

**MECHANICAL BEHAVIOUR OF 3D
BRAIDED NATURAL FIBRE FABRIC
REINFORCED BIODEGRADABLE
COMPOSITES**

Thesis

Submitted in partial fulfillment of the requirements for the degree of

DOCTOR OF PHILOSOPHY

by

SATEESHKUMAR KANAKANNAVAR



DEPARTMENT OF MECHANICAL ENGINEERING
NATIONAL INSTITUTE OF TECHNOLOGY KARNATAKA,
SURATHKAL, MANGALORE – 575025

FEBRUARY, 2022

DECLARATION

I hereby *declare* that the Research Thesis entitled “**MECHANICAL BEHAVIOUR OF 3D BRAIDED NATURAL FIBRE FABRIC REINFORCED BIODEGRADABLE COMPOSITES**” which is being submitted to the **National Institute of Technology Karnataka, Surathkal** in partial fulfillment of the requirements for the award of the Degree of **Doctor of Philosophy in Department of Mechanical Engineering** is a *bonafide report of the research work carried out by me*. The material contained in this Research Thesis has not been submitted to any University or Institution for the award of any degree.

Register Number : 177038ME017

Name of the Research Scholar : SATEESHKUMAR KANAKANNAVAR

Signature of the Research Scholar:

Department of Mechanical Engineering

Place : NITK, Surathkal

Date :

C E R T I F I C A T E

This is to *certify* that the Research Thesis entitled “**MECHANICAL BEHAVIOUR OF 3D BRAIDED NATURAL FIBRE FABRIC REINFORCED BIODEGRADABLE COMPOSITES**” submitted by **Mr. SATEESHKUMAR KANAKANNAVAR** (Register Number: **177038ME017**) as the record of the research work carried out by him, is *accepted as the Research Thesis submission* in partial fulfillment of the requirements for the award of degree of **Doctor of Philosophy**.

Research Guide

Dr. P. Jeyaraj
Associate Professor
Department of Mechanical Engineering

Chairman – DRPC

Date:

ACKNOWLEDGEMENT

I would like to extend my sincere gratitude to Dr. Jeyaraj Pitchaimani, Associate Professor Department of Mechanical Engineering, National Institute of Technology Karnataka, Surathkal, for their invaluable constructive guidance and encouragement extended throughout my study. Sincere gratitude is expressed to Dr. Arunkumar Thalla, Department of Civil Engineering, National Institute of Technology Karnataka, Surathkal, for their encouragement and help extended.

I would like to thank Research Progress Assessment Committee Members Dr. M. R. Ramesh, and Dr. T. Nasar for their valuable inputs. Useful discussions and suggestions are deeply appreciated.

I would like to thank former head of department Prof. Narendranath S., Prof. Shrikantha S Rao, Prof. S. M. Kulkarni, and Prof. Ravikiran Kadoli Head of Mechanical Engineering Department and all the faculty members at Mechanical Engineering Department for their support throughout this research work.

Constant encouragement of my family to pursue higher studies has made it possible for me to reach at this stage. I wish to thank all my family members for love, help and encouragement provided. I express my sincere thanks to Dr. M. Rajesh, Dr. Sunil Waddar, Mr. Vijay G., Mr. Sailesh Raju, Mr. Twinkle C.M., and our research team for their help and kind cooperation extended throughout this research work. Special note of thanks to all my friends and well-wishers for their constant help, encouragement and understanding.

ABSTRACT

Synthetic fibre reinforced composites (such as glass, carbon and kevlar) have high specific strength and modulus and popularly used in the applications of automotive, aerospace and wind energy sectors. These composites are non-degradable and their disposal after the end use is a significant problem. Hence the research in the development of more sustainable and renewable natural fibre filled bio-composites is extremely topical. In this study, to fabricate the biodegradable composites flax fibre is used as filler material and polylactic acid (PLA) polymer is used as matrix material. Flax fibre braided yarn is prepared by solid braiding method, followed by this the plain woven fabric is prepared using a handloom machine. Before the preparation of the composite laminates, PLA and natural fibre braided yarn fabric (NFBF) sheets are prepared by solution casting method. Film stacking method and hot press compression molding methods are used to prepare the composites with the different weight fraction of fibre. In this work, influence of NFBF reinforcement in PLA resin on mechanical properties, thermal buckling, water absorption, biodegradability, wear, fracture toughness, mechanical buckling and free vibration characteristics are investigated.

Initially, geometrical and tensile properties of the prepared braided yarn and woven fabric are studied. Mechanical properties of the composites are characterised experimentally in the warp and weft directions of the composite surface plies. The NFBF/PLA composites results are compared with the pristine PLA results. It is observed that the mechanical properties of the composites are improved with the reinforcement of NFBF compared to pure PLA. Warp direction loaded composites showed higher mechanical properties compared to weft direction loaded composites. The NFBF/PLA composites are compared with the other natural fibre PLA composites results reported in literature and it is noticed that the NFBF/PLA composites have moderate tensile strength, higher flexural and impact strengths.

Thermal properties (flammability, DSC, TGA, HDT and thermal deflection) of the NFBF/PLA composites are determined experimentally. Thermal deflection behaviour of pure PLA and NFBF/PLA composites are carried out on an in house built experimental set up at different temperature loading conditions. Effect of NFBF reinforcement, its weight percentage, loading direction (warp and weft) of the

composites and nature of temperature load change on deflection behaviour of the PLA and NFBBF/PLA composites are studied. Results revealed that, burning rate of the NFBBF/PLA composites is reduced compared to pure PLA. Meanwhile, enthalpy (ΔH_m), percentage crystallinity (X_c), thermal stability and HDT are enhanced for the NFBBF reinforced PLA composites over pure PLA. Thermal deflection of the composites is reduced compared to pristine PLA and it further decreased with the increase in fibre content. Due to higher modulus and strength associated with the NFBBF/PLA composites. Similarly, the warp direction loaded composites showed higher reduction in deflection compared to pure PLA and weft direction loaded composites. The reinforcement of NFBBF improved the thermal resistance property and this result for the reduction in thermal deflection peak temperature for different heating cases. Reinforcement also enhanced the thermal sustainability of the composites.

Influence of environmental conditions on NFBBF/PLA composites are analysed by performing water absorption and soil incubation tests. Water absorption, thickness swelling, flexural tests are performed in different loading directions (warp and weft) of the composites. Similarly, biodegradation study is carried out in a compost soil medium at different incubation time periods (0, 15, 30, 60, 90 days). Biodegradation study is analysed based on weight loss measurement, change in FTIR spectra and reduction in tensile strength. Results revealed that water absorption and thickness swelling are increased with the reinforcement of NFBBF, the weft direction loaded composite showed higher water absorption and thickness swelling values. Warp direction loaded composites showed maximum flexural strength and modulus. These values are decreased after water absorption. The NFBBF reinforcement also enhanced the biodegradability of the NFBBF/PLA composites compared to neat PLA. Tensile properties are decreased with the increase in the incubation time. Biodegradability analysis revealed that NFBBF reinforcement enhanced the resistance against degradation than other types of reinforcement. It is due to the high fibre aspect ratio associated with short fibre reinforcement that increases the interaction with water molecules, whereas it is low for braided reinforcement.

Friction co-efficient and wear rate of the composites are analysed using pin-on-disc tribometer under dry contact sliding condition and various operating conditions (velocity and load) for a fixed sliding distance of 3000 m. The reinforcement of NFBBF with the PLA reduced the polymer film generation and improved the surface roughness significantly. Wear rate of the composites are decreased drastically compared to pure PLA. Also, fracture toughness study is performed on single-edge-notched-bend (SENB) specimens using three point bending method. It is found that plane-strain fracture toughness (K_{IC}) and strain energy release rate (G_{IC}) values of the PLA composites are higher than pure PLA for NFBBF35 reinforcement. K_{IC} values of the NFBBF reinforced PLA composites are much high compared to similar natural fibre composites reported in literature. This is attributed to high resistance offered by the interweaving yarns of the braided fabric hence more energy is required to begin crack propagation compared to other typical forms of reinforcement.

Influence of mechanical edge load on free vibration frequencies of NFBBF/PLA beam is studied experimentally. Initially, the buckling load of the beam is calculated. Then variation of natural frequencies with and without compression loads is analysed. Buckling strength of the PLA beam is enhanced by NFBBF reinforcement. Increase in the axial load results in reduction in the frequencies and the effect is very significant for the lowest frequency for the loads around the buckling load. Furthermore, the lowest frequency increase is very significantly for the loads higher than critical load due to the increase in geometric stiffness.

Keywords: Braided yarn fabric; PLA; Biodegradable composites; Mechanical properties; Thermal properties; Wear properties; Fracture toughness; Buckling; Free vibration.

CONTENTS

ACKNOWLEDGEMENT	i
ABSTRACT.....	ii
CONTENTS.....	v
LIST OF FIGURES	ix
LIST OF TABLES	xv
ABBREVIATIONS	xvi
1 INTRODUCTION AND LITERATURE REVIEW	1
1.1 Fibre sources	3
1.2 Yarns	3
1.2.1 Braided yarn.....	4
1.3 Textile preform.....	6
1.3.1 Woven fabrics	6
1.4 Bio-matrix	7
1.5 Literature review	8
1.5.1 Braided fibre composites	8
1.5.2 Natural fibre PLA composites	8
1.5.3 Thermal deflection	10
1.5.4 Water absorption.....	11
1.5.5 Biodegradability.....	12
1.5.6 Wear study	13
1.5.7 Fracture toughness study.....	14
1.5.8 Buckling under axial compressive load	15
1.6 Closure	16
1.7 Motivation	16
1.8 Objectives.....	17
1.9 Outline of the thesis.....	17
2 MATERIALS AND METHODS	19
2.1 Materials.....	19
2.2 PLA resin.....	19
2.3 Flax fibre	20

2.4	Preparation of braided yarn and woven fabric	21
2.5	Geometrical and mechanical characterization of braided yarn and fabric	23
2.6	Composite laminate preparation.....	26
2.7	Mechanical characterization of composites	28
2.7.1	Tensile, flexural, impact and interlaminar shear strength (ILSS) tests..	28
2.7.2	SEM Analysis	29
2.8	Thermal properties	29
2.8.1	Flammability	29
2.8.2	Differential scanning calorimetry (DSC) analysis	30
2.8.3	Thermogravimetric analysis.....	30
2.8.4	Heat deflection temperature	31
2.8.5	Thermal deflection	31
2.9	Water absorption and Biodegradability tests	34
2.9.1	Water absorption.....	34
2.9.2	Biodegradability test	34
2.10	Wear and fracture toughness study	37
2.10.1	Density test.....	37
2.10.2	Wear test	38
2.10.3	Plane strain fracture toughness test.....	40
2.11	Buckling and free vibration properties.....	42
2.11.1	Buckling under axial compression.....	42
2.11.2	Free vibration	43
3	MECHANICAL PROPERTIES OF BRAIDED YARN, FABRIC AND COMPOSITES.....	45
3.1	Introduction	45
3.2	Geometric and tensile properties of braided yarn and woven fabrics	45
3.3	Mechanical properties of the composites	48
3.3.1	Tensile properties.....	49
3.3.2	Flexural properties	54
3.3.3	Impact properties of NFBF reinforced PLA composites	58
3.3.4	Interlaminar shear strength (ILSS).....	60
3.4	Conclusions	63

4	THERMAL PROPERTIES OF COMPOSITES	65
4.1	Introduction	65
4.2	Flammability	65
4.3	Crystallisation and melting behaviour.....	66
4.4	Thermogravimetric analysis.....	68
4.5	Heat deflection temperature	70
4.6	Thermal deflection study.....	71
4.7	Conclusion.....	81
5	WATER ABSORPTION, THICKNESS SWELLING AND BIODEGRADABILITY OF COMPOSITES	83
5.1	Water absorption	84
5.1.1	Transport coefficients	85
5.1.2	Effect of water absorption on flexural properties	87
5.2	Biodegradability study	90
5.3	Conclusion.....	100
6	TRIBOLOGICAL BEHAVIOUR AND FRACTURE TOUGHNESS OF COMPOSITES.....	102
6.1	Introduction	102
6.2	Density	103
6.3	Wear studies	104
6.3.1	Coefficient of friction	105
6.3.2	Wear rate.....	107
6.3.3	Specific wear rate.....	109
6.3.4	Worn surface morphology	112
6.4	Plane strain fracture toughness.....	115
6.4.1	Tensile properties.....	115
6.4.2	Fracture toughness	117
6.5	Conclusion.....	124
7	BUCKLING AND FREE VIBRATION PROPERTIES.....	126
7.1	Density and void content.....	126
7.2	Buckling under axial compression	127
7.3	Free vibration response under axial compressive load.....	131

7.4	Property comparison plots.....	133
7.5	Conclusion.....	135
8	SUMMARY AND CONCLUSIONS.....	136
8.1	Summary.....	136
8.2	Conclusion.....	137
	SCOPE FOR FUTURE WORK.....	140
	REFERENCES.....	141
	LIST OF PUBLICATIONS.....	159
	BIO-DATA.....	161

LIST OF FIGURES

Figure 1.1 Types of unidirectional preforms (a) spun yarn, (b) continuous filament yarn (Wambua and Anandjiwala 2011)	4
Figure 1.2 Commingled yarn schematic arrangement (Shonaike et al. 1996).....	4
Figure 1.3 Braiding principle with three yarns (a) Braided lace (b) Braided natural fibre Yarn (c) Jute flat braided yarn (Kyosev 2015; Rajesh and Pitchaimani 2017b)...	5
Figure 1.4 Types of tubular braiding (Bairstow 2018; Sakaguchi et al. 2000).....	5
Figure 1.5 Most common woven fabric structures (a) Plain, (b) Twill, (c) Satin (d) Basket (e) Mock leno (f) Leno (John and Thomas 2008).....	6
Figure 2.1 Flax plants (Katherine 2012)	20
Figure 2.2 Simply twisted yarn	21
Figure 2.3 Braiding principle with four simply twisted yarns (Poole 2020)	21
Figure 2.4 Photographs of a) 3D braided yarn, b) 3D braided yarn closer view, c) showing four simply twisted strands of yarns in braided yarn	22
Figure 2.5 Flax braided yarn plain woven fabric	23
Figure 2.6 a) Braided yarn tensile test specimen and b) sample kept in UTM for the tensile test.....	24
Figure 2.7 a) GSM cutter b) specimen for GSM calculation c) GSM scale	25
Figure 2.8 Braided yarn woven fabric tensile test specimens for a) warp direction loading, b) weft direction loading	26
Figure 2.9. Flow-chart representing composite fabrication process	27
Figure 2.10 Flammability test set up.....	30
Figure 2.11 Schematic of thermal buckling testing set up.....	32
Figure 2.12 Schematic of thermal buckling test specimen	32
Figure 2.13 Schematic representation of a) case 1: decrease, b) case 2: Decrease – Increase and c) case 3: Increase – decrease	33
Figure 2.14 Crates with samples	36
Figure 2.15 Sketch of burial test crate	36
Figure 2.16 Tensile specimens before and after biodegradability test.....	37
Figure 2.17 Schematic diagram of pin-on-disc wear testing set up.....	38
Figure 2.18 Schematic of composite specimen sliding direction	39

Figure 2.19 SENB (single-edge-notch bending) specimen and fixture for three point bending test	41
Figure 2.20 Representing estimation of critical buckling load (P_{cr}) from (a) DTM and (b) MBC methods for NFBF2 composites.....	43
Figure 2.21 Schematic experimental set up of free vibration test under axial compressive load.....	44
Figure 2.22 Schematic representation of composite test specimen configuration.....	44
Figure 3.1. Optical photographs of 3D braided yarn a) longitudinal view, b) cross-sectional view.....	45
Figure 3.2 Stress-strain curve of the braided yarn	46
Figure 3.3 SEM image of the flax fabric woven using 3D braided yarns	47
Figure 3.4 Tensile stress-strain curves of braided yarn fabric in warp and weft direction loading	47
Figure 3.5. Tensile stress–strain curves for PLA and NFBF/PLA composites under warp direction loading	50
Figure 3.6. Ultimate tensile strength and tensile modulus of PLA and NFBF/PLA composites under warp direction loading	50
Figure 3.7. Tensile stress–strain curves of PLA and NFBF/PLA composites under weft direction loading	50
Figure 3.8. Ultimate tensile strength and tensile modulus of PLA and NFBF/PLA composites under weft direction loading	51
Figure 3.9. Micrographs of tensile test specimen fractured surfaces a) warp direction loaded and b) weft direction loaded composites.....	52
Figure 3.10. Flexural response curves for PLA and NFBF/PLA composites under warp direction loading	54
Figure 3.11 Flexural strength and flexural modulus of neat PLA and NFBF/PLA composites under warp direction loading	54
Figure 3.12. Flexural response curves for PLA and NFBF/PLA composites under weft direction loading	55
Figure 3.13. Flexural strength and flexural modulus of neat PLA and NFBF/PLA composites under weft direction loading	55

Figure 3.14. Micrographs of flexural test specimen fractured surfaces a) warp direction and b) weft direction loaded composites	56
Figure 3.15. Impact strength of PLA and NFBB/PLA composites under warp direction loading.....	59
Figure 3.16. Impact strength of PLA and NFBB/PLA composites under weft direction loading.....	59
Figure 3.17 Fractured surface photographs of impact test specimen a) warp direction loading and b) weft direction loading of NFBB composites.....	60
Figure 3.18 Load - displacement curves of PLA and NFBB composites	61
Figure 3.19 Microscopic image of the NFBB/PLA composite specimen (a) before and (b) after the SBS test	61
Figure 3.20 Interlaminar shear strength of PLA and NFBB composites	62
Figure 3.21 Microscopic images of the fractured composite samples from SBS test carried out on a) NFBB11, b) NFBB22 and c) NFBB33 composites	63
Figure 4.1 Burning rate of pure PLA and NFBB/PLA composites.....	66
Figure 4.2 DSC thermograms of PLA and NFBB/PLA composites for (a) first heating scan and (b) second heating scan	68
Figure 4.3 Thermogravimetric analysis of (a) Flax fibre, (b) PLA (c) NFBB11, (d) NFBB22 and (e) NFBB33 composites.	69
Figure 4.4 Heat deflection temperature of PLA and NFBB/PLA composites	71
Figure 4.5 Thermal deflection curves of PLA (NFBB0) and NFBB/PLA composites	72
Figure 4.6 Thermal deflection curves for decrease case in (a) warp direction and (b) weft direction loading of PLA and NFBB/PLA composites.....	74
Figure 4.7 Thermal deflection curves for decrease-increase case in (a) warp direction and (b) weft direction loading of PLA and NFBB/PLA composites	74
Figure 4.8 Thermal deflection curves for increase-decrease case in (a) warp direction and (b) weft direction loading of PLA and NFBB/PLA composites	74
Figure 4.9 Comparison of deflection of NFBB/PLA composite beam under warp and weft direction heating in case 2	75
Figure 4.10 Images of PLA specimen under case 3 heating a) before test, b) after test	77

Figure 4.11 Images of the NFBF/PLA composites under case 3 heating a) before test, b) after test	77
Figure 4.12 Heat transfer in pure PLA.....	77
Figure 4.13 Heat transfer in NFBF/PLA composite	78
Figure 4.14 Time required attaining 80 °C surface temperature for PLA and NFBF/PLA composites under (a) warp and (b) weft direction loading.....	79
Figure 4.15 Heating profile effect on deflection of NFBF22/PLA under (a) warp and (b) weft directions heating	80
Figure 5.1 Schematic of manufacturing of braided flax yarn woven reinforced PLA composites.....	83
Figure 5.2 Water absorption of PLA and NFBF/PLA composites under (a) warp and (b) weft direction loading.....	85
Figure 5.3 Thickness swelling of PLA and NFBF/PLA composites under (a) warp and (b) weft direction loading.....	85
Figure 5.4 Flexural stress of PLA and NFBF/PLA composites for warp direction.....	88
Figure 5.5 Flexural modulus of PLA and NFBF/PLA composites for warp direction	88
Figure 5.6 Flexural stress of PLA and NFBF/PLA composites for weft direction	88
Figure 5.7 Flexural modulus of PLA and NFBF/PLA composites for weft direction.	89
Figure 5.8 SEM images of the fractured surface of NFBF/PLA composites a) before water absorption, b) after water absorption	89
Figure 5.9 Percentage weight loss of PLA and NFBF/PLA composites as a function of burial time	91
Figure 5.10 FTIR spectra of NFBF44 composites before (0 day) and after (90 days) biodegradation test.....	93
Figure 5.11 SEM photomicrographs of pure PLA and NFBF/PLA composites before and after (90 days) biodegradation test a) PLA, b) NFBF44%	94
Figure 5.12 Stress-strain curves of PLA and NFBF/PLA composites (a) before and (b) after the biodegradation test.....	94
Figure 5.13 Effect of compost soil burial on tensile strength of the PLA and NFBF/PLA composites	96
Figure 5.14 Effect of compost soil burial on Young's modulus of the PLA and NFBF/PLA composites.....	96

Figure 5.15 SEM micrograph of the tensile fractured surface of the NFBF44 composite before biodegradability.....	98
Figure 5.16 SEM micrographs of the tensile fractured surface of the NFBF44 composite after 30 days of soil burial test	98
Figure 5.17 SEM micrographs of the tensile fractured surface of the NFBF44 composite after 60 days of soil burial test	98
Figure 6.1 Cross-sectional views of PLA and NFBF/PLA composites with different number of fabric reinforcement.	102
Figure 6.2 (a) Frictional force and (b) Height loss of PLA and NFBF/PLA composites under 30N load.....	105
Figure 6.3 Coefficient of friction versus applied load for NFBF/PLA composites of (a) NFBF0 (PLA), (b) NFBF18, (c) NFBF26, and (d) NFBF35.	106
Figure 6.4 Effect of load and speed on wear rate for NFBF/PLA composites (a) neat PLA, (b) NFBF of 18 wt. %, (c) NFBF of 26 wt. %, and (d) NFBF of 35 wt. % ...	108
Figure 6.5 Specific wear rate versus applied load for 1 m/s of PLA and NFBF/PLA composites.....	109
Figure 6.6 Specific wear rate versus applied load for 2 m/s of PLA and NFBF/PLA composites.....	110
Figure 6.7 Specific wear rate versus applied load for 3 m/s of PLA and NFBF/PLA composites.....	110
Figure 6.8 Specific wear rate versus sliding distance for PLA and NFBF/PLA composites at 1 m/s sliding velocity and 10 N applied load.....	111
Figure 6.9 Percentage variation of specific wear rate minimum and maximum values of PLA and NFBF/PLA composites	112
Figure 6.10 SEM images of worn surfaces of pure PLA and NFBF/PLA composites for 10 N applied normal load and 1 m/s velocity (a) NFBF0, (b) NFBF18, (c) NFBF26 and (d) NFBF35	113
Figure 6.11 Worn surfaces SEM micrographs of pure PLA and NFBF/PLA composites for 30 N applied load and 3 m/s velocity of (a) NFBF0, (b) NFBF18, (c) NFBF26 and (d) NFBF35	114
Figure 6.12 Wear debris micrographs of (a) NFBF0, (b) NFBF35	115
Figure 6.13 Stress-strain curves of PLA and NFBF/PLA composites.....	116

Figure 6.14 Ultimate tensile stress and modulus of the pure PLA and NFBF/PLA composites.....	116
Figure 6.15 Typical load versus displacement curves of PLA and NFBF/PLA composites.....	117
Figure 6.16 Measurement of P_Q from load versus displacement curve for (a) pure PLA and (b) NFBF18 composite.....	118
Figure 6.17 K_{IC} of PLA and NFBF/PLA composites for different fibre weight percentage	120
Figure 6.18 G_{IC} of PLA and NFBF/PLA composites for different fibre weight percentage	120
Figure 6.19 SEM micrographs of fractured surfaces of SENB specimens a) pure PLA, b) NFBF18, c) NFBF26 and d) NFBF35 composites	122
Figure 6.20 Fracture toughness (K_{IC}) plotted against fibre content from available literature studies	123
Figure 7.1 Axial load vs. displacement curves of samples according to NFBF content	127
Figure 7.2 Critical buckling load of PLA and its composites obtained from DTM and MBC techniques.....	128
Figure 7.3 NFBF/PLA composite specimen representative images (a) before and (b) after buckling test.....	128
Figure 7.4 SEM micrograph presenting fibre matrix bonding of NFBF11 composite	130
Figure 7.5 Buckling strength and modulus of the PLA composites with different fabric content	131
Figure 7.6 Representative frequency response function of NFBF11 composite sample	132
Figure 7.7 Influence of increase in axial-compressive load on natural frequencies of (a) 1 st , (b) 2 nd and (c) 3 rd modes	133
Figure 7.8 Comparison of the critical buckling load of NFBF/PLA composites with other similar composites	134

LIST OF TABLES

Table 2.1 Properties of PLA polymer*	20
Table 2.2 Chemical components of flax fibres (Yan et al. 2014)	21
Table 2.3. Chemical properties of the compost soil used for biodegradation test	35
Table 2.4 Parameters used for wear test	39
Table 3.1. Tensile properties of the braided yarn	46
Table 3.2. Tensile properties of natural fibre braided yarn fabric (NFBF)	48
Table 3.3 Comparison of tensile properties of NFBF/PLA composites with different natural fibre PLA composites (Percentage (+) increase or (-) decrease of the composites is calculated with respect to neat PLA)	53
Table 3.4 Comparison of flexural properties of NFBF/PLA composites with different natural fibre PLA composites (Percentage (+) increase or (-) decrease of the composites is calculated with respect to neat PLA)	57
Table 4.1 Thermal characteristics of the PLA and NFBF/PLA composites for first heating scan	67
Table 4.2 Thermal characteristics of the PLA and NFBF/PLA composites for second heating scan	67
Table 4.3. Effect of thermogravimetric temperature on weight loss of PLA and NFBF/PLA composites	70
Table 4.4 Peak values of the deflection and temperature of pure PLA and NFBF/PLA composites	81
Table 5.1 The maximum moisture uptake, diffusion coefficient and permeability of pure PLA and NFBF/PLA composites	86
Table 5.2 Comparison of water absorption results of NFBF/PLA composites with other natural fibre/PLA composites	90
Table 5.3 Comparison of biodegradability results of NFBF/PLA composites with other natural fibre/PLA composites	99
Table 6.1 Density and void content of the PLA and NFBF/PLA composites	103
Table 7.1 Density and void content of the composites	127

ABBREVIATIONS

ASTM	: American society for materials and testing
CNT	: Carbon nano tube
CV	: Coefficient of variation
DCM	: Dichloromethane
DIM	: Direct-injection-molding
DSC	: Differential scanning calorimetry
DSF	: Dynamic sheet former
DTM	: Double tangent method
EIM	: Extrusion-injection-molding
FFT	: Fast fourier transform
FG-GRC	: Functionally graded graphene reinforced composite
FRF	: Frequency response function
FTIR	: Fourier transform infrared
GSM	: Gram per square metre
HDT	: Heat deflection temperature
ILSS	: Interlaminar shear strength
IR	: Infrared
ITR	: Interfacial thermal resistance
LVDT	: Linear variable differential transducer
MBC	: Modified Budiansky criteria
MMT	: Montmorillonite clay
NFBF	: Natural fiber braided yarn fabric
PLA	: Polylactic acid
PLLA	: Poly-L-lactic acid

SBS	: Short beam shear
SEM	: Scanning electron microscope
SENB	: Single edge notched bending
SiC	: Silicon carbide
SWR	: Specific wear rate
TGA	: Thermogravimetric analysis
UTM	: Universal testing machine

1 INTRODUCTION AND LITERATURE REVIEW

Usage of plastic bottles, cans, grocery bags and different types of food packaging elements leads to a burning solid waste management problem as these plastics are basically non-biodegradable materials. During the fabrication process also these materials emit green-house gases. Similarly, most of the fibre reinforced composites are used in different applications also made of synthetic (man-made) fibres (such as glass, kevlar and carbon) and non-biodegradable resins such as epoxy and polyester. Disposal of these materials after their end use is also an important environmental concern. Hence, these kind of materials are mainly responsible for environmental pollution (Khan et al. 2016). To reduce the pollution problems and to keep environment green and safe, it is necessary to reduce the usage of these materials and develop the substitution by bio-based “eco” materials (Orue et al. 2018a). Biodegradable materials made from natural resources are the perfect alternatives to these materials. Biodegradable materials are sustainable and degrade easily after its disposal at the end of the service. Globally, the development of these environmentally sustainable materials using natural resources for high-performance engineering applications is growing (Adomavičiūtė et al. 2015). Recently, several researchers developed biodegradable composite materials using natural fibres for example flax, hemp, bamboo, jute, sisal etc., as reinforcement.

For mankind synthetic polymers are priceless endowment of present day science and technology. These materials became the integral part to our life style with their extensive variety of applications in numerous fields inclusive of agriculture, industry, clinical appliances, food, construction substances, purchaser (consumer) products, aerospace substances etc. The serious concern of these polymers is resistance to physical, chemical and biological deterioration, whilst it is utilized in regions including surgery, agriculture, pharmacology and the environment (Luckachan and Pillai 2011). Disposal of these materials creates various levels of land fill problems. To deal with this problem, much consideration has been paid to produce biodegradable polymers from renewable sources. Starch, cellulose, chitosan and proteins are natural resources of bio-polymers from animal and plant origins. The degradation of biopolymers is frequently prompted by microorganisms such as fungi

and bacteria through enzymatic catalysis process in disposed landfills. Biomass, water, CO₂, CH₄ and other natural substances are the end products of the biodegraded biopolymers, which helps in balancing the greenhouse gas and other environmental impacts (Zhong et al. 2020).

Natural fibres can be utilised as fillers in thermosetting or thermoplastic polymers, replacing the conventional artificial fibres (such as carbon, glass, aramid etc.). Compared to conventional fibres these fibres are advantageous regarding specific weight, flexibility in processing, no toxic gas release during processing, low cost, thermal stability, dimensional stability, lower environmental impact, chemical resistance, good strength and modulus, agro-waste utility, fully biodegradable, renewable, recyclable and required low energy for processing (Georgiopoulos et al. 2018; Ngaowthong et al. 2019). Several researchers also demonstrated that types of fibre, forms of reinforcement, size of fibre, harvesting process of fibre, environmental conditions affects the stiffness and strength of the natural fibre filled composites (Alimuzzaman et al. 2015; Alix et al. 2009; Fazita et al. 2014; Huang et al. 2018; Ochi 2008).

Natural fibres can be reinforced in a short form (with random distribution) and woven textile fabric form. Though natural fibre reinforcement improves the characteristics of the composites, the enhancement in the strength is not up-to-level because of non-uniform stress distribution in short fibre composites (Rajesh et al. 2018b; Rajesh and Pitchaimani 2017a). Due to amorphous nature of random short natural fibres, composites filled with these fibres showed comparatively poor mechanical properties and are not appropriate for structural components (Goutianos et al. 2006; Rajesh et al. 2018a). In woven fabrics, fibres are tightly attached together; fibre pull-out is quite impossible and requires more strength to break down of these woven fabric reinforced composites. Also, the weaving architecture of the fibres gives an interlocking and gives better strength than the short-random fibre composites (Khan et al. 2016). The woven fabric reinforcement provides excellent integrity, stability and conformability for advanced structural applications (Alavudeen et al. 2015; Aruchamy et al. 2019).

Fibres play the most important role in the production of textile fabric filled composites. Consequently the initial phase in development of textile fabric composites is the determination of natural fibres, which ought to have high strength and modulus to withstand higher loads in the structural applications.

1.1 Fibre sources

Depending on the use of natural fibres, plants may be grouped as, primary plants and secondary plants. The plants grown particularly for their fibre content are known primary plants examples are jute, sisal, kenaf, and hemp. In the plants where the fibres are processed as by product are called secondary plants. For example, pineapple, banana, oil palm, flax and coir are secondary plant fibres (Faruk et al. 2012). Natural fibres can be further classified based on the extraction from plant part such as leaf fibres (manila, caraua, palm, sisal etc.), fruit fibres (coir, coconut etc.), bast fibres (flax, kenaf, jute, ramie, hemp etc.) and seed fibres (kapok, cotton etc.). Low pollution emission, improved energy recovery, low density, abundance, non-toxicity, biodegradability, acceptable specific properties, versatility, renewability, low cost, non-corrosive nature and less skin and respiratory irritation are the specific benefits of the natural fibres (Kumar et al. 2018; Nam et al. 2011; Sgriccia et al. 2008).

In the present study flax fibre is used as filler material. Flax fibre is a natural fibre and is found in fibre groups in a layer of the bark called as the bast layer. These fibres are normally used in polymer composite applications. Flax fibres are made up of hemicellulose and cellulose, and lignin or pectin which acts as some form of matrix to bond together (Shanks et al. 2005). Flax fibres have excellent mechanical properties and hence it is known as one of the strongest fibre among the natural fibres. Due to this the polymer composites reinforced with flax fibres are used in several industrial applications including packaging, textile and automotive industries (Eselini et al. 2019).

1.2 Yarns

Yarns comprises of fibres grouped together in a straight assemblage to form a continuous strand (Wambua and Anandjiwala 2011). Yarn is the conventional term

used for a continuous strand of fibres, materials or filaments in a structure appropriate for weaving, knitting or otherwise interlacing/intertwining to make a textile texture. There are different types of yarns such as spun yarn (single and ply), continuous filament (twisted and no-twist), commingled yarn and braided yarn. Different types of unidirectional yarn preforms are shown in Figure 1.1. Similarly, schematic diagram of formation of commingled yarn is shown in Figure 1.2.

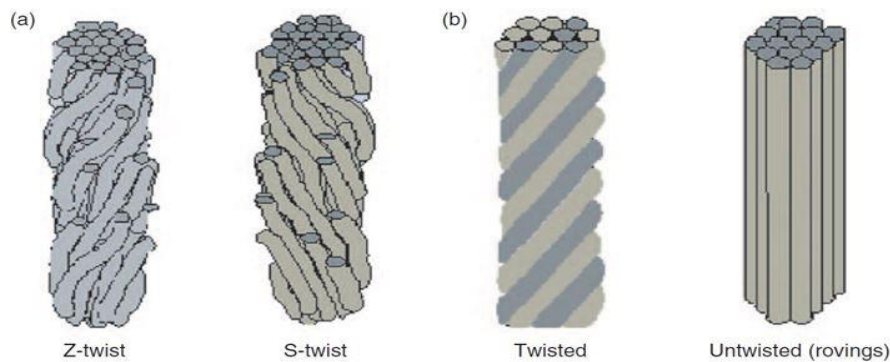


Figure 1.1 Types of unidirectional preforms (a) spun yarn, (b) continuous filament yarn (Wambua and Anandjiwala 2011)

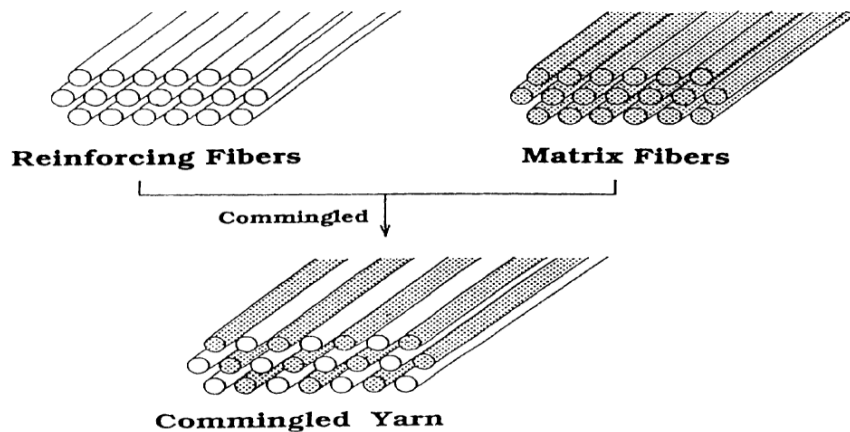


Figure 1.2 Commingled yarn schematic arrangement (Shonaik et al. 1996)

1.2.1 Braided yarn

Braiding is a method, in which three or more conventional yarns are interlaced diagonally along the axis of the product, so as to get a thick and strong yarn. Braids can be straight items (ropes and chords), plane shell, solid or curved structures (fabrics of 1, 2 or 3-dimensional) with variable or fixed cross-section (Kyosev 2015). Basic principle of making braided yarn using three typical yarns is shown in Figure

1.3(a). Different types of tubular braiding forms are shown in Figure 1.4. Common round braided yarn types are solid braid, hollow braid, double braid and maypole braid. These braids are usually used in rope and lace making. In Figure 1.3, in the initial step the left yarn is interlaced, so this yarn moves over right yarn, and in the step two, the right yarn is interlaced, hence the right yarn moves over left yarn. A flat cross-sectioned braid is the resulting product, known as flat-braid. The tubular braiding method is carried out by following the same flat braiding steps, but in this braiding technique even-number of yarns organized in a circle.

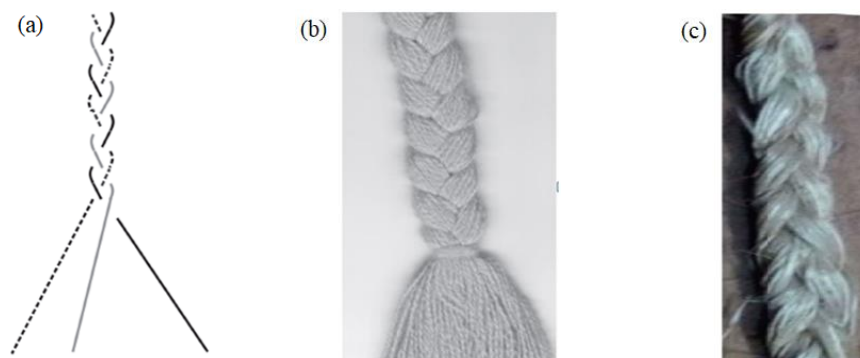


Figure 1.3 Braiding principle with three yarns (a) Braided lace (b) Braided natural fibre Yarn (c) Jute flat braided yarn (Kyosev 2015; Rajesh and Pitchaimani 2017b)

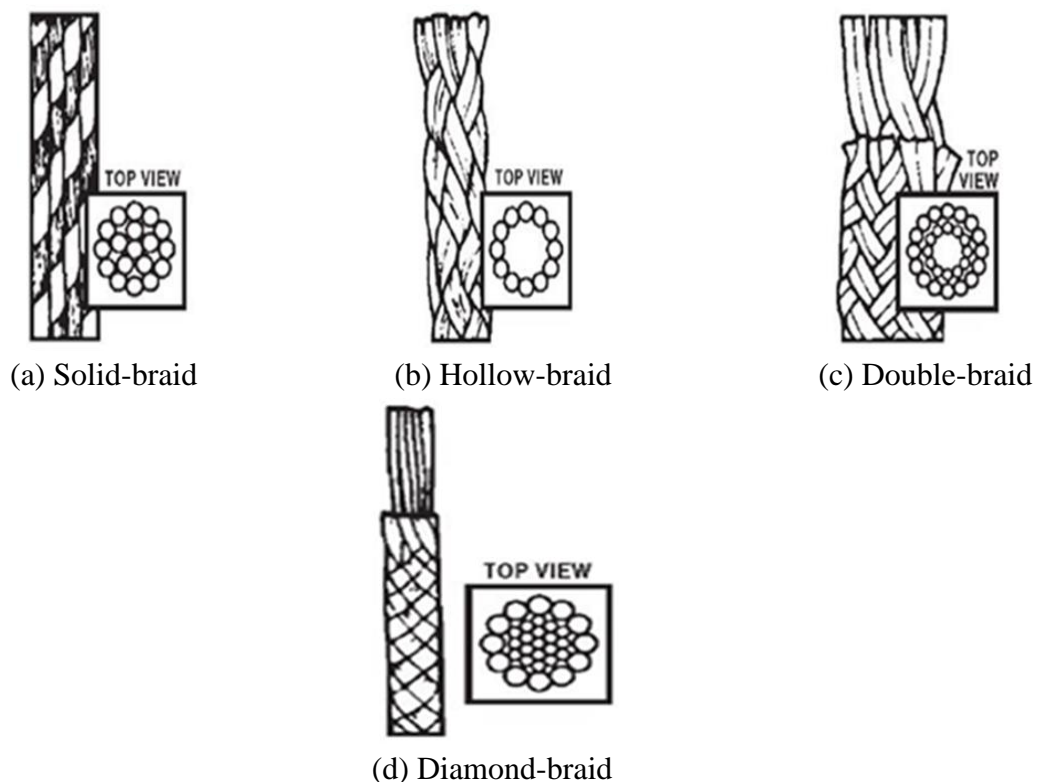


Figure 1.4 Types of tubular braiding (Bairstow 2018; Sakaguchi et al. 2000)

1.3 Textile preform

Fibrous materials for example fibres, yarns and fabrics are explicitly gathered in a unconsolidated (i.e., without adding matrix) way are known as textile preform (Wambua and Anandjiwala 2011). In recent years the analysts are pulled in towards these textile preforms because of their exceptional mechanical characteristics, like improved transverse moduli, strength, increased damage tolerance and shear resistance. These materials also give great dimensional stability and near net shape fabricating capability (Byun and Chou 1989). Textile preforms are further divided into three kinds like woven, knitted and braided fabrics (Tan et al. 1997).

1.3.1 Woven fabrics

These are manufactured by using two sets of interlaced yarns (warp and weft). The yarn along the fabric longitudinal direction is known as warp yarn and the yarn along the fabric width (transverse) direction is known as weft yarn or fill (Byun and Chou 1989). These preforms are characterised by their higher resistance to damage, intra and inter laminar strengths (Aly 2017). The woven fabrics common types are; plain, twill, satin, basket, mock leno and leno as shown in Figure 1.5.

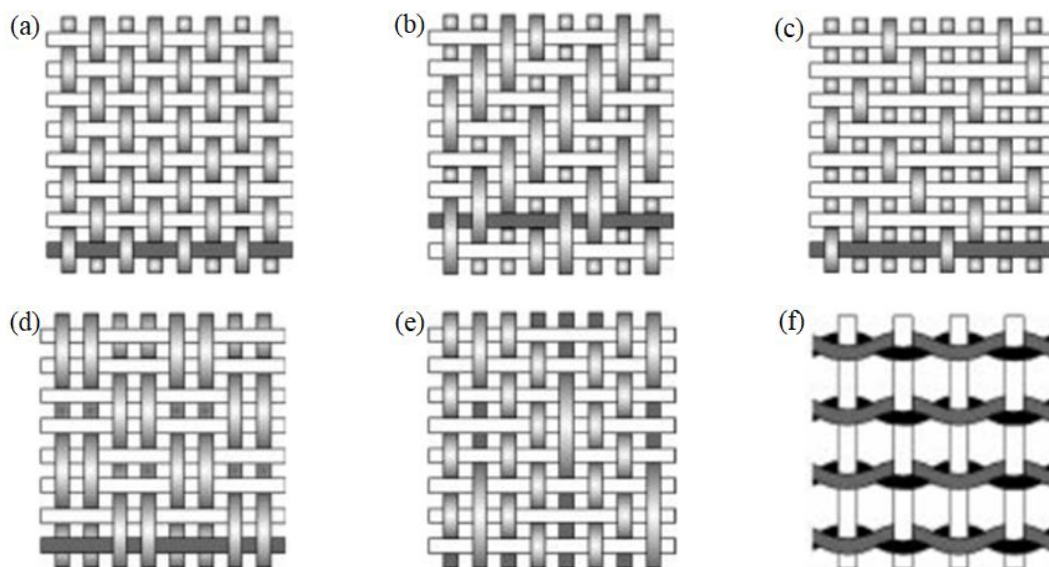


Figure 1.5 Most common woven fabric structures (a) Plain, (b) Twill, (c) Satin (d) Basket (e) Mock leno (f) Leno (John and Thomas 2008)

1.4 Bio-matrix

The composites based on synthetic polymers are prompting exorbitant waste in the landfill and takes extensive stretch to degrade and are destructive to the environment (Anuar et al. 2016). Since early 1990s advancement in the plastics industry has changed the paths dramatically towards the development of durable bio-plastics having high bio-based substance (Nagarajan et al. 2016). These materials have specific physical and chemical properties but the key limitation on the utilization of these materials is their higher cost (Bogoeva-Gaceva et al. 2007).

Polyvinyl alcohol, polyvinyl acetate, polylactic acid and polycaprolactone are the some examples for biodegradable polymer resins (Netravali and Chabba 2003). In the present study PLA (Polylactic acid) is used as polymer resin. PLA is a fully bio-based polymer extracted from agricultural based materials (corn, potato, sugar beet etc.) by fermentative processes (Orue et al. 2018b). PLA polymer has excellent barrier capacity, good mechanical properties, and can be easily processed for different applications. Despite of these features, it has limitations such as high-brittleness, slow crystallization rate, water-sensitivity, low heat deflection temperatures, higher cost and low impact strength (Bajpai et al. 2013; Huerta-cardoso et al. 2020; Kumar et al. 2010). PLA is already been used for the packaging applications such as cups, bowls, bags and jars for beverages, salads, potato chips and yogurts (Aznar et al. 2019). However, the various research studies showed that PLA can also be used as polymer matrix to incorporate the fibres in the composites. Products made of natural fibre filled PLA composites are already available in the market. The biodegradable urns are produced from Jacob Winter (Satzung, Germany) using flax and PLA by hot press molding method. NEC Corporation (Tokyo, Japan) and UNITIKA Ltd. (Osaka, Japan) jointly manufactured bio-plastic mobile phone (FOMA N701iECO) casing using kenaf fibres and PLA matrix. Also, biodegradable composites made of kenaf fibre and PLA are used in automobile industry as spare tire cover in Toyota RAUM (Graupner et al. 2009; Koronis et al. 2016). To reduce the cost and improve material properties for commercial applications, researchers are trying to manufacture natural fibre reinforced biodegradable PLA composites in different forms.

1.5 Literature review

A substantial quantity of research has been conducted to characterise the mechanical properties of the natural fibre reinforced composites fabricated using different manufacturing methods such as injection, compression and extrusion molding methods. From the experimental investigations, various researchers are demonstrated that the influence of reinforcement of fibre architecture (short-random fibre, unidirectional-woven and bidirectional-woven) and variation in fibre weight fraction can be utilised effectively to improve the mechanical properties of the natural fibre filled composites for different possible commercial and industrial applications.

1.5.1 Braided fibre composites

Braiding is a process in which three or more yarns are interlaced along the length of the axis of the thread, to obtain a thick and strong thread. It is a cost effective and versatile process to make the yarn structures, which are effectively used in wide-range of applications such as ropes, insulation material in sports, recreation activities, composites and biomedical uses (Rawal et al. 2015). Khondker *et al.* (2006) produced microbraided yarn, in which jute yarn is used as core and polymer matrix fibres (PLA and homo-polypropylene) are braided around the jute yarn through the tubular braiding process. They reported that mechanical properties of tubular braided yarn composites are enhanced by improved wettability of matrix over fibre bundles, interfacial bonding and uniform distribution of fibre-matrix. Rajesh and Pitchaimani (2016) manufactured flat braided yarn interlaced basket type woven fabric reinforced composites using polyester resin as matrix and reported that storage modulus of the braided yarn fabric composites is high compared to knitted and conventional woven fabric reinforced composites. Rajesh and Pitchaimani (2017) also reported that the braided yarn fabric composites have superior properties compared to conventional woven fabric and short fibre reinforced composites.

1.5.2 Natural fibre PLA composites

Numerous studies are conducted on the natural fibre filled PLA composites, to investigate the impact of the reinforcement on the biodegradability, mechanical

properties, temperature and water resistances of the composites. Researchers used different types of natural fibres, varied fibre content, different types of the reinforcement (such as short-random fibre, non-woven mat and woven fabrics) and also treatment of fibre surface to analyse the same. Fabrication of natural fibre reinforced PLA composites is done by using injection molding, compression molding, extrusion and fused deposition molding (3D printing) (Bourmaud et al. 2020; Du et al. 2014; Duigou et al. 2019).

Tensile and Charpy impact tests are carried out on the injection molded flax/PLA and Cordenka/PLA composites by varying the fibre content (Bax and Müssig 2008). Cordenka reinforced PLA composites showed higher tensile strength and impact strength at 30% fibre mass, while the flax/PLA composites showed higher Young's modulus. Kumar et al. (2010) fabricated the woven flax reinforced and montmorillonite clay (MMT) added PLA bio-composites. They observed that the addition of MMT enhanced the modulus and water resistance property of the composites. Ben et al. (2012) prepared kenaf fabric (unidirectional and cross-ply) reinforced PLA composites and found that the unidirectional composites have higher strength compared to neat PLA and cross-ply composites. Benzoyl Peroxide treated and un-treated banana/sisal fibre hybrid PLA composites are prepared by Asaithambi et al. (2014) and they concluded that properties of the treated hybrid composites are higher than untreated hybrid composites and virgin PLA. Arao et al. (2015) used twin-screw-extruder to compound PLA and jute pellets using long and short jute fibres and then prepared the composites using injection molding technique. Tensile results showed that composites made from short jute fibre have better strength and modulus compared to long jute fibre reinforced composites.

Thermo-mechanical characteristics of the novel *manicaria saccifera* palm fabric reinforced PLA composites are studied by Porras et al. (2016). They developed composites using compression molding technique and characterised for thermal (TGA), tensile, flexural and Izod impact properties. The *manicaria saccifera* fabric reinforced PLA composite showed lower thermal degradation temperature and improved mechanical properties compared to neat PLA. Pickering and Efendy (2016) done an experimental investigation on PLA strengthened by discontinuous alkali

treated natural fibre (harakeke and hemp) mats produced by dynamic sheet former (DSF) method. These shown that the mechanical characteristics of these natural fibre mat composites are much higher than the virgin PLA. Chaitanya and Singh (2017) prepared short and long sisal fibre strengthened PLA composites using two different manufacturing methods such as direct-injection-molding (DIM) method and extrusion-injection-molding (EIM) method. Short sisal fibre reinforced PLA composites exhibited significant enhancement in the tensile and flexural strengths compared to long sisal fibre reinforced PLA composites manufactured using both the methods. Long-fibre reinforced PLA composites prepared using DIM process showed highest impact strength. They also showed that the composites manufactured from DIM process are having superior properties compared to composites prepared using EIM process. Also, hybrid composites prepared by incorporating sisal and hemp in PLA through injection molding showed the significant enhancement in the properties (Pappu et al. 2019).

1.5.3 Thermal deflection

During the service the thin walled structures are exposed to heat as a consequence thermal stress develop whenever there is a restriction to thermal expansion. The thermal stress will alter the structure/member stiffness, which intern changes the dynamic features of the structure.

George et al. (2016) studied experimental and theoretical deflection behaviour of the non-uniformly heated aluminium beam. Their results revealed that for the non-uniformly heated beam the deflection behaviour is totally different from uniformly heated beam and also concluded that the critical temperature of the beam significantly vary with respect to the position of the heating source. George et al. (2017) analysed the functionally graded CNT (carbon nanotube) strengthened composite plates are exposed to non-uniform temperature profile for the deflection and free vibration characteristics with the help of FE (finite element) method. They showed that, type of CNT dispersion pattern and type of temperature field are two factors which have significant impact on buckling strength of the polymer composites. Thermal deflection study on non-uniformly heated aluminium cylindrical panel indicates that

thermal deflection is affected by location of heat source (Bhagat and Jeyaraj 2018). Functionally graded graphene filled composite (FG-GRC) cylindrical panels are investigated for thermal deflection behaviour analysis is carried out by Bhagat et al. (2018). They found that thermal deflection strength is significantly influenced by the GRC grading pattern and geometrical parameters (thickness and curvature ratio) of the cylindrical panel. Functionally graded ceramic metal nano-plate is analysed by Bouazza et al. (2018) considering the small scale effect.

Waddar et al. (2018b) conducted thermal deflection test on fly ash cenosphere-epoxy syntactic foam composites with three types of non-uniform heating cases. The temperature versus deflection curves showed snap-through deflection behaviour of syntactic foams and the deflection of syntactic foam varies with cenosphere content in the composite. Bouazza et al. (2019) performed thermal deflection study on laminated composite beams with the help of hyperbolic refined shear deformation theory. Thermal deflection behaviour study is carried out on syntactic foam sandwich composites manufactured from fly ash cenosphere reinforced epoxy syntactic foam core and sisal fabric reinforced epoxy skin. Results revealed that sandwich beams undergo snap-through deflection due to viscoelastic behaviour of the syntactic foam sandwich composites (Waddar et al. 2020). Thermal deflection behaviour of hybrid sisal/glass epoxy composites under non-uniform heating is analysed by Gilorkar et al. (2020). They reported that the pure sisal composites have high deflection compared to hybrid sisal/glass composites. However, the angle ply composites showed lower deflection than cross ply composites.

1.5.4 Water absorption

Natural fibres are hydrophilic in nature and reinforcement of these fibres limits their susceptibility to water absorption. Due to this the fibre swelling occurs which influences the mechanical and dimensional characteristics of the composites (Muñoz and García-Manrique 2015). Shanks et al. (2005) fabricated the PLA composites by reinforcing acetone washed polymerization treated flax fibres. It is found that the water absorption resistance property and storage moduli of the polymerization treated with acetone washed flax fibres are higher than unwashed flax fibres. Duigou *et al.*

(2009) also conducted sea water ageing studies on flax/PLLA composites at different temperature (20 and 40° C). At the 40° C of sea water temperature the tensile strength and stiffness of the flax/PLLA composites are reduced due to hydrolysis of the matrix, structural changes in the composites, degradation of fibre-matrix interface, fibre swelling and fibre degradation. Siengchin et al. (2013) conducted water absorption study on woven flax PLA composites fabricated using hot press method. It is found that the water absorption of flax/PLA is high and it is reduced after the incorporation of alumina particles. PLA/flax commingled yarns and PLA/flax sandwich structures are manufactured by thermoplastic pultrusion (Linganiso et al. 2014) by keeping the non-woven material as core and commingled yarn as outer layers. They reported that water uptake of non-woven composites is much higher than that of commingled composites. Duigou et al. (2015) studied the effect of water absorption on stiffness of the PLLA/Flax composites. Unidirectional flax-PLLA composites have shown 40% reduction in stiffness after the immersion for a two months period. The water absorption study is performed on non-oxidized TiO₂ coated and oxidized TiO₂ coated unidirectional flax fabric reinforced PLA composites (Foruzanmehr et al. 2016). It is noticed that the TiO₂ grafting reduced the moisture uptake of the fibre and is 18% lower than the as received one.

1.5.5 Biodegradability

Natural fibre strengthened PLA composites gets degraded easily due to the interaction of the natural soil, compost, active sludge, lake, and marine environment. Researchers used natural fibres and starch in the PLA matrix and enhanced the strength of the composite without compromising the biodegradation (Macedo and Rosa 2016). Ochi (2008) prepared unidirectional green composites with kenaf fibre and PLA (emulsion type) resin. The biodegradability of a prepared composite is carried out in a garbage processing machine, and observed 38% of weight loss after four weeks. A comparative study on biodegradability has been carried out by Yussuf et al. (2010) on PLA/kenaf and PLA/rice husk composites for 90 days in normal garden soil. It is concluded that reinforcement of kenaf fibre with PLA showed higher biodegradability compared to the rice husk reinforcement. Kumar and Yakubu (2010) prepared composites by reinforcing woven and nonwoven flax fibre with PLA using hot-press

compression and observed 5-25% of weight loss after 90 days of the farmland soil incubation test. Lv et al. (2017) mixed starch and wood flour with PLA and conducted the biodegradation experiment in the outdoor soil environment. They found that the addition of starch in the PLA increased the degradation rate than the wood flour, as it acts as a biological fuel. Rajesh et al. (2019) investigated the biodegradable behaviour of short sisal fibre reinforced PLA composite by analysing the weight reduction, mechanical strength, and surface roughness before and after soil incubation test. They found that PLA composites kept in soil for 90 days shows higher weight loss and significant reduction in the tensile strength. They reported that PLA composite could degrade at a reasonable speed in the soil environment.

1.5.6 Wear study

During the relative movement of solid surfaces, wear and friction are the two significant parameters in the field of tribology used to characterise energy dissipation and material deterioration. Fibre reinforcement is one way of improving the tribological behaviour of a polymer. Fibre strengthened composites are as of now being used in a variety of applications, in which the common mode of failure is abrasive wear (Bijwe et al. 2007). Comprehensive research is being carried out on polymers reinforced with synthetic fibre to analyse the tribology characteristics. Literature also indicates that there has been enough work carried out on natural fibres (nettle, *grewia optiva*, sisal, kenaf, *lantana camara*, rice husk char, oil palm, coir) reinforced synthetic polymer (polypropylene, polyurethane, epoxy, polyester etc.) composites to study friction and wear characteristics of the composites for tribology application (Bajpai et al. 2012; Deo and Acharya 2009; Narish et al. 2010; Samantrai et al. 2014; Yousif 2008; Yousif and El-Tayeb 2015). Composites strengthened by fabric have higher thermal and mechanical stability, higher strength, stiffness and high fatigue. Similarly, they are also used in components such as seals, cams and bearings which require better tribological properties (Guo et al. 2010).

Goriparthi et al. (2012) studied frictional and wear characteristics of the chemically surface-modified jute fibre-filled PLA composites. Surface treatment of the fibre improved the interfacial bonding and further enhanced the tribological properties.

Bajpai et al. (2013) prepared laminated bio-composites using grewia optiva, nettle and sisal fibre mats reinforced into PLA polymer and performed tribological studies under dry contact condition. The results showed that natural fibre loading enhanced wear performance of PLA and the coefficient of friction value of fibre reinforced composites is less compared to PLA. It is also noticed that, the wear performance is influenced by the variation of the load applied than the sliding speed.

1.5.7 Fracture toughness study

Fracture toughness is a material's ability to prevent or resist the crack propagation. Several research studies are performed to analyse the fracture toughness of the bio-composites. For instance, Alvarez et al. (2003) produced bio-composites by reinforcing alkali treated sisal fibres with biodegradable thermoplastic matrix. Fracture test results of these materials showed that the critical strain energy release rate (G_{IC}) is enhanced by treated fibres compared to untreated fibres. Alvarez et al. (2006) also conducted fracture toughness test on SENB bio-composite specimens prepared using short sisal fibre reinforced starch-based matrix with injection molding process. The findings revealed that the fracture toughness of the composites increased due to the fibre reinforcement.

The accelerated ageing effect on the alkali-treated and untreated long hemp fibre strengthened PLA composites is carried out by Islam et al. (2010a) for four different interval of time using UV irradiation and water spray at 50° C. They found that the plane-strain fracture toughness (K_{IC}) of the SENB specimens enhanced due to alkali treatment of the fibre. Islam et al. (2010b) also studied effect of hygrothermal ageing on alkali-treated and untreated woven hemp PLA composites by immersing the samples in distilled water at 50° C for 3 months. They found that fracture toughness of the samples decreases with increase in hygrothermal ageing temperature. Sawpan et al. (2011) investigated mode-I plane-strain fracture toughness of treated aligned long and short random hemp fibres filled PLA composites with different fibre weight fractions. They found that the strain energy release rate and fracture toughness are decreased with increase in fibre weight percentage. Pickering et al. (2011) investigated the effect of alkali treatment, crystallinity and loading rate on fracture

toughness. They performed fracture toughness studies on SENB specimens prepared from random hemp fibre strengthened PLA bio-composites. They reported that K_{IC} values decreased with increase in loading rate, fibre content and crystallinity.

1.5.8 Buckling under axial compressive load

Composite structures have outstanding engineering/mechanical properties and most likely to play a significant role in the design of various structural applications such as marine, automobile, aircrafts and building industries. These laminated composites have ability to replace conventional metallic structures. Fracture, fatigue and buckling are the some important structural failure behaviours of composites. Buckling is the special kind of failure mode of structural members subjected to axial compression. In this failure mode, structure fails suddenly under axial-compressive loads, at this point the failure compressive strength is lower than the ultimate compressive strength at which the member is capable to sustain (Bozkurt et al. 2019; Rajesh and Pitchaimani 2017c).

The anisotropic laminated composite beams buckling and post buckling under axial compressive load analysis is carried out by Li and Qiao (2015) using von Karman-type kinematic nonlinearity and shear deformation theory. Rajesh and Pitchaimani (2017c) performed experimental study to investigate buckling and free vibration characteristics of jute fabric filled polyester composite beam under axial compressive loads. They noticed buckling strength of the composite is significantly influenced by weaving structure of the fabric and also they reported increase in compressive load decreases the natural frequency of the composite beam. Nano-clay incorporated S-glass/epoxy composites lateral and axial buckling characteristics are investigated by Bozkurt et al. (2019) with varying fibre orientation and nano-clay content. The test results revealed that the addition of nano-clay of 1 wt.% enhanced the critical buckling load and further increase in nano-clay content reduced the critical buckling load. Further, angle of orientation of fibre (0/90°) showed highest buckling load compared to other direction of loading. Rezaiee-Pajand et al. (2019) used Timoshenko beam theory to analyse the carbon nanotube reinforced composite beam under axial compressive loads. Effect of volume fraction of fibre, fibre orientation angles, depth

of the crack, location of the crack on post buckling property of fibre reinforced composites subjected to compressive load is investigated by Akbas (2019) numerically using finite element method. Results revealed that the crack depth, crack location, volume fraction of fibre and fibre orientation angle have significant effect on the post buckling behaviour of the composites. Waddar et al. (2019) studied the syntactic foam core and natural (sisal) fibre fabric composite facing sandwich composite beam buckling and vibration properties under compressive loads. Study reveals that the critical-buckling load is enhanced with the cenosphere content and vibration frequencies are reduced with respect to increase in axial-compressive load. Ozbek (2021) carried out an experimental study on silica nano-particle added kevlar/epoxy composites to determine the mechanical buckling properties and it is reported that 1.5 wt.% of nano-silica added composite has highest critical-buckling load and buckling load of the composites reduced further increase in nano-silica content due to decreased bonding between nano-silica and epoxy.

1.6 Closure

Most important advantages of the natural fibre reinforced bio-composites are biodegradability, renewability and environment friendliness are attracted the researchers to develop the composites with improved mechanical properties. Literature study shows that the reinforcement of natural fibres enhances the properties of the polymer matrix irrespective of type of fibre used. Most of the investigations are carried out on the short and random fibre reinforced composites. Study also shows that the biodegradability, water absorption, mechanical and thermal characteristics of the natural fibre composites can be improved by surface modification. Researchers also demonstrated that the architecture of the reinforcement such as fibre orientation (short, long, unidirectional and random distribution), yarn, non-woven mat and woven fabric influences the properties of the composites.

1.7 Motivation

Natural fibre reinforced biodegradable composites have low density, eco-friendly, less health hazards compared to synthetic fibre strengthened composites. These composites can replace the synthetic fibre strengthened composites where the strength

of the material is least considered such as in car dash board, interiors and seat backs. Textile fabric reinforced composites are gaining great attention from past two decades. Composites fabricated from braided and woven fabric reinforcements have found potential uses in the marine, automobile and aerospace industries. This is due to their superior out of plane stiffness, toughness and strength characteristics, as well as their low manufacturing cost and simple to handle in production.

1.8 Objectives

From the literature it is observed that, least work has been carried out on the natural fibre 3D braided yarn fabric reinforced bio-composites. These composites might be used as the alternatives for the synthetic fibre strengthened polymer composites in certain extent. So, it is necessary to find out the mechanical properties of natural fibre braided composites. Main objective of the proposed research work is,

- To characterise mechanical properties of natural fibre 3D braided yarn and its fabric.
- To characterise mechanical properties such as tensile, flexural, impact and fracture toughness of natural fibre 3D braided yarn fabric NFBF/PLA biodegradable composites.
- To perform thermal deflection study of NFBF/PLA composites through experiments.
- To characterise the tribological behaviour of NFBF/PLA composites.
- To study stability and free vibration behaviour of NFBF/PLA composite beams under axial compression.

1.9 Outline of the thesis

In the present work, the systematic investigation is carried out with regard to the above objectives is discussed and the important outcomes are presented as conclusions. The following sections give the brief explanation of thesis structure.

Chapter 1 provides the required information of the research on natural fibre reinforced bio-composites and their advantages and disadvantages over synthetic fibre reinforced

composites. Also it deals with the literature survey, objective and the scope for the research work.

Chapter 2 deals with the materials used, preparation of braided yarn and fabric and processes used for fabrication of bio-composites. Also, it explains the methodology of different tests carried out on the proposed composite materials.

Chapter 3 focuses on the results and discussions related to braided yarn and fabric characterization, change in mechanical properties of the composites for different loading directions (warp and weft) of the surface plies of the composite and fibre weight percentage.

Chapter 4 presents the flammability, crystallinity, melting temperature, heat deflection temperature and thermal stability of the composites. Also, it deals with thermal deflection behaviour of natural fibre braided yarn woven fabric reinforced PLA composites under non-uniform heating conditions.

Chapter 5 presents the effect of water absorption and thickness swelling on flexural characteristics of the composites. The characteristics of composites for biodegradation are discussed, as well as the effect of biodegradation on the tensile strength and modulus of the composites.

Chapter 6 discussed tribological behaviour of natural fibre braided yarn woven fabric composites under various applied load and velocity conditions. The plane strain fracture toughness of the composites is also discussed.

Chapter 7 presents studies carried out on buckling and free vibration behaviour of composites subjected to axial compressive load. Conclusions and future scope of the work are presented at the end.

2 MATERIALS AND METHODS

2.1 Materials

In the present work polylactic acid (PLA) is used as matrix material and natural fibre extracted from flax is used as the reinforcement in woven form. PLA is selected because it has good strength, easy processability and cleanliness. The fibre was selected on the basis of availability, cost and strength. The flax fibre is easily available in India, also the cost of the flax fibre is very less compared to ramie and hemp fibres. Review study carried out by Pickering et al. (2016) indicates that the flax fibre has good strength compared to the other natural fibres. The details of the constituent materials are discussed in the following sections.

2.2 PLA resin

Among the biodegradable polymers, in particular, poly lactic acid (PLA) is being used in several commercial applications. PLA is a thermoplastic material produced from lactic acid monomer. The lactic acid monomer is obtained from fermentation of corn, potato, sugar beet and sugar cane (Nam et al. 2012). PLA is one such type of polymer which is produced from the agriculture products and it is biodegradable (Fazita et al. 2014). PLA polymer has several advantages such as good mechanical properties, thermal plasticity, bio-compatibility, easy process ability, good aesthetics and strength. PLA has desirable mechanical properties including greater strength and stiffness compared to conventional plastics such as polystyrene, polyethylene and polypropylene (Mamun et al. 2013). This polymer material has some disadvantages such as poor toughness, brittleness and high production cost (Fazita et al. 2014; Huda et al. 2006; Porras and Maranon 2012). Enhancement of mechanical properties of PLA can be achieved through the reinforcement of natural fibres, such as kenaf, cellulose, hemp and abaca fibres (Siengchin et al. 2013).

Nature works 3052D bio-polymer PLA is purchased in the pellet form from Nature Tech India Ltd. Chennai, Tamil Nadu, India. Properties of the PLA received from the supplier are listed in Table 2.1. Dichloromethane (DCM) is used as a solvent to

dissolve the PLA pellets, and it is supplied by Sri Durga Laboratory Equipment Suppliers, Mangalore, India.

Table 2.1 Properties of PLA polymer *

Properties	Test method	Value
Specific gravity	D792	1.24
MFR, g/10 min (210°C, 2.16kg)	D1238	14
Relative viscosity		3.3
Glass transition temperature (°C)	D3418	55-60
Crystalline Melt temperature (°C)	D3418	145-160

* As provided by the supplier

2.3 Flax fibre

Flax belongs to Linaceae family. It is being used over 5000 years and it has 230 different species. It grows up to 0.5 to 1.25 m height with 16 to 32 mm diameter of stem and it is an annual crop (Chaitanya and Singh 2017), Figure 2.1 shows image of the typical flax plants. The literature survey shows that the flax fibre has high density and tensile strength and moderate Young's modulus comparing to other natural fibres. Bleached 25 count flax yarn (Figure 2.2) is purchased from The Matrix Enterprises Tiruppur, Tamil Nadu, India. The chemical compositions of flax fibre are presented in Table 2.2.



Figure 2.1 Flax plants (Katherine 2012)



Figure 2.2 Simply twisted yarn

Table 2.2 Chemical components of flax fibres (Yan et al. 2014)

Chemical component	%
Cellulose	64.1-75
Hemicellulose	16.7-20.6
Lignin	2-2.5
Pectin	1.8-2.2
wax	1.5-1.7
Moisture content	8-12

2.4 Preparation of braided yarn and woven fabric

In this study, flax fabric woven using 3D braided yarns is used as reinforcement to improve the mechanical properties of the PLA composites. Initially, flax simply twisted yarns are altered into braided yarn using a solid braiding method, as shown in Figure 2.3.

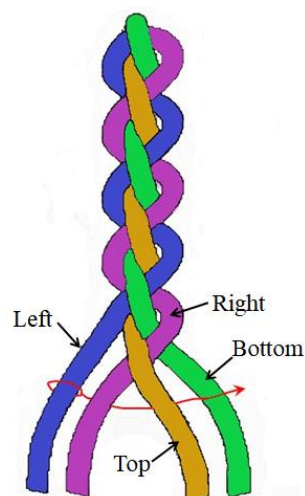


Figure 2.3 Braiding principle with four simply twisted yarns (Poole 2020)

Figure 2.3 represents the principle of making a braided yarn using four strands of simply twisted yarns. Initially, the right yarn goes left moving below the top yarn. Then left yarn moves right passing below the top yarn and right yarn and above the bottom yarn (red line arrow in Figure 2.3). The top yarn moves downwards and the bottom yarn moves upwards. Like this the first interlacement is completed. This procedure is continued up to the required length. Finally, the resulting product is a solid type of braided yarn. The architecture of the prepared 3D braided yarn can be seen properly from the longitudinal and cross-sectional view of the braided yarn in Figure 2.4 and its average diameter is measured as 0.52 mm. From Figure 2.4c, one can clearly observe that four strands of simply twisted yarn used to make the braided yarn.

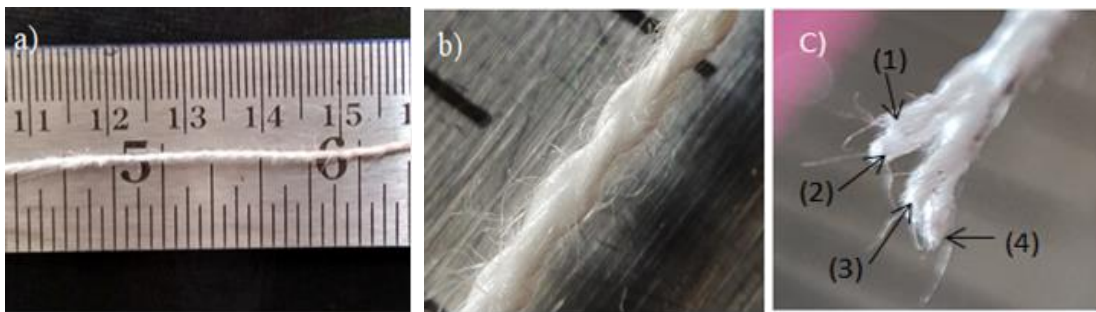


Figure 2.4 Photographs of a) 3D braided yarn, b) 3D braided yarn closer view, c) showing four simply twisted strands of yarns in braided yarn

Followed by this fabric woven with plain architecture is prepared by interlacing the braided yarn in warp and weft directions with the help of a handloom weaving machine. Rajesh and Pitchaimani (2017b) reported that reinforcement of fabric woven with plain and basket weaving pattern enhances mechanical properties of the composites. Hence, in this study fabric with plain weave architecture is used as reinforcement (Figure 2.5). Thickness of the prepared natural fibre 3D braided yarn fabric (NFBF) is measured as 0.9 mm to 1 mm.

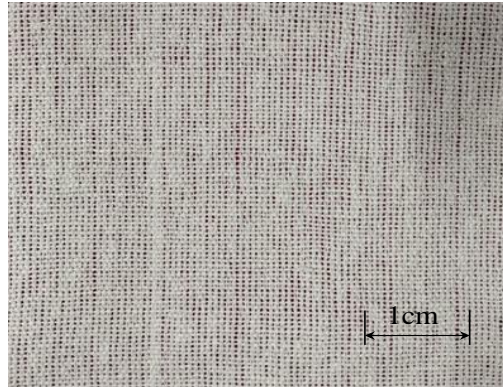


Figure 2.5 Flax braided yarn plain woven fabric

2.5 Geometrical and mechanical characterization of braided yarn and fabric

Prepared 3D braided yarn is characterised for its density, yarn number and tensile properties. Density test of yarn is carried out according to ASTM D3800-16. Density test is conducted on ten flax yarn specimens of length 1 m with the help of an analytical balance machine (manufactured by Contech Instruments Ltd. Navi Mumbai, India). Yarn number is calculated as outlined in ASTM D1059-17. For this test ten specimens of 3D braided yarns of length 1 m are cut. Then weights of these specimens are measured in a digital electronic weighing balance with an accuracy of four decimal places. Equation used to calculate the yarn number is as follows;

$$Yarn\ number = \frac{G \times K}{M} \quad (2.1)$$

where, G is weight of the yarn, M is length of the yarn and K is the constant ($K= 1000$ for Tex and $K=9000$ for Denier). Tensile properties of braided yarn are obtained according to ASTM D2256-10 using Tinius Olsen 75KS universal testing machine (UTM) with a cross head speed of 5 mm/min. Yarn specimens of gauge length 50 mm are used for testing and cardboard rectangles of $50 \times 25\text{ mm}^2$ are used to secure the yarn in tensile test machine jaws as shown in Figure 2.6b.

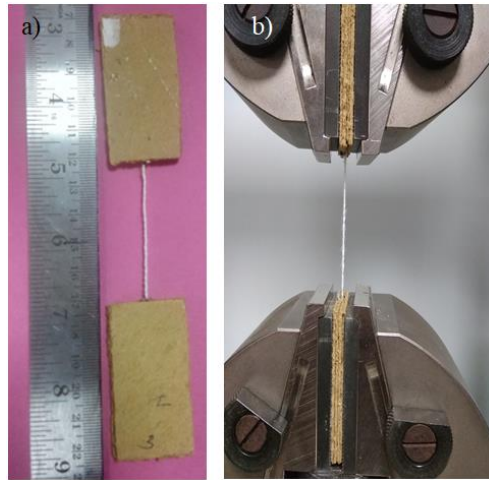


Figure 2.6 a) Braided yarn tensile test specimen and b) sample kept in UTM for the tensile test.

3D braided plain woven fabric is characterised for its yarn count, yarn crimp, fabric GSM (gram per square meter), moisture content and tensile properties. Yarn counts of the fabric along the warp and weft directions are measured according to ASTM D3775-17. Square area of 75 mm × 75 mm is marked on the fabric and total number of yarns along warp and weft directions present in the marked area is counted. This has been repeated for five different places of the fabric and average value is reported along with the co-efficient of variation (CV). The number of yarns per centimetre is calculated using Equation (2.2).

$$Yarn\ count = \frac{Counts}{B} \text{ (yarns/cm)} \quad (2.2)$$

In Equation 2.2, *counts* is number of yarns counted and *B* is width of fabric in cm. Crimp test for the 3D braided plain woven fabric braided yarn is done according to ASTM D3883-04. Yarn crimp is a relation between yarn length in the fabric (*F*) and yarn length after its removal from the fabric (*Y*). Yarn crimp is calculated by using Equation (2.3).

$$Yarn\ Crimp\ C = \frac{Y - F}{F} \times 100 \quad (2.3)$$

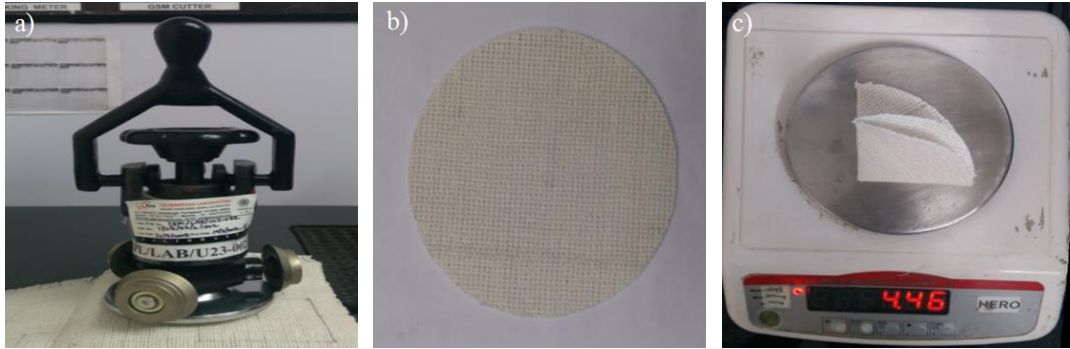


Figure 2.7 a) GSM cutter b) specimen for GSM calculation c) GSM scale

GSM of the 3D braided yarn fabric is calculated based on ASTM D3776-09. A circular fabric specimen of diameter 112.9 mm is cut by a GSM cutter as shown in Figure 2.7(a & b). Three specimens are prepared and GSM of the fabric is evaluated by weighing in a GSM scale manufactured by Hero Magic Inc. Delhi, India. Moisture content study of the woven fabric is conducted as outlined in ASTM D2495-07. Equation (2.4) is used to measure the amount of moisture in the fabric.

$$\text{Moisture content (\%)} = \frac{W_i - W_d}{W_i} \times 100 \quad (2.4)$$

where, W_i is initial weight of specimen, W_d is weight of the specimen after the oven drying. Tensile behaviour of 3D braided plain woven fabric is analysed based on ASTM D5035-11. Fabric specimen with a gauge length of 50 mm is tested in a UTM with 5 mm/min cross head speed. Characterization of the braided yarn fabrics is done in both warp and weft directions (five replicates of each). The warp and weft direction fabric tensile specimens are shown in Figure 2.8.

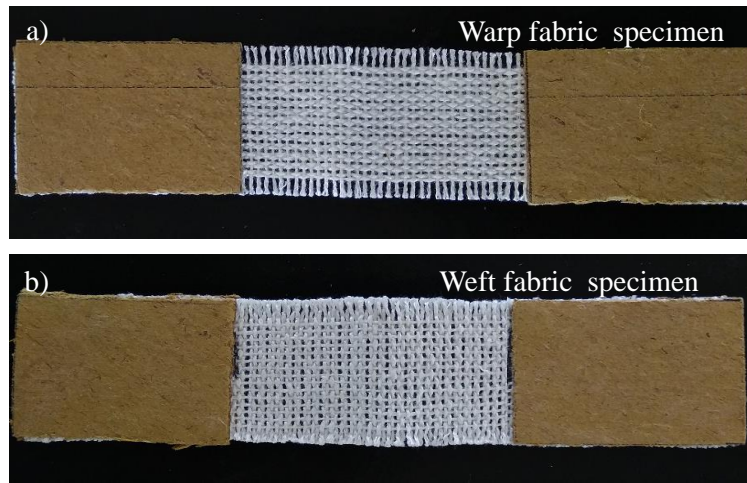


Figure 2.8 Braided yarn woven fabric tensile test specimens for a) warp direction loading, b) weft direction loading

2.6 Composite laminate preparation

In present work, film stacking and compression molding processes are used to fabricate the composite laminates. Initially the neat PLA and NFBF/PLA thin sheets are prepared by solution casting method. Literature study shows that the solution casting improves the fibre impregnation and wettability in the polymer and avoids the fibre strength reduction due to thermal deterioration (Goriparthi et al. 2012; Kumar et al. 2010). In this study, DCM is selected as solvent to prepare PLA solution for solution casting (Chalid and Prabowo 2015; Kowalczyk et al. 2011). For this, the solution of PLA and DCM is prepared by dissolving calculated amount of PLA pellets in 600 ml of DCM using a mechanical stirrer. The pure PLA sheet is prepared by pouring this solution in a square aluminium tray of dimension 200 mm × 200 mm × 10 mm as shown in Figure 2.9. Similarly, NFBF/PLA sheet is produced by pouring a small amount of solution in another aluminium tray and on this solution 200 mm × 200 mm fabric is laid using hand-lay-up method. On this fabric another small quantity of solution is poured and these two trays are kept for 48 hours for the evaporation of DCM in room temperature.

Followed by this, the prepared PLA and NFBF/PLA sheets are arranged alternatively (such as PLA-NFBF/PLA-PLA) and placed between two aluminium plates. Composite laminates with 3 mm thickness are fabricated by placing 3 mm thick

spacer at the centre. Releasing agent (silicone grease) is applied on both the aluminium plates and spacer for easy removal of composite laminate. Then the compression molding is carried out in hydraulic hot-press machine. Pressure is set to 5 MPa and maintained for 15 minutes at 180° C. Before de-molding composites are cooled down to 40° C. After de-molding, specimens are cut from the composites according to different experimental standards. Percentage weight of the fibre (W_F) in the composites is calculated using Equation (2.5).

$$W_F = \frac{w_{ff}}{w_{mm} + w_{ff}} \times 100 \quad (2.5)$$

where, w_{ff} is weight of flax woven fabric and w_{mm} is weight of matrix material (Khan et al. 2016).

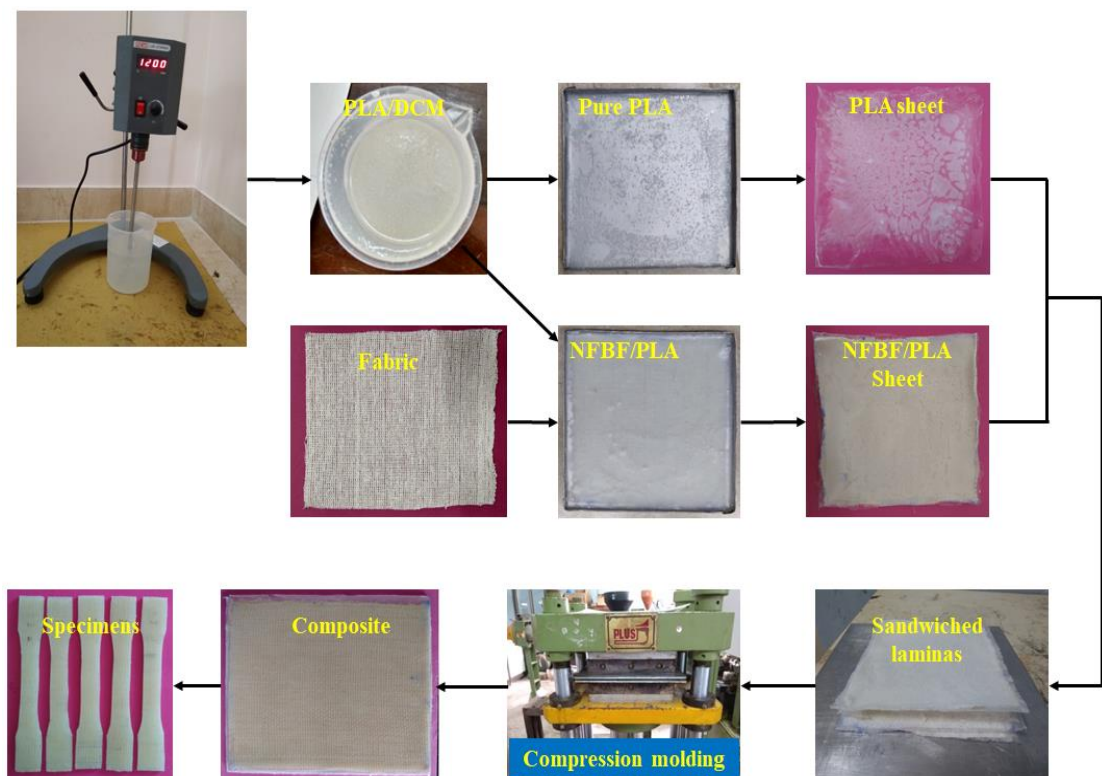


Figure 2.9. Flow-chart representing composite fabrication process

In this work composites with 3 different thicknesses are prepared such as 3 mm, 1.5 mm and 4 mm respectively. Composite specimens with 3 mm are considered for the characterization of mechanical properties such as tensile, flexural, impact and

buckling properties. For Biodegradability test 1.5 mm (Morales et al. 2017) composites are considered and for wear and fracture toughness study 4 mm thick composite plates are used. In this study, natural fibre braided yarn woven fabric (NFBF) reinforced composites are represented as 'NFBFxx' and 'xx' indicates the fabric weight percentage. The neat PLA polymer samples are represented as NFBF0.

2.7 Mechanical characterization of composites

2.7.1 Tensile, flexural, impact and interlaminar shear strength (ILSS) tests

Characterization of tensile and flexural properties of NFBF laminated composites is done in room temperature on the universal testing machine (H75KS, 50 KN load cell capacity, Tinius Olsen make, UK). Tensile test is performed as outlined in ASTM D638-14. The dumbbell shaped test specimens are prepared with the dimensions of gauge length 50 mm, width 13 mm at narrow section, length between grips 115 mm, width 19 mm and overall length of 165 mm. This test is conducted on five specimens with the operating speed of 5 mm/min and average value is presented with standard deviation. Flexural strength of the composites is measured according to ASTM D790-17. The specimen having dimensions of 127 mm x 12.7 mm x 3 mm is considered and cross head speed used is maintained as 1.3 mm/min. The loading of specimen is done on specimen in three-point-bending with span to thickness ratio of 16:1. Impact strength evaluation is done on Zwick/Roell HIT50P impact testing machine (manufactured by Zwick Roell Testing Machines Pvt. Ltd. Chennai, India) following ASTM D256-10. This study considered an un-notched specimen of dimensions 64 mm x 12.7 mm x 3 mm and it is conducted on five specimens. Tensile, flexural and impact experiments are performed in warp and weft directions of the composites. For this the specimens are cut such that the warp specimen axis is parallel to the warp yarns of the surface plies. Similarly weft specimens are cut by maintaining specimen axis parallel to the weft yarns of the surface plies.

SBS (short beam shear) test is carried out to determine the interlaminar shear strength (ILSS) of the pure PLA and braided flax PLA composites in accordance with ASTM D2344-16. For this test, specimens of dimensions 20 mm × 6.5 mm × 3 mm are used with a span to-depth ratio of 4:1. This test is performed in a UTM (Zwick/Roell Z020)

under three point bending test condition with the upper head velocity of 1 mm/min. To evaluate the interlaminar shear strength (ILSS) of the composites Equation (2.6) is used.

$$ILSS = 0.75 \times \frac{P_m}{b \times h} \quad (2.6)$$

where, *ILSS* is the interlaminar shear strength (*MPa*), *P_m* represents the maximum load (*N*), *b* represents the measured specimen width (*mm*) and *h* is the measured specimen thickness (*mm*).

2.7.2 SEM Analysis

Scanning electron microscope (SEM) image analysis is performed on Jeol JSM-6380LA scanning electron microscope to investigate the composite surface appearance of the fractured specimens after the mechanical tests. Gold sputtering is done on the composite specimen surface to avoid charging.

2.8 Thermal properties

Flammability, DSC, TGA and thermal deflection experiments are performed to characterise burning rate, glass transition temperature, thermal stability and deflection of PLA and its composites. Brief explanations about these tests are discussed in the following sections.

2.8.1 Flammability

Flammability test of the composite specimen is carried out by a horizontal burning test method as per ASTM D635-18. In this study, the test specimen is held horizontally at one end and at the other end the gas fuelled flame is applied to light as shown in Figure 2.10. Time to reach the flame from 25 mm reference point to 100 mm from reference point is measured and presented.

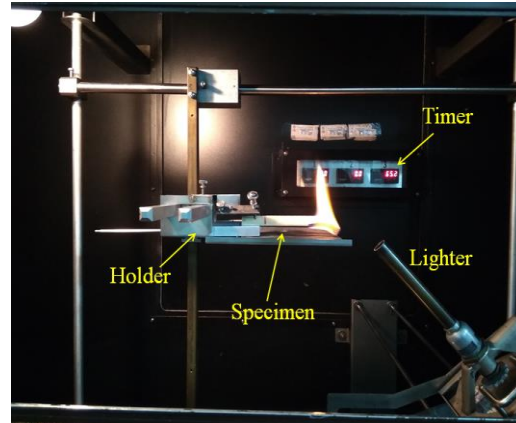


Figure 2.10 Flammability test set up

2.8.2 Differential scanning calorimetry (DSC) analysis

DSC study is carried out on a DSC 404F1, Pegasus, NETZSCH, German make, equipment under the nitrogen environment. The pure PLA and NFBBF/PLA composites are first heated from 20° C to 220° C at a rate of 10° C/min and then the samples are cooled down to 20° C. From 20° C the same samples are again heated up to 220° C under the same heating rate. From the first and second heating scans glass transition temperature (T_g), cold crystallization temperature (T_c), melting temperature (T_m) and enthalpy for melting (ΔH_m) are determined. The percentage crystallinity of the PLA and NFBBF/PLA composites are evaluated utilizing the following Equation:

$$X_c (\% \text{ crystallinity}) = \frac{\Delta H_m}{\Delta H_{m0}(1 - m_f)} \times 100 \quad (2.7)$$

where, $\Delta H_{m0} = 93 \text{ J/g}$ is the 100% crystalline PLA sample enthalpy of melting and $(1 - m_f)$ is the PLA weight fraction in the sample (Islam et al. 2010c; Yang et al. 2016).

2.8.3 Thermogravimetric analysis

Thermogravimetric analyzer (Exstar TG/DTA 6300 manufactured by Seiko Instruments, Japan) is used for measuring thermal degradation properties of flax fibre, pure PLA and NFBBF/PLA composites. The analysis is carried out from 25° C to 500° C in a nitrogen environment at a rate of 10° C/min (Huang and Netravali 2007).

2.8.4 Heat deflection temperature

Heat deflection temperature (HDT) analysis is performed on a HDT analyser according to ASTM D648-18. The samples (127 mm × 12.7 mm × 3 mm) are analysed in 3 point bending mode with an applied load of 0.455 MPa at a uniform temperature rate of 2° C/min. In this study minimum three specimens are tested and average values are reported.

2.8.5 Thermal deflection

In the HDT test, the specimen is subjected to uniform temperature with constant applied load of 0.455 MPa (in 3 point bending condition) inside the oil chamber. However, in the case of thermal deflection test, a beam like specimen is subjected to non-uniform temperature load in the fixed-fixed condition and change in lateral deflection of the beam with increase in temperature is analysed.

Deflection of a beam like structure, subjected to different temperature variations is studied. Deflection of NFBF/PLA composite beam in lateral direction due to increase in temperature is used to obtain the deflection temperature. Figure 2.11 represents the schematic of an in-house developed thermal deflection testing set up (George et al. 2016; Waddar et al. 2018, 2020). For this test, specimen of 275 mm × 13 mm × 3 mm (Figure 2.12) is used and clamped for the 25 mm portion on both the sides as shown in Figure 2.12. Infrared (IR) heater (1000W/230V single-tube short-wave IR lamps) is utilised as a source of heating and it is mounted 30 mm away from the specimen. Here, heating of the specimen takes place through radiation heat transfer. Lateral deflection of the specimen due to thermal load is obtained using Honeywell MVL7 Linear Variable Differential Transducer (LVDT), which has a temperature range of -50° C to + 125° C and ± 1 in., stroke length. K-type thermocouple with 41 µV/°C sensitivity is used to measure the specimen's surface temperature and the reported temperature results are fed to a computer via DAQ (data acquisition) system. The IR heater ON / OFF switch is operated by a relay unit (ABB A9-30-10 industrial relay) in light of the thermocouple results using a LabVIEW computer program.

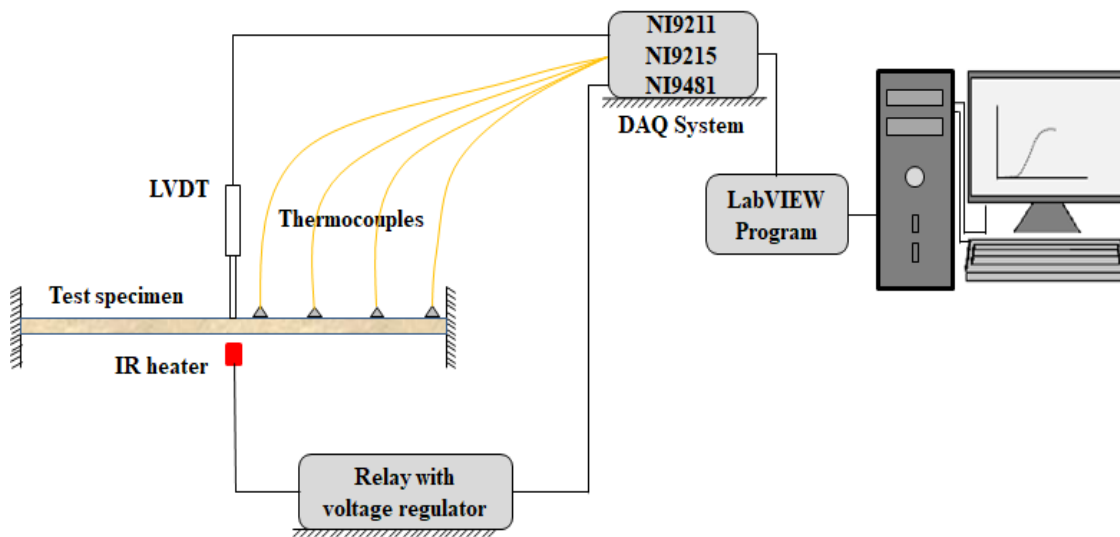


Figure 2.11 Schematic of thermal buckling testing set up

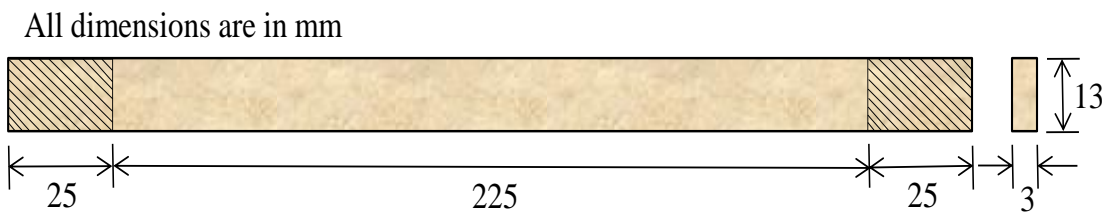


Figure 2.12 Schematic of thermal buckling test specimen

The DAQ framework has three different data acquisition modules to monitor the different parameters through the computer and LabVIEW user interface. The NI9211 DAQ is used to read the temperature measurement results given from the K-type thermocouple and the specimen deflection is determined using the NI9215 DAQ module and it uses the analogue voltage output of the LVDT as an input. NI9481 DAQ module is used to control the temperature with the switching ON/OFF IR heater by triggering relay unit according to LabVIEW program. Shift registers are used to store deflection and temperature into an array to plot the deflection and temperature curves. Preliminary tests are performed to determine the specimen's maximum ideal heating temperature and the same is used as the user input to the LabVIEW program up to which the specimen is to be heated. When the temperature of the specimen exceeds this ideal temperature, the program turns off the heater automatically. Using the statistical palette, the RMS (root mean square) value of the LVDT information got from the NI9215 DAQ is separated before the temperature-deflection data array is

established to be used to map the curves. Using the write command, all the data is compiled into a Microsoft Excel file.

Three kinds of temperature variations (case-1, case-2 and case-3) are considered in this study to analyse the influence of temperature variation on thermal deflection. The IR heaters are located in different positions to achieve these three types of variation in temperature as shown in Figure 2.13. For case-1, i.e. decrease (Figure 2.13a), the IR heater is placed at one end of the specimen. In this condition, the maximum temperature occurs at the beam end where IR heater placed. In the second case, i.e., case of decrease-increase, IR heaters are mounted at both ends of the specimen separately as shown in Figure 2.13b. In this case, higher temperature occurs at both ends of the specimen. Figure 2.13c shows an increase-decrease case (case 3) where a single IR heater is placed around the centre of the specimen and specimen experiences a maximum temperature at the centre.

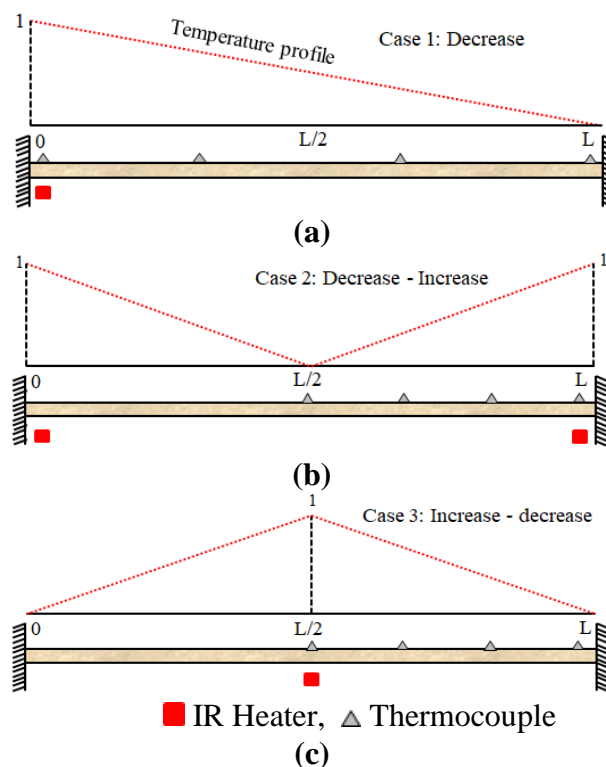


Figure 2.13 Schematic representation of a) case 1: decrease, b) case 2: Decrease – Increase and c) case 3: Increase – decrease

2.9 Water absorption and Biodegradability tests

Behaviour of PLA and NFBF/PLA composites under different environmental conditions (such as, distilled water immersion and compost soil incubation) is analysed by conducting water absorption and biodegradability tests.

2.9.1 Water absorption

Water absorption study of pure PLA and its composites is performed as per ASTM D570. Pure PLA (NFBF0) and PLA composites with different weight fractions (NFBF11, NFBF22 and NFBF33) are considered for this study. Before the test, initial weight and thickness of each specimen are measured, and conditioned specimens are soaked in the distilled water at room temperature. For every 24 hour intervals of time, specimens are taken out from the water and water at the surface of the specimen is wiped out with cotton cloth before the thickness and weight measurement. This process is continued until specimen mass reaches a constant value. Equation (2.8) is used to evaluate the percentage of water absorption.

$$\text{Water absorption (\%)} = \frac{W_2 - W_1}{W_1} \times 100 \quad (2.8)$$

where, W_1 is specimen initial weight, and W_2 is specimen weight after immersion. The percentage of swelling of the specimen is calculated using Equation (2.9).

$$\text{Thickness swelling (\%)} = \frac{h_f - h_i}{h_i} \times 100 \quad (2.9)$$

where, h_i is the initial thickness, and h_f is thickness after wetting. The flexural test is conducted before and after water absorption of the composite specimen using ASTM D790. For this test, specimens of size 127 mm × 13 mm × 3 mm are used and tested on a UTM with a crosshead speed of 1.3 mm/min.

2.9.2 Biodegradability test

In this present work, municipal compost soil is used to study the aerobic biodegradation of the pure PLA and its composites. Municipal compost soil is

collected from Unique Waste Processing Company Ltd. Mangalore, India. Chemical properties of the compost soil are reported in Table 2.3. Values given in Table 2.3 are provided by the supplier. In plastic crates size of 600 mm × 400 mm × 285 mm, the compost soil is filled up to a height of 250 mm, and holes are created at the bottom of the crate to release the excess water. The dumbbell-shaped specimens are cut from the prepared PLA and NFBF/PLA composite laminates. The PLA and NFBF/PLA composite specimens are buried in the compost soil at 125 mm deep from the soil surface. Positioning of the samples inside the compost for the biodegradation test is shown in Figure 2.14 and Figure 2.15. Then the crates are placed at outdoors and watered every day (except on the rainy days) to maintain the moisture of compost soil. After 15, 30, 60, 90 days of incubation, specimens are taken from compost and cleaned with distilled water to remove compost components from the specimen surface. Finally, the specimens are vacuum dried for 12 hours at 50° C to remove moisture content and achieve constant weight. Followed by this, these specimens underwent weight loss measurement, tensile test, FTIR spectra and SEM image analysis.

Table 2.3. Chemical properties of the compost soil used for biodegradation test

Chemical property	%
Moisture content	23.64
Total organic carbon (air-dry basis)	14.79
Total nitrogen as N (air-dry basis)	2.06
Total phosphorous as P ₂ O ₅ (air-dry basis)	0.74
Total potassium as K ₂ O (air-dry basis)	0.46
C: N ratio	7.18
pH value (1:2) (air dry basis)	7.28
Bulk Density	0.5068 g/cc



Figure 2.14 Crates with samples

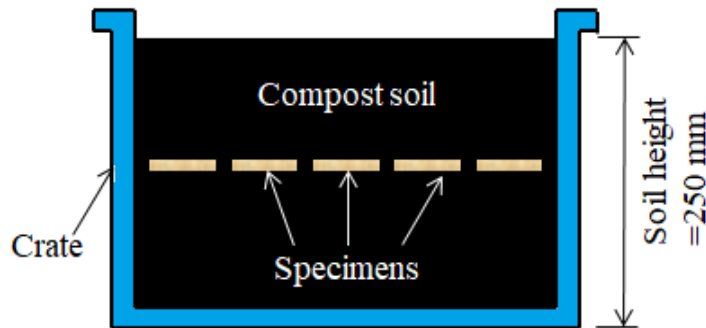


Figure 2.15 Sketch of burial test crate

Biodegradability of the prepared PLA and NFBF/PLA composites is assessed based on weight loss, reduction in tensile properties (strength and modulus), change in FTIR spectra and surface appearance. Equation (2.10) is used to calculate the sample percentage weight loss (W_L).

$$W_L = \frac{W_b - W_a}{W_b} \times 100 \quad (2.10)$$

where, W_b is the sample weight before soil incubation, and W_a is the sample weight after soil incubation.

2.9.2.1 Fourier transform infrared (FTIR) spectroscopy

The infrared spectra of the composites specimens before and after biodegradation are recorded on a Bruker Alpha 400 FTIR spectrometer equipped with silicon carbide as an IR source. The samples were recorded with 24 scans having a resolution of 4 cm^{-1} with the spectrum range of $500 - 4000 \text{ cm}^{-1}$.

2.9.2.2 Tensile testing before and after biodegradability

Tensile testing is performed on dumbbell-shaped specimens of PLA and its composites (Figure 2.16) according to ASTM D638 using a universal testing machine (Tinius Olsen 75KS, UK) with 5 mm/min crosshead speed to evaluate the reduction in tensile strength after the biodegradability test. SEM image analysis is performed to study the composite surface appearance before and after the biodegradation test.



Figure 2.16 Tensile specimens before and after biodegradability test

2.10 Wear and fracture toughness study

Void content, wear properties and plane strain fracture toughness are evaluated based on the following experimental procedures.

2.10.1 Density test

Density of the prepared 3D braided composites is evaluated as outlined in ASTM D792-13. Theoretical densities (ρ^{th}) of the NFBF/PLA composites are evaluated with the relation between mass fraction and density of the filler and matrix material (Equation 2.11) (Bajpai et al. 2013).

$$\frac{1}{\rho^{th}} = \frac{W_f}{\rho_f} + \frac{W_m}{\rho_m} \quad (2.11)$$

where, W denotes weight fraction and ρ denotes density, suffixes m represents matrix and f represents fibre respectively. The air gap in the composite materials known as void content (ϕ_v) is evaluated as per Equation (2.12) (Waddar et al. 2018).

$$\phi_v = \frac{\rho^{th} - \rho^{exp}}{\rho^{th}} \times 100 \quad (2.12)$$

2.10.2 Wear test

Friction and wear characteristics of the PLA and NFBF/PLA composites are analysed using a pin-on-disc tribometer (Ducom, India). Experiments are conducted as per ASTM G99-17 at ambient conditions. Schematic diagram of wear test set up is shown in Figure 2.17. The wear properties of the NFBF/PLA composites and pure PLA are investigated on EN-31 steel rotor disc. Sliding friction takes place between the stationary specimen (pin) clamped in the holder and rotating steel disc. The sliding velocity and load are varied during the test and their values are summarised in Table 2.4.

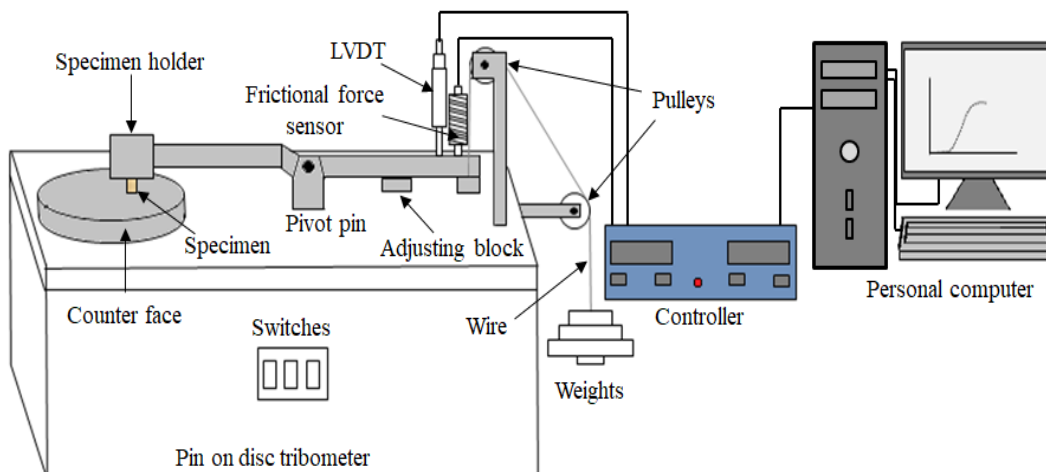


Figure 2.17 Schematic diagram of pin-on-disc wear testing set up

Table 2.4 Parameters used for wear test

Input parameters	Values
NFBF (wt. %)	0, 18, 26, 35
Applied normal load, F_n (N)	10, 20, 30
Sliding distance, D_s (m)	3000
Sliding velocity, V (m/s)	1, 2, 3

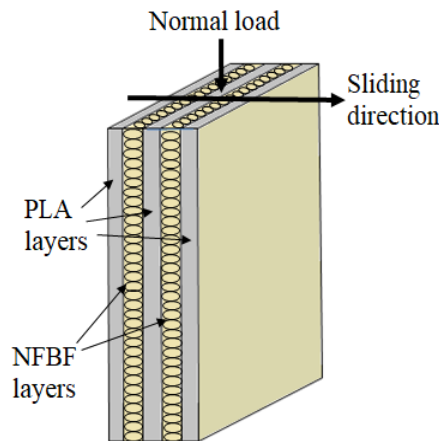


Figure 2.18 Schematic of composite specimen sliding direction

The composite specimens of dimension 20 mm × 12 mm × 4 mm are cut from the prepared composite laminates. In order to maintain proper initial roughness, the composite samples are rubbed with silicon carbide (SiC) 800 grits and 1500 grits of abrasive paper prior to the wear test. This method helps to maintain the proper surface contact of the composite specimen with the rotor disc counter surface. Schematic diagram of composite specimen sliding direction against rotor disc counter surface is presented in Figure 2.18.

The friction force and height loss is measured with the help of friction force sensor and LVDT (Linear Variable Differential Transducer). From each composition of sample minimum three specimens are tested and reported average values. From these results the co-efficient of friction (μ) is calculated using Equation (2.13).

$$\mu = \frac{F_f}{F_n} \quad (2.13)$$

where, F_f and F_n indicate frictional force (N) and applied normal load (N). Similarly, wear rate can be written as below:

$$w_t = \frac{V_L}{D_s} \quad (2.14)$$

where, V_L and D_s are volume loss (mm^3) and sliding distance (mm). Specific wear rate (w_s) represents the load carrying capacity and it is calculated as,

$$w_s = \frac{w_t}{F_n} \quad (2.15)$$

The composites worn surface morphology study is done on Scanning Electron Microscope (Jeol JSM-6380LA, Jeol India Pvt. Ltd. India).

2.10.3 Plane strain fracture toughness test

In this investigation, tensile and fracture properties are analysed in a universal testing machine (H75KS, 50KN load cell capacity, Tinius Olsen made, UK). Tensile test is carried out on dumbbell shaped composite specimens as per ASTM D638-14 with an upper head speed of 5 mm/min. Fracture toughness study is performed on SENB specimens as outlined in ASTM D5045-14. Specimens of size 127 mm \times 13 mm \times 4 mm are used for the fracture toughness test. Initial crack length (a) of 6.5 mm between $0.45 < a/W < 0.55$ is introduced by 0.25 mm (Shen et al. 2014) hacksaw blade and a fresh razor blade at notch tip. Support span length of 52 mm ($S = 4W$) is used and the test is conducted with a cross-head speed of 10 mm/min. Figure 2.19 shows the SENB specimen and fixture of the mode-I plane-strain fracture toughness test. Following relationship is used to calculate the Mode-I plane-strain fracture toughness (K_{IC}) of SENB specimen;

$$K_Q = \left(\frac{P_Q}{BW^{1/2}} \right) f(x) \quad (2.16)$$

where, B , W and P_Q are specimen thickness, width and maximum load respectively, and

$$f(x) = 6x^{1/2} \frac{[1.99 - x(1-x)(2.15 - 3.93x + 2.7x^2)]}{(1+2x)(1-x)^{3/2}} \quad (2.17)$$

where, $x=a/W$, here 'a' represents the initial length of crack. Then the strain energy release rate (G_{IC}) is calculated using Equation (2.18).

$$G_{IC} = \frac{U}{(BW\varphi)} \quad (2.18)$$

$$\varphi = \frac{18.64 + A}{dA/dx} \quad (2.19)$$

where,

$$A = [16x^2 / (1-x)^2] \times [8.9 - 33.717x + 79.616x^2 - 112.952x^3 + 84.815x^4 - 25.672x^5]$$

$$\begin{aligned} dA/dx = & [16x^2 / (1-x)^2] \times [-33.717 + 159.232x - 338.856x^2 + 339.26x^3 - 128.36x^4] \\ & + [32x / (1-x)^3] \times [8.9 - 33.717x + 79.616x^2 - 112.952x^3 + 84.815x^4 - 25.672x^5] \end{aligned}$$

Following size criterion must be satisfied to consider the K_{IC} as the plane-strain fracture toughness K_{IC} :

$$B, a, (W - a) > 2.5(K_{IC} / \sigma_t)^2 \quad (2.20)$$

where, σ_t is the tensile strength of the composite specimens, obtained by performing tensile test. SEM image analysis is done on the fractured surfaces of the composites to examine the surface morphology.

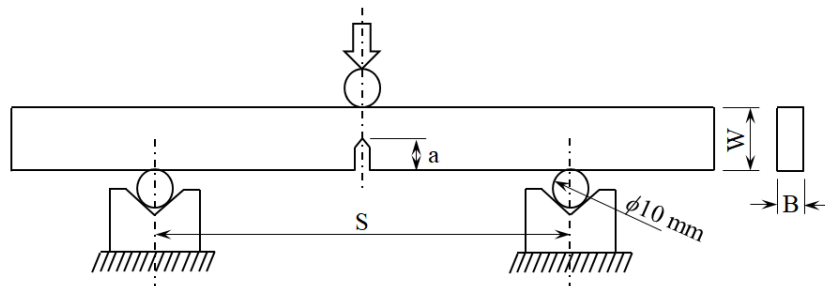


Figure 2.19 SENB (single-edge-notch bending) specimen and fixture for three point bending test

2.11 Buckling and free vibration properties

This section explains testing procedures used to determine critical buckling load and natural frequencies of composites subjected to axial-compressive load.

2.11.1 Buckling under axial compression

Mechanical buckling of PLA and NFBB/PLA composites under edge compression is performed on Tinius Olsen universal testing machine (H75KS, 50 KN load cell, UK made) with fixed-fixed conditions at a cross-head velocity of 0.2 mm/min. For this test, specimens having dimension of 310 mm × 13 mm × 3 mm (length, width and thickness) are used and five trials are made for each case. Based on preliminary tests, pre and post buckling deflection behavioural changes of composite beams subjected to axial-compressive load are characterised by maintaining 0.5 mm end shortening limit. The schematic of mechanical buckling and free vibration experimental test set-up under axial-compressive load is depicted in Figure 2.21. From the load-deflection curve the critical buckling load (P_{cr}) is determined using two different graphical methods (Double Tangent Method (DTM) and Modified Budiansky Criteria (MBC)) (Matsunaga 1996; Tuttle et al. 1999). In the DTM approach tangents are drawn (as shown in Figure 2.20a) to the pre and post buckling zones of the load-deflection curve. The intersection of the pre and post-deflection tangents gives the P_{cr} (critical axial buckling load) as illustrated in Figure 2.20a. Similarly, in the MBC method bisector is drawn from the pre and post-deflection tangents intersection point to the load deflection curve as shown in Figure 2.20b. The bisector point on the load-deflection curve corresponds to the critical buckling load (P_{cr}) of the composite.

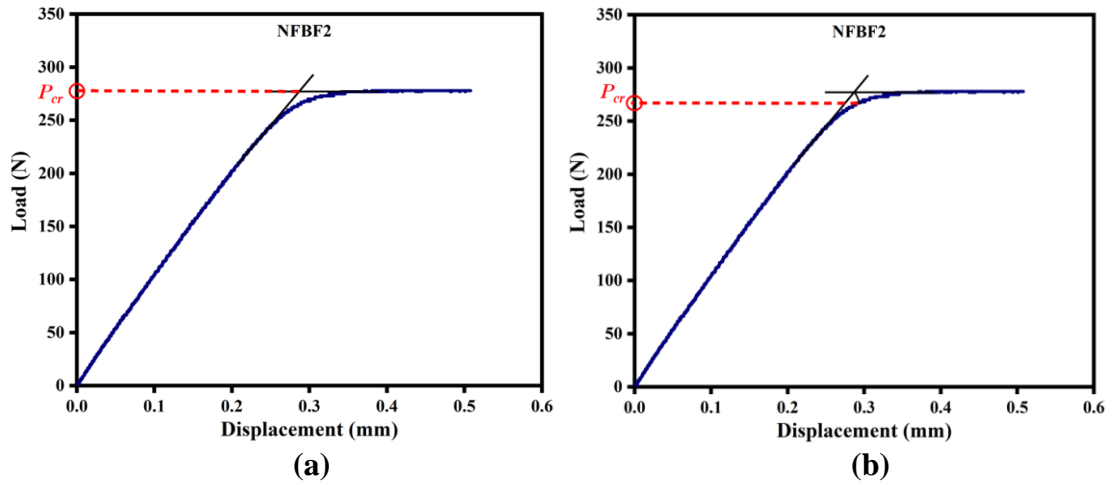


Figure 2.20 Representing estimation of critical buckling load (P_{cr}) from (a) DTM and (b) MBC methods for NFBF2 composites

2.11.2 Free vibration

Natural frequencies corresponding to first three (1st, 2nd and 3rd) bending modes of the PLA and NFBF/PLA composite beams under edge compressive load in clamped-clamped boundary condition are determined using experimental modal analysis. Schematic of experimental test rig of free vibration study of the composite beams under axial-compressive load is presented in Figure 2.21. The impulse hammer (Model:8778A500, sensitivity: 10mV/g, operating range: ± 500 g, Kitsler make) is used to excite composite beams and uniaxial type light weight accelerometer (Model: 9722A2000, the sensitivity of 10 mV/N, Kitsler make) is used to acquire the vibration response signals. An accelerometer is mounted on the composite specimen surface (as shown in Figure 2.21) with the help of bee's wax. Response signals are recorded using software called DEWESoft and this software uses FFT (Fast Fourier Transform) algorithm to transform time-domain signals into frequency-domain which is further used to calculate the natural frequencies. Modal-analysis experiment is performed from zero load to critical buckling load (P_{cr}) at every 30 N incremental load. In every increment of load, experimental modal-analysis is paused for 2 min to excite the specimen at marked positions (Figure 2.21) and capture the respective frequency of the beam. This procedure is followed for all compositions of composite beams. The schematic of testing of braided flax-PLA composite specimen used for the axial buckling and free vibration test is shown in Figure 2.22. The test specimen with a

shaded portion at both the ends is used for the holding in UTM fixture and the gauge length (210 mm) of the specimen is divided into seven equal parts with having a distance of 30 mm each. These marked positions are used as impulse hammer excitation locations.

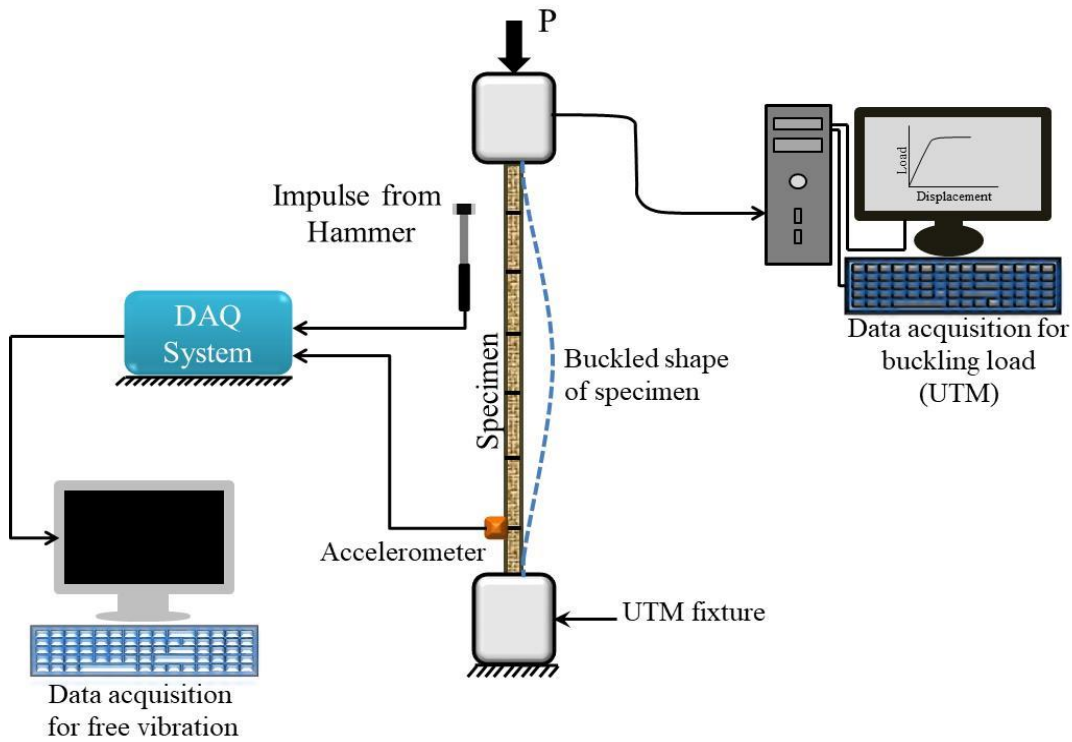


Figure 2.21 Schematic experimental set up of free vibration test under axial compressive load

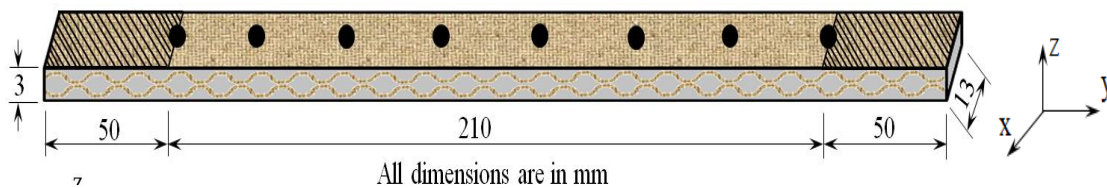


Figure 2.22 Schematic representation of composite test specimen configuration

Results and discussion associated with various tests explained in this chapter are presented in detail in the following chapters.

3 MECHANICAL PROPERTIES OF BRAIDED YARN, FABRIC AND COMPOSITES

3.1 Introduction

In this chapter geometrical and tensile properties of the braided yarn and its fabrics are presented. Then effect of natural fibre braided yarn fabric (NFBF) reinforcement on mechanical properties such as tensile, flexural impact and ILSS properties of the PLA is presented. Characterization of the composites is carried out in different loading directions (warp and weft) of the surface plies for different possible structural applications in automotive, food packaging, aerospace and electronics industries. Finally the results of the NFBF composites are compared with the results available literature for other types of natural fibre reinforced PLA composites.

3.2 Geometric and tensile properties of braided yarn and woven fabrics

The longitudinal and cross-sectional views of a 3D braided yarn sample are shown in Figure 3.1. One can clearly observe the braiding pattern of the yarn as shown in Figure 3.1(a). Similarly, interlacing of four simply twisted yarns to form a braided yarn can be seen clearly in Figure 3.1(b). The prepared braided yarn has a braiding angle of 22° . The average density of flax yarn is evaluated as 1.374 g/cm^3 and it falls within the established flax fibre densities ranging from 1.2 g/cm^3 to 1.5 g/cm^3 (Pickering et al. 2016; Zhang et al. 2013). For yarn number evaluation, average yarn weight ‘G’ is measured as 0.2542 gram and the braided yarn number is calculated as 2288.43 in Denier and 254.27 in Tex.

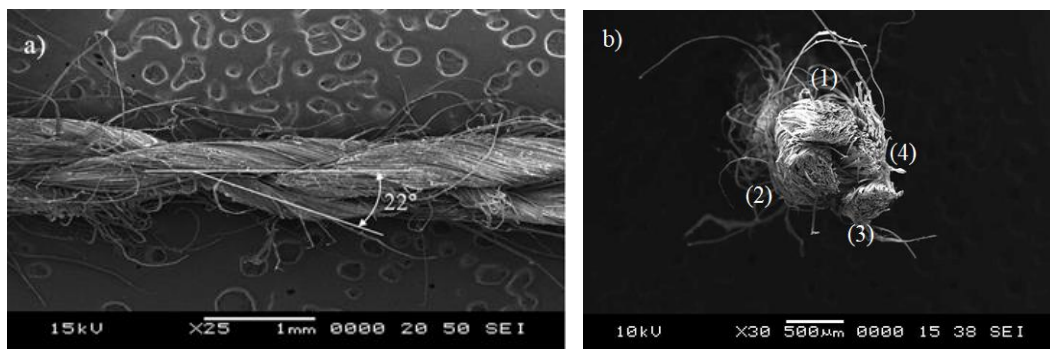


Figure 3.1. Optical photographs of 3D braided yarn a) longitudinal view, b) cross-sectional view

In general, the physical and mechanical characteristics of a natural fibre inherently dependent on the state of the soil in which the plant is grown, the method of fibre extraction and the maturity of the plant (Porrás and Marañón 2012). Tensile properties of the braided yarn are presented in Figure 3.2 and Table 3.1 with standard deviation. Young's modulus and ultimate stress of the yarns vary due to variation in chemical composition of fibre, force-elongation properties, fibre diameter, the fibres fibril angle and packing factor (Graupner et al. 2009; Huang and Netravali 2007). Tensile strength and modulus of the braided yarn depend on the braiding angle. Tensile strength and elastic modulus of the braided yarn reduces with the increase in braiding angle (Naik et al. 1994; Sun and Qiao 1997; Tate et al. 2006). The prepared braided yarn has the tensile strength and modulus of 250.33 MPa and 4.29 GPa respectively.

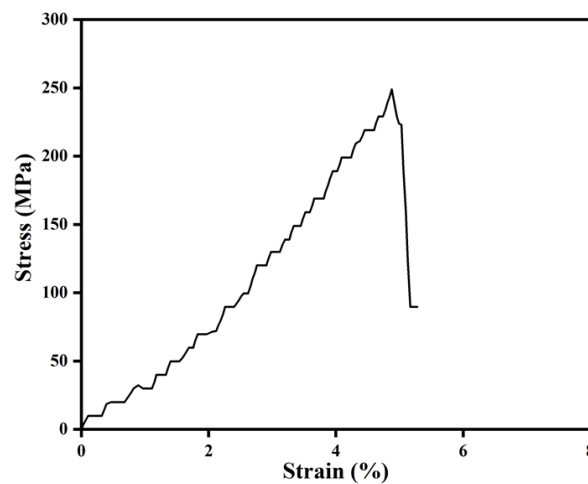


Figure 3.2 Stress-strain curve of the braided yarn

Table 3.1. Tensile properties of the braided yarn

Ultimate stress (MPa)	Ultimate strain (%)	Young's modulus (GPa)
250.33 ± 12.51	4.29 ± 0.88	4.29 ± 0.23

Fabric used as reinforcement in present study has plain type weaving pattern as shown in Figure 3.3. Yarn count associated with the fabric along warp and weft directions are 10 yarns/cm and 6 yarns/cm with coefficient of variation of 1.04% and 1.88% respectively. The prepared fabric has higher yarn count in the warp direction compared to weft direction.



Figure 3.3 SEM image of the flax fabric woven using 3D braided yarns

Yarn crimp of the woven fabric yarn along warp and weft directions are evaluated as $11.86 \pm 1.247\%$ and $3.86 \pm 0.471\%$ respectively. The length of the yarn along the warp direction is greater than that of the yarn length along the weft. This is due to the interlacement of the warp yarn in the fabric which results in higher crimp for the warp yarns. GSM of the natural fibre braided yarn woven fabric is measured as $444.33 \pm 1.247 \text{ g/m}^2$ and the moisture content of the fabric is evaluated as $9.012 \pm 0.016 \%$. Moisture content in the natural fibres influences the fibre-matrix compatibility and mechanical performance of the composites. Moisture content value of the flax fibre studied is within the limit of 8 – 12% (AL-Oqla et al. 2015).

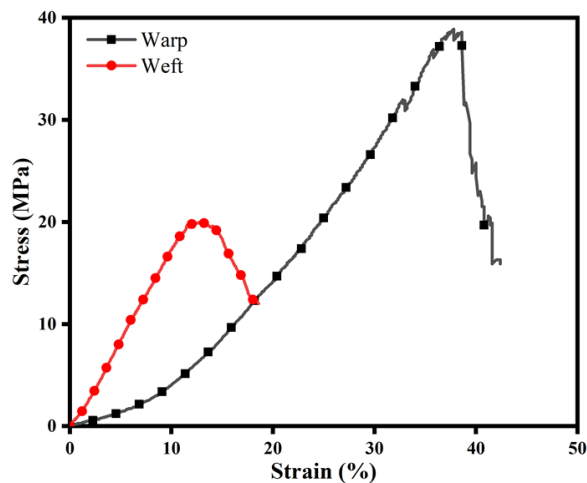


Figure 3.4 Tensile stress-strain curves of braided yarn fabric in warp and weft direction loading

Table 3.2. Tensile properties of natural fibre braided yarn fabric (NFBF)

Test direction	Ultimate stress (MPa)	Ultimate strain (%)	Young's modulus (MPa)
Warp	38.18 ± 3.16	39.02 ± 3.06	98.45 ± 5.91
Weft	18.80 ± 2.20	13.85 ± 1.56	167.82 ± 8.39

Tensile properties such as ultimate breaking stress, modulus and percentage elongation at break of NFBF when loaded along warp and weft directions of fabric specimens are listed in Table 3.2 and tensile stress-strain curves are shown in Figure 3.4. From Table 3.2, it is found that the tensile properties of the NFBF specimens along warp and weft directions are different. This could be due to the difference in yarn density of the fabric along the warp and weft directions. Tensile strength and elastic modulus of the NFBF under warp direction loading are 38.18 MPa and 98.45 MPa, while under weft direction loading the corresponding values are 18.80 MPa and 167.82 MPa respectively. From the results, it is clear that tensile strength of the NFBF is higher under warp direction loading and it is low for weft direction loading. This is due to higher number of denier yarns present in the warp direction. Due to higher crimp associated with the warp direction loaded fabric, it showed higher strain and lower modulus. When the load is applied in the warp direction, the braided yarns initially loose their crimp and the load required to straighten the yarn is lower than that required to stretch the yarns (Chabba and Netravali 2005). Due to this reason, warp direction loaded fabric specimen showed lesser value of tensile modulus. The ultimate tensile stress and Young's modulus of the braided yarn woven fabrics are lower than that of braided yarn specimens. This can be attributed to the cross-linking of the yarns in the fabric, yarn crimp and gap between the consecutive yarns in the fabric. Huang and Netravali (2007) also noticed lower tensile properties for the fabric compared to yarn properties.

3.3 Mechanical properties of the composites

PLA composite reinforced with one, two and three layers of NFBF is considered for this study. These composites are named as NFBF11, NFBF22 and NFBF33 based on their fibre weight percentage. For example, wt.% of the fabric in single layered fabric

reinforced PLA composite is 11% and it is represented as NFBF11. Different properties of the NFBF/PLA composites are compared with the virgin PLA (NFBF0).

3.3.1 Tensile properties

Typical stress-strain curves of warp and weft direction loaded PLA composites are shown in Figure 3.5 and Figure 3.7 respectively. Similarly, the ultimate stress and modulus of warp and weft direction loaded composites are shown in Figure 3.6 and Figure 3.8 respectively. Error bars on the ultimate stress and modulus shows the standard deviation of the repeated experiments.

The stress-strain curves (Figure 3.5 and Figure 3.7) are initially linear at low strains, followed by this there is a small change in the slope of the curve. This represents the non-linear behaviour of composites. This nonlinearity in the stress-strain curves shows the beginning of crack in the polymer matrix and starting of fibre failure. Beyond the ultimate tensile stress a sudden drop is observed in the stress-strain curve, due to fibre fracture and fibre pull-out (Figure 3.9). The average values of tensile strength and modulus of the virgin PLA are 32.84 MPa and 1.19 GPa respectively. Incorporation of the NFBF enhanced the tensile properties (strength and modulus) of the composites considerably and these properties further enhanced with increase in fibre content for both warp and weft loading. This enhancement is might be due to good fibre matrix bonding and this helps to transfer stress from polymer matrix to strong fibres (Oksman et al. 2003). The composite reinforced with 33 wt.% of braided yarn fabric showed higher tensile properties. For the warp direction loading PLA composite with 33 wt.% of NFBF has the average tensile strength and modulus values are 45.24 MPa and 2.09 GPa respectively. Similarly, the corresponding values for weft direction loading of the PLA composite with 33 wt.% of NFBF are 38.34 MPa and 1.83 GPa respectively. According to the results reported by the other researchers, tensile strength of the flax woven fabric reinforced PLA composite is 21 MPa (Kumar et al. 2010) and flax knitted fabric PLA composite is 28 MPa (Adomavičiūtė et al. 2015). Tensile strength values of the bio-composites produced by reinforcing braided yarn fabric are comparatively higher than that of woven PLA composites with other forms of fabric reinforcement.

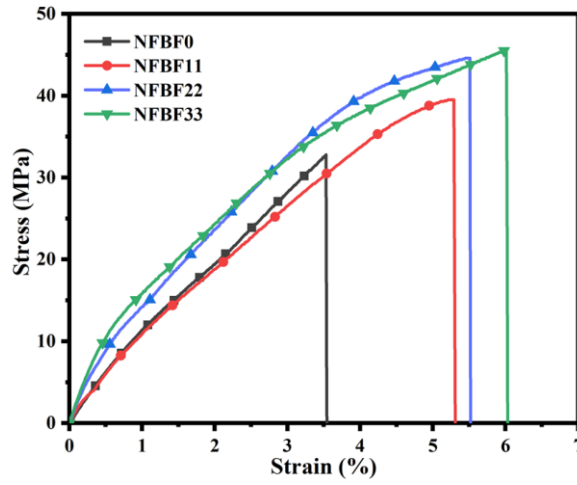


Figure 3.5. Tensile stress–strain curves for PLA and NFBF/PLA composites under warp direction loading

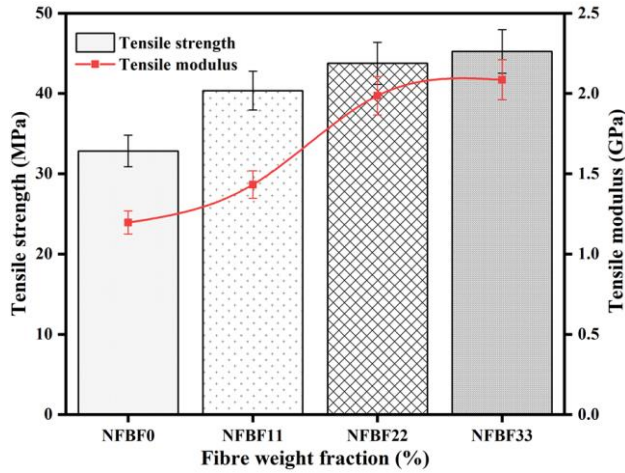


Figure 3.6. Ultimate tensile strength and tensile modulus of PLA and NFBF/PLA composites under warp direction loading

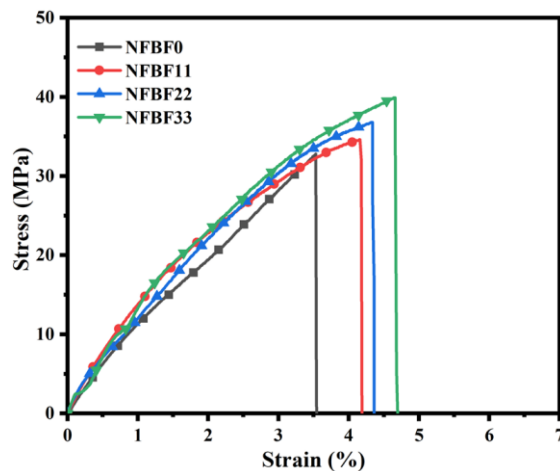


Figure 3.7. Tensile stress–strain curves of PLA and NFBF/PLA composites under weft direction loading

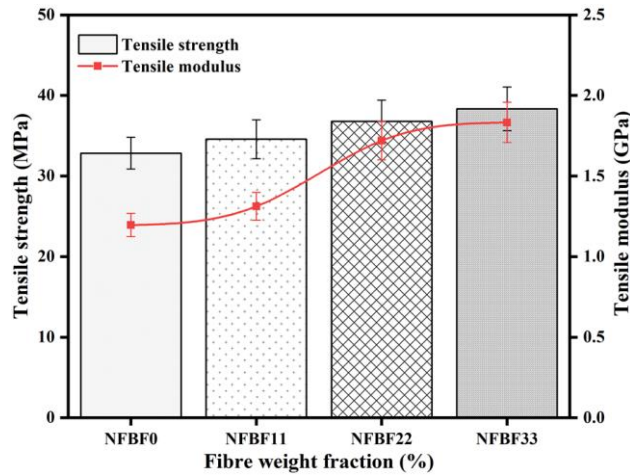


Figure 3.8. Ultimate tensile strength and tensile modulus of PLA and NFBF/PLA composites under weft direction loading

The warp direction loaded composites showed 38% and 76% increase in tensile strength and modulus values respectively compared to virgin PLA. Similarly, compared to weft direction loaded composites these values are 18% and 15% higher. The weft direction loaded composites have lesser number of yarns compared to warp direction composites, hence the NFBF composites showed poor mechanical characteristics. When the tensile load is applied on the composites reinforced with woven fabric, at the crimped sections of fibre overlaps produces the transverse loads and this tries to straighten the fibre. This reduces the transfer of stress from fibre to fabric and reduces creep rupture and fatigue performance (Khan et al. 2016). During the tensile test, extension of warp yarns is more due to higher crimp associated with these yarns. For this reason, higher strain percentage is noticed for the warp direction loading compared to the weft direction loading.

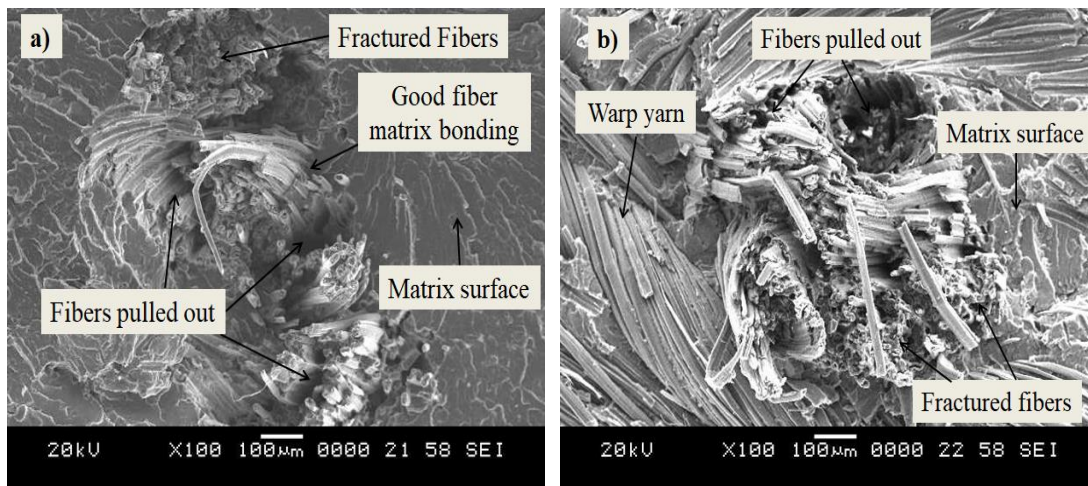


Figure 3.9. Micrographs of tensile test specimen fractured surfaces a) warp direction loaded and b) weft direction loaded composites

Tensile characteristics of the present composites are compared with the results of other similar PLA composites reported in literature as seen in Table 3.3. In this comparative study (Table 3.3), different manufacturing methods, fibre matrix blending or compounding processes and types of natural fibres used for composite preparation are considered. Tensile strength and Young's modulus of the natural fibre composites are listed as the percentage increase (+) or decrease (-) with respect to pure PLA samples of the other research studies. Except for the jute fabric and sisal fabric reinforced composites, the tensile strength of the composites present NFBF/PLA is higher. Lower strength of the present composite may be due to process used for fibre matrix blending, lower strength of the fibres and also the braided yarn angle. Young's modulus of the present braided yarn composites is low compared to other flax fibre, flax fabric, jute fabric and sisal fabric composites. Bax and Mussig (2008) conducted experiment with and without extensometer and showed 12% increment in the modulus of the composites compared to no-extensometer used one. Tensile properties of the present composite can be enhanced using the braided yarn with smaller diameter with reduced braiding angle and reducing the distance between the yarns of the fabric by increasing the number of yarns in both warp and weft direction.

Table 3.3 Comparison of tensile properties of NFBF/PLA composites with different natural fibre PLA composites (Percentage (+) increase or (-) decrease of the composites is calculated with respect to neat PLA)

Manufacturing method	Fibre matrix compounding	Kind of Fibres	Fibre mass (%)	Tensile Strength (%)	Young's Modulus (%)	References	
Compression molding	Solution casting	Flax braided yarn fabric	33	+38	+76	This study	
	Twin screw extrusion	Flax	30	+6	+144	(Oksman et al. 2003)	
		Flax non-woven mat	20	-15	n.s	(Siengchin 2014)	
		Flax twill woven fabric	40	+3.14	+271	(Nassiopoulos and Njuguna 2015)	
	Roller carding	Cotton	40	+32	+11	(Graupner et al. 2009)	
		Hemp	40	+27	+111	(Hu and Lim 2007)	
	Barbender mixer	Hemp	20	-26	+13	(Masirek et al. 2006)	
		Hemp plain fabric	20	+8.6	+32	(Song et al. 2012)	
		Hemp twill fabric	20	+12	+40	(Song et al. 2012)	
		Bamboo fabric	35	+34	+68	(Rawi et al. 2013)	
		Carding and needle-punching	Jute fabric	40	+60	+179	(Kandola et al. 2018)
			Sisal fabric	40	+48	+165	(Kandola et al. 2018)
Injection molding	Twin screw extrusion	Coconut	30	-13	+71	(Sujaritjun et al. 2013)	
		Chicken feather	10	-21	+8.33	(Cheng et al. 2009)	
		Banana/sisal	30	+32	+80	(Asaithambi et al. 2014)	
	Roller carding	Flax	30	+23	+103	(Bax and Müssig 2008)	
		Cordenka	40	+32	+58	(Bax and Müssig 2008)	

3.3.2 Flexural properties

The flexural strength and flexural modulus of PLA and its composites under warp and weft direction loadings are given in Figure 3.10, Figure 3.11, Figure 3.12 and Figure 3.13 respectively. Incorporation of NFBF with PLA significantly enhanced the flexural strength and modulus of the composites compared to virgin PLA. Flexural properties are also improved with respect to increase in NFBF content in the composite. From Figure 3.10 and Figure 3.12 it is observed that the PLA samples are failed abruptly with average flexural strength and modulus of 52.65 MPa and 2.07 GPa respectively. The sudden failure can be attributed to stiff and brittle nature of PLA polymer (Oksman et al. 2003).

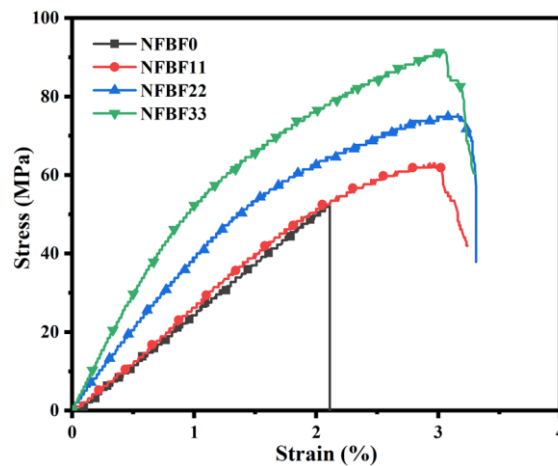


Figure 3.10. Flexural response curves for PLA and NFBF/PLA composites under warp direction loading

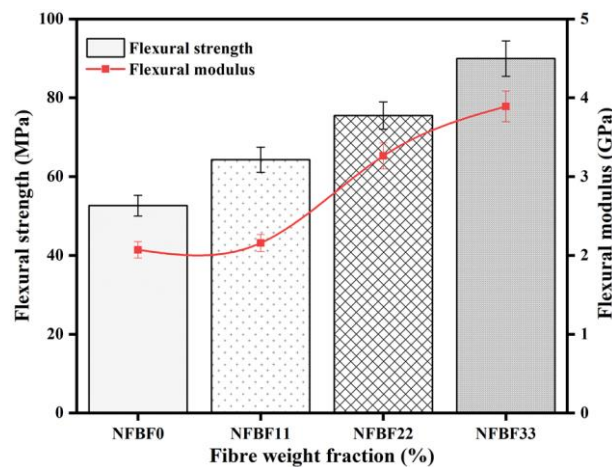


Figure 3.11 Flexural strength and flexural modulus of neat PLA and NFBF/PLA composites under warp direction loading

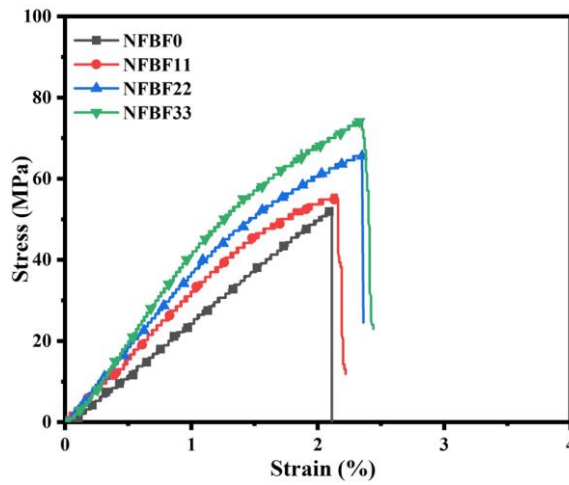


Figure 3.12. Flexural response curves for PLA and NFBF/PLA composites under weft direction loading

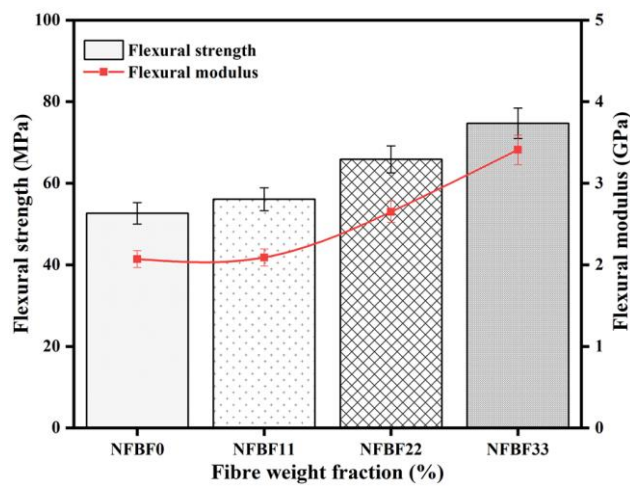


Figure 3.13. Flexural strength and flexural modulus of neat PLA and NFBF/PLA composites under weft direction loading

In this study also, the composites loaded in warp direction showed better flexural strength and modulus compared to the weft loading. The composite with 33 wt.% of NFBF showed maximum strength and modulus of 89.96 MPa and 3.89 GPa respectively. These values are 71% and 88% greater than the pristine PLA and these corresponding values are 20% and 14% high for the weft direction loading. The flexural strength of the flax fibre un-commingled yarn plain fabric and double faced rib knitted fabric reinforced PLA composites is 10.90 MPa and 5.22 MPa respectively (Kannan et al. 2012). The flexural strength of NFBF33 composite is much higher compared to these values.

The SEM micrographs of the flexural test specimen fractured surfaces are presented in Figure 3.14 and fibre fracture is commonly noticed. In Figure 3.14(b) one can notice the river like structure formed in the matrix due to yarn detachment. This behaviour shows that the fracture of specimen took place along the warp yarn, due to lower polymer matrix presence and higher stress concentration along the warp yarn. Similar trend is noticed in fractured surface of weft direction loaded tensile specimen in Figure 3.9(b). This is also might be reason for the lower tensile and flexural properties associated with the weft direction loaded composites.

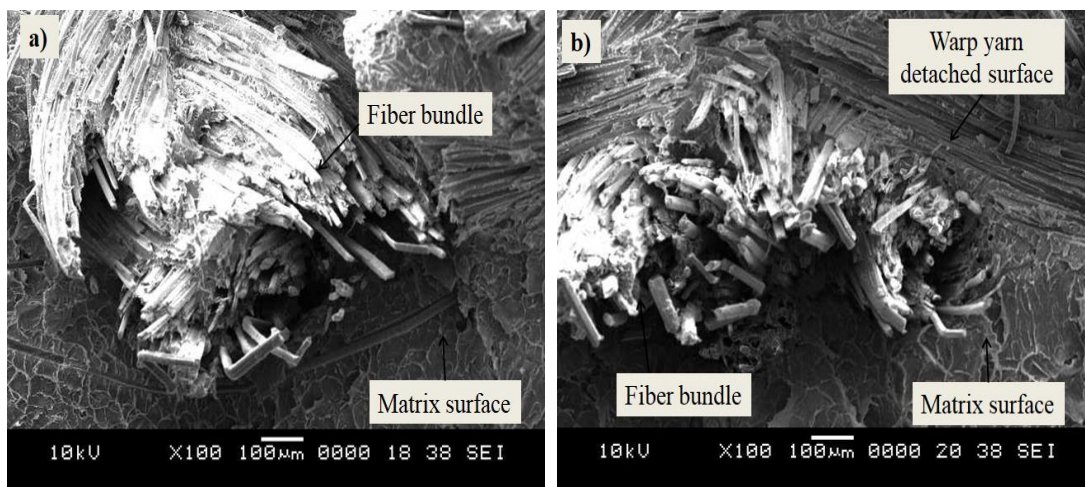


Figure 3.14. Micrographs of flexural test specimen fractured surfaces a) warp direction and b) weft direction loaded composites

Flexural properties of the present NFBF reinforced PLA composites are compared with the flexural properties of other natural fibre reinforced PLA composites available in literature. Flexural properties are also compared with the corresponding PLA values and listed as percentage increase (+) or decrease (-) in Table 3.4. From Table 3.4, it is observed that flexural strength of the current NFBF/PLA composites are higher than the other PLA composites. Flexural modulus of the present NFBF/PLA composites is also in an acceptable range. This study demonstrates that the reinforcement of natural fibre braided yarn woven fabric (NFBF) enhances the tensile strength, tensile modulus, flexural strength and flexural modulus of PLA composites.

Table 3.4 Comparison of flexural properties of NFBF/PLA composites with different natural fibre PLA composites (Percentage (+) increase or (-) decrease of the composites is calculated with respect to neat PLA)

Manufacturing method	Fibre matrix compounding	Kind of Fibres	Fibre mass (%)	Flexural Strength (%)	Flexural Modulus (%)	References
Compression molding	Solution casting	Flax braided yarn fabric	33	+71	+88	This study
		Bamboo fabric	35	+23	+22	(Rawi et al. 2013)
	Two-roll mill	Ramie	30	+11	n.s	(Tao et al. 2009)
		Jute	30	+7	n.s	(Tao et al. 2009)
		Ramie	30	+11	+22	(Yu et al. 2014)
Injection molding	Twin screw extruder	Abaca	20	-4	+57	(Shibata et al. 2003)
		Glass	20	+48	+90	(Wang et al. 2019)
		Banana/sisal	30	+15	+16	(Asaithambi et al. 2014)
	Coating die and extruder	Abaca	30	+24	+107	(Bledzki et al. 2009)

Based on the mechanical properties study, it is concluded that the NFBF/PLA composites can be used in the different applications. These composites can be used in consumer applications such as furniture, combs, telephone stands, flower pots, watchcases, trays and toys. These composites are also useful for the commercial applications for example automobile seat backs, door panel, rear parcel shelves, spare tyre cover and other interior trim. Because these composites mechanical properties are comparable with the other commercially available natural fibre composites, such as bast fibre/polypropylene, wood fibre/acrylate have tensile strength of 18-30 MPa, 25-30 MPa (Graupner et al. 2009) and bending strength for natural fibre reinforced unsaturated polyester composites is 70 MPa (Holbery and Houston 2006). By considering these values the present NFBF/PLA composites can be used in different areas of applications.

3.3.3 Impact properties of NFBF reinforced PLA composites

Impact strength of the composites along weft and warp directions are compared with pure PLA and the results are plotted in Figure 3.15 and Figure 3.16 respectively. One can clearly observe from the results that the variation in fibre reinforcement influences impact strength of composites. It can be seen from Figure 3.15 that the impact strength of the NFBF/PLA composites for addition of NFBF 11% and NFBF 22% is lower than the pure PLA. Literature study also shows that impact strength of PLA reduces due to the natural fibre reinforcement. For instance, Oksman et al. (2003) prepared PLA biocomposites by reinforcing heckled flax fibre filled in the form of handmade roving using twin screw extruder and compression molding. Neat PLA polymer showed impact strength of 14 KJ/m^2 and composite filled with 40 wt.% flax fibre showed 12 KJ/m^2 approximately. This flax/PLA composite impact strength is 14% less than virgin PLA. Asaithambi et al. (2014) carried out the impact strength study on 30 wt.% banana/sisal fibre filled PLA hybrid composites prepared by injection molding process and then the composites results are compared with the neat PLA. This study presents that the impact strength of the hybrid composites is 30% lower than the neat PLA. Plackett et al. (2003) used film stacking and hot-press compression molding methods to fabricate non-woven jute mat PLA composites with 40 wt.% of jute fibre. They recorded the impact strength for pure PLA is 15.4 KJ/m^2 and for jute/PLA it is 14.3 KJ/m^2 . The jute/PLA impact strength value is 7.14% less compared to neat PLA. Taib et al. (2014) prepared kenaf fibre PLA composites with 40 wt.% of fibre using compression molding method. From impact experiment they noted that the PLA polymer has impact strength of 7.83 KJ/m^2 and the kenaf-PLA has 6.27 KJ/m^2 . This study also shows the impact strength of the composite is lesser (20%) than the neat PLA. From literature also it is noticed that the impact strength of the thermoplastics reduces with the addition of agro-fibres (Plackett et al. 2003). Further, from Figure 3.15, it is also observed that with the increase in fibre content from 11 wt.% to 33 wt.% the impact strength of the braided flax fibre PLA biocomposites is also increases. Bax and Mussig (2008) also observed the same trend for 10, 20 and 30 wt.% of flax fibre reinforced PLA composites. The present composites filled with 33 wt.% fibre showed impact strength of 18.58 KJ/m^2 and this value is

12.38% higher than pristine PLA value of 16.53 KJ/m². This indicates that the composites with higher fibre content are able to sustain higher impact load compared to the composites with lower fibre content. The PLA composite with 33 wt.% of braided flax fibre showed excellent energy absorption capability compared to other composites (11% and 22%) and pristine PLA.

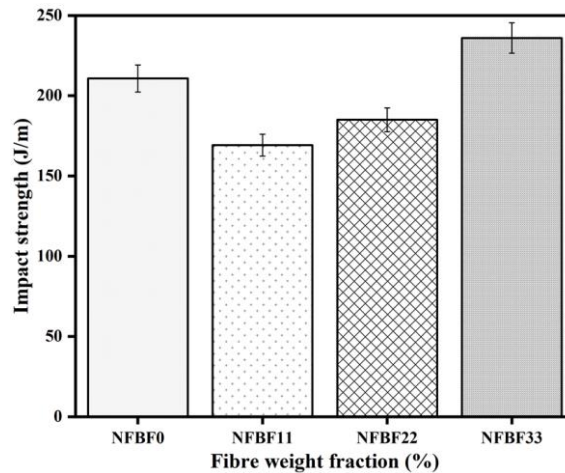


Figure 3.15. Impact strength of PLA and NFBF/PLA composites under warp direction loading

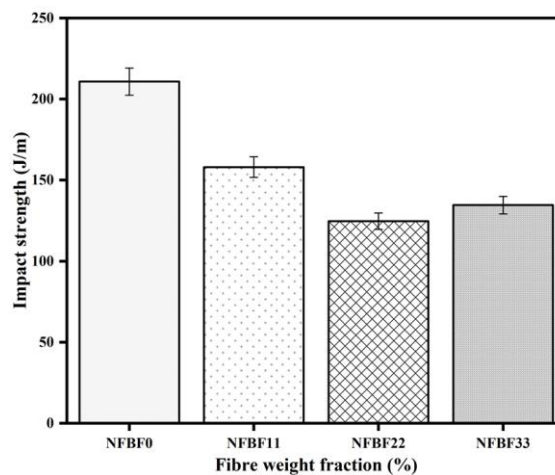


Figure 3.16. Impact strength of PLA and NFBF/PLA composites under weft direction loading

In Figure 3.16, NFBF/PLA composites showed the poor impact strength compared with the pure PLA along weft direction. In this loading condition pendulum hits the specimen along the warp direction. More number of yarns present in the warp direction creates stress concentration. Hence very small amount of energy is required

for the crack initiation. As a result of this, the impact resistance of un-notched natural fibre reinforced thermoplastic composites decreases (Plackett et al. 2003).

The SEM micrographs of the impact fractured NFBF composites in both warp and weft directions are represented in Figure 3.17. Figure 3.17a shows failure of the impact test specimen due to brittle failure of matrix and fibre fracture under warp loading direction. Figure 3.17b shows the presence of air gap, fibre fracture and warp yarn bundle present in the composite. This reveals that the failure occurred due to stress concentration and lack of matrix material along the warp direction and hence there may be less energy absorption in weft direction loading compared to warp direction loading.

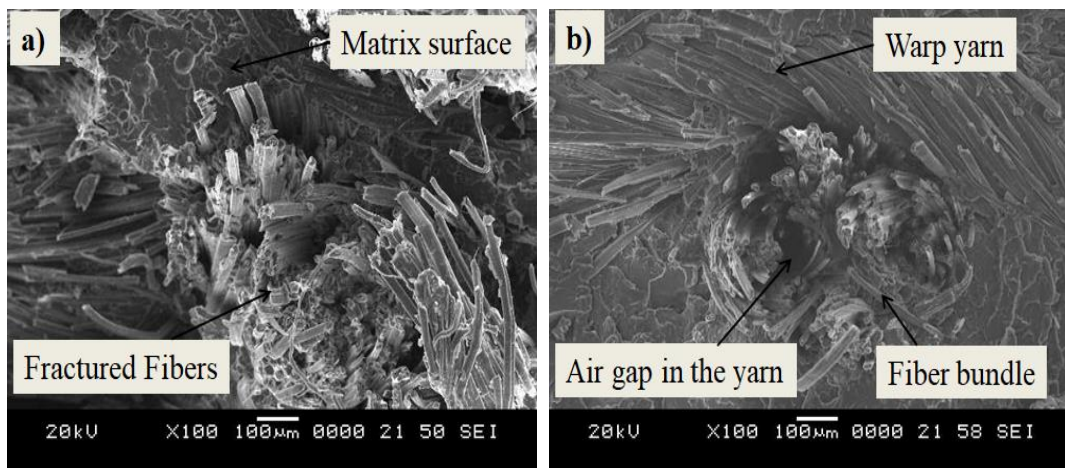


Figure 3.17 Fractured surface photographs of impact test specimen a) warp direction loading and b) weft direction loading of NFBF composites

3.3.4 Interlaminar shear strength (ILSS)

From the tensile, flexural and impact tests it is observed that the strength is more for the warp direction loading compared to the weft direction loading. Hence, the interlaminar shear strength of the NFBF/PLA composites is studied only for warp loading.

SBS tests are performed in order to investigate the interlaminar shear strength (ILSS) of the NFBF/PLA composites. Typical load-displacement diagram of the pure PLA and NFBF composites is shown in Figure 3.18. Pure PLA and NFBF composite materials showed similar trend in load-displacement response curves. From Figure

3.18, it is noticed that the load bearing capacity of the PLA is enhanced with the reinforcement of NFBF. Reinforcement of NFBF also improved the damage tolerance of the PLA, hence it requires higher load for failure. NFBF33 composite achieved highest peak load compared to other NFBF composites and neat PLA. The microscopic image of composite sample (NFBF22) before and after the ILSS test is shown in Figure 3.19. After the SBS test specimen showed crack at the lower side of the specimen and also presented the fibres bridging.

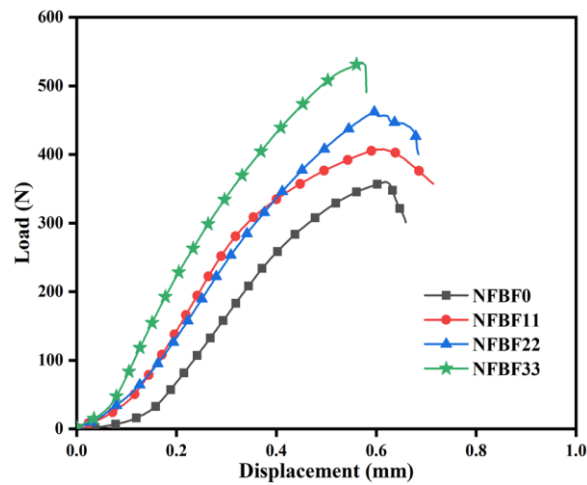


Figure 3.18 Load - displacement curves of PLA and NFBF composites

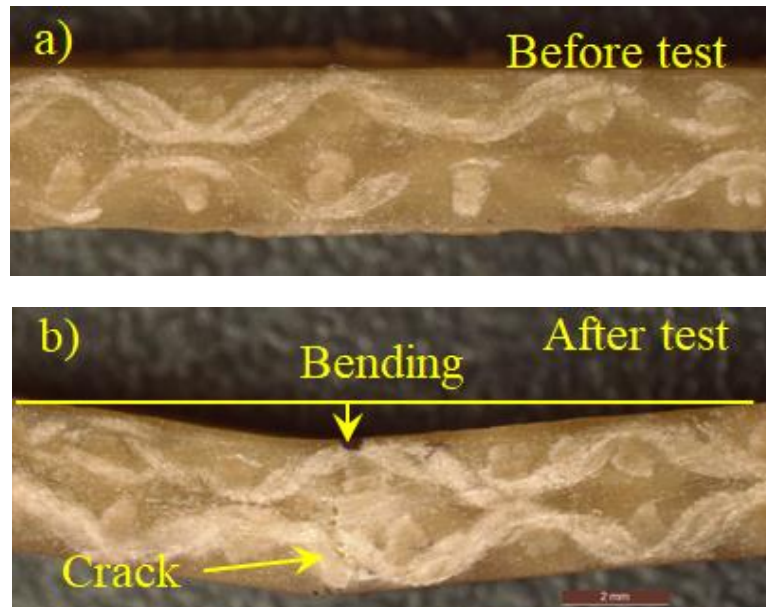


Figure 3.19 Microscopic image of the NFBF/PLA composite specimen (a) before and (b) after the SBS test

ILSS is calculated from the load histories using Equation 2.6. ILSS is calculated as the average of five samples for each composite and the results are presented in Figure 3.20. As received PLA sample showed shear strength of about 15 MPa. The NFBF reinforcement enhanced the ILSS of composites and it increases with increase in wt.% of fabric. The same trend is observed for the plain woven carbon fibre reinforced plastics (Baran et al. 2018; Naik 1995) also. This indicates that the in-plane shear properties are enhanced due to the reinforcement. This enhancement can be attributed to improved stiffness and load bearing capacity of the composites with the reinforcement of solid braided yarn woven fabric. Also, presence of strong interfacial bonding between fibre-matrix enhances the strength of the composite (Dhal and Mishra 2013; Sadasivuni et al. 2019). Since, strong fibre-matrix interfacial bonding helps in uniform load transition between matrix and filler. Maximum shear strength of about 20 MPa is observed for NFBF33 composite which is 33.33% high compared to pristine PLA.

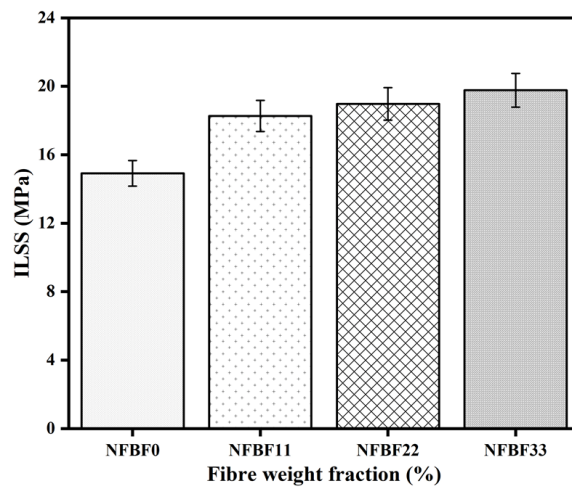


Figure 3.20 Interlaminar shear strength of PLA and NFBF composites

Figure 3.21 (a-c) shows the micrographs of fractured surfaces of the SBS test specimens. The typical failure mechanisms such as fibre bridging, interlaminar shear crack and normal cracks are showed by NFBF composites. Composites exposed to SBS are subjected to ordinary or normal cracks since the interlaminar shear failure does not generally happen at the mid-plane of the composite laminate (Thiagamani et al. 2019). From micro-scale results it is also observed that the flax braided fibres have played bridging roles on the interfacial adhesion between fibre and matrix plies. This

improves the stress-transfer capability of the composites. Interlaminar properties of the composites enhances with the flax fibres bridging (Zhang et al. 2013).



Figure 3.21 Microscopic images of the fractured composite samples from SBS test carried out on a) NFBF11, b) NFBF22 and c) NFBF33 composites

3.4 Conclusions

Geometrical and mechanical characterization is done on 3D braided yarn and fabric woven using the 3D braided yarns. Results indicate that the tensile strength and modulus of braided yarn woven fabrics are reduced compared to braided yarn. The warp direction of fabric showed higher ultimate stress compared to weft direction.

Flexural, tensile, impact and SBS experiments are carried out on prepared composites. Reinforcement of NFBF enhanced the tensile and flexural strength of the composites. Compared to virgin PLA, composites reinforced with NFBF showed 38%, 76%, 71% and 88% increase in the tensile strength, Young's modulus, flexural strength and flexural modulus respectively for 33 wt.% of NFBF. Highest impact strength of 236

J/m (18.58 KJ/m^2) also observed for the NFBF33 composite. Incorporation of braided flax fibre woven fabric enhanced the interlaminar shear strength of the composites compared to pure PLA. Further with increase in fibre content the shear strength is increased and the composite with 33 wt.% of fabric showed higher improvement of about 33.33% compared to virgin PLA. From micro-graphs it is noticed braided flax fibre bridging and this mechanism is responsible for enhancement in the interlaminar shear property.

Warp direction loaded composites showed good mechanical properties compared to weft direction loaded composites. Comparative study of present NFBF composite with other natural fibre composites showed good mechanical properties. According to the present findings, the NFBF bio-composites could be used in light weight applications.

4 THERMAL PROPERTIES OF COMPOSITES

4.1 Introduction

Excellent application-oriented thermal characteristics are also discovered in relation to the mechanical characteristics of the natural fibre reinforced composites and these thermal properties are contingent upon a few parameters, for example, density, homogeneity and the morphology of composite materials (Sair et al. 2019). In materials science, thermal analysis is an important aspect as physical, chemical and mechanical characteristics of the materials are examined as an element of temperature and time (Krishnasamy et al. 2019). In civil, automotive, aerospace, electronics and other commercial applications it is essential to study structural behaviour of composites under thermal loading conditions (Demosthenes et al. 2019). Apart from the study on typical thermal properties such as flammability, DSC, TGA and HDT of a newly developed material, it is also important to study effect of heating on deflection of a structure made of a new material. Beam like structure made of NFBF/PLA composite exposed to different kinds of temperature variation along the length of the beam is investigated in this study. Transverse deflection of the beam as a function of temperature is analysed with the help of an in-house developed set-up.

4.2 Flammability

Natural fibre composites are expected to be used in several engineering applications in the process of reduce the use of conventional material. During their service these composites may be exposed to fire. Hence, knowledge of the composites behaviour under fire conditions is a key requirement (Chapple and Nandjiwala 2010; Kozłowski and Władyska-Przybylak 2008). The burning rate of the pure PLA and NFBF/PLA composites is presented in Figure 4.1. Pure PLA shows the higher burning rate than the natural fibre filled composites. As seen from Figure 4.1, the burning rate of the NFBF/PLA composites is low compared to pure PLA. It is also observed that the burning rate reduces with increase in filler content. From these results, it is clear that the flame retardancy of the PLA polymer is enhanced due to the reinforcement of NFBF. Burning rate of NFBF33 is 75.41% lower than the pure PLA. Fire resistance

of the natural fibre reinforced composites depends on the chemical composition of the fibre (cellulose, hemicellulose, lignin and silica or ash), fibre microstructure, higher crystallinity and lower polymerization (Dittenber and Gangarao 2012).

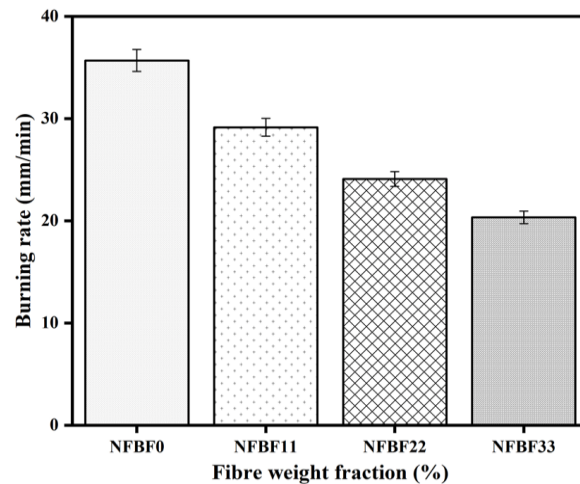


Figure 4.1 Burning rate of pure PLA and NFBF/PLA composites

4.3 Crystallisation and melting behaviour

DSC results for the first and second heatings of PLA and NFBF/PLA composites are presented in Figure 4.2 and the evaluated thermal properties are summarised in Table 4.1 and Table 4.2 for first and second heating conditions respectively. During the thermal scanning of the each sample endothermic melting peaks are observed. No exothermic peaks are found; the results could be clarified by the low molecular mass of PLA polymer (Adomavičiūtė et al. 2015; Ahmed et al. 2009; Cao et al. 2003). Results presented in Table 4.1 and Table 4.2 indicate that there is no significant change in the glass transition temperature (T_g) of the PLA and NFBF/PLA composites for both the heatings. There is a small variation (-1.6 to 1.1° C) in glass transition temperature (T_g) of PLA is observed due to the NFBF reinforcement. This indicates that the fibre reinforcement does not affect much on the glass transition temperature of PLA. This is due to, no alter in the mobility of the polymer chain with the reinforcement (Triki et al. 2013). From Figure 4.2 and Table 4.1 it is clear that the crystallisation temperature (T_c) of the pure PLA is high, due to the reinforcement of NFBF the crystallisation temperature of the composite is reduced in first heating. Results of second heating of the pure PLA and NFBF/PLA composites (Table 4.2)

showed that the crystallisation temperature of the PLA improved due to reinforcement of the NFBF because of nucleation effect of the natural fibre (NFBF) (Lee and Wang 2006). Figure 4.2 shows a small variation in the melting temperature (T_m) peaks, which is improved by 4° C (for first heating condition) and 5° C (for second heating condition) for the NFBF/PLA composites compared to the pure PLA. Enthalpy for melting (ΔH_m) and percentage crystallinity (X_c) are enhanced for the NFBF/PLA composites over pure PLA. This can be attributed to the nucleating ability of the natural fibre to enhance the PLA crystallisation. As a result of chemical and mechanical interlocking between fibre and matrix help the fibre surface to act as nucleation sites for the PLA crystallisation and this promotes the transcrystalline regions on the fibre surface (Islam et al. 2010c). It is noteworthy that these crystallinity results are in good agreement with some other available natural fibre/PLA composites (Adomavičiūtė et al. 2015; Islam et al. 2010c; Pilla et al. 2008, 2012; Rosa et al. 2011; Yang et al. 2016).

Table 4.1 Thermal characteristics of the PLA and NFBF/PLA composites for first heating scan

Sample	T_g (°C)	T_c (°C)	T_m (°C)	ΔH_m (J/g)	X_c (%)
NFBF0	67.0	127.9	155.1	14.62	15.72
NFBF11	65.4	119.5	158.2	41.61	50.27
NFBF22	65.8	118.0	155.2	32.04	44.16
NFBF33	68.1	119.7	159.3	23.03	36.96

Table 4.2 Thermal characteristics of the PLA and NFBF/PLA composites for second heating scan

Sample	T_g (°C)	T_c (°C)	T_m (°C)	ΔH_m (J/g)	X_c (%)
NFBF0	66.0	122.3	150.6	5.60	6.025
NFBF11	68.1	124.4	155.0	37.30	45.06
NFBF22	66.0	122.2	152.9	30.18	41.60
NFBF33	70.0	127.3	155.9	22.76	36.52

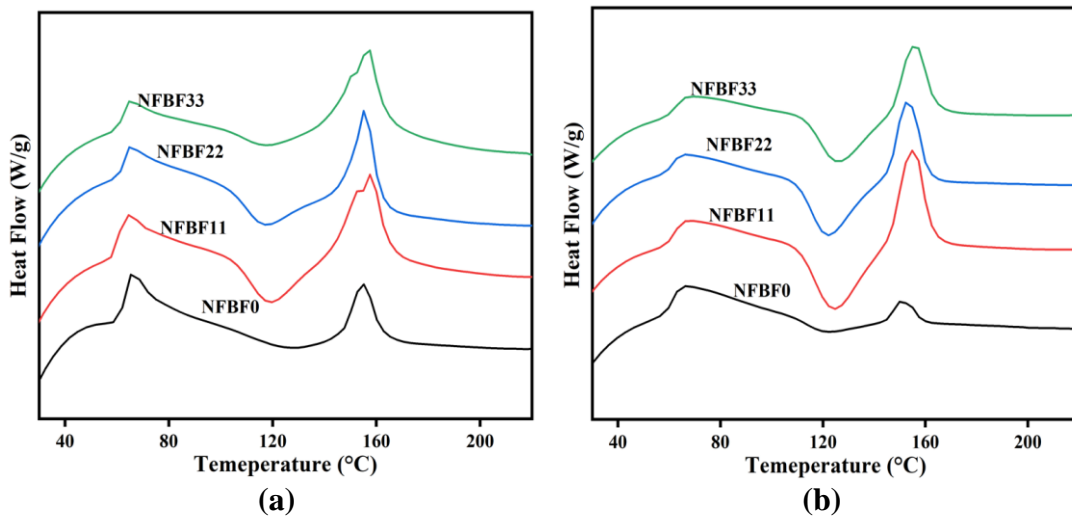


Figure 4.2 DSC thermograms of PLA and NFBF/PLA composites for (a) first heating scan and (b) second heating scan

4.4 Thermogravimetric analysis

TGA thermograms of flax fibre, pure PLA and NFBF/PLA composites are shown in Figure 4.3. In which, thermal degradation of materials is divided into two stages based on the nature of the graph. The first stage of the degradation starts at the temperature range of 30° C to 250° C. In this stage, there is a small weight loss or thermal degradation of materials occurs in the range of 0.82% to 10.87%. This degradation occurs by evaporation of moisture content from the flax fibre, PLA and composites. Observation shows that the flax fibre has a higher content of moisture about 10.87%. Hydrophilic nature of the natural fibre is responsible for the moisture absorption from the surrounding environment. The pure PLA has very less moisture content and the moisture content of the composite increases with the fibre content. NFBF33 composite showed higher weight loss of about 5.18% due to the moisture evaporation. Very deep reduction in the percentage of weight loss is observed in the temperature range of 230° C to 350° C. This signifies drastic decrease in thermal or heat stability of the flax fibre, PLA and NFBF/PLA composite. In the second stage, the shoulder is obtained at the end of the process around 280° C – 350° C as shown in Figure 4.3. This is due to the residual mass of fibre, polymer and composites left after thermal degradation and this residual mass is called as char (Devallencourt and Capitaineh 1996; Dobircau et al. 2009; Kumar et al. 2013).

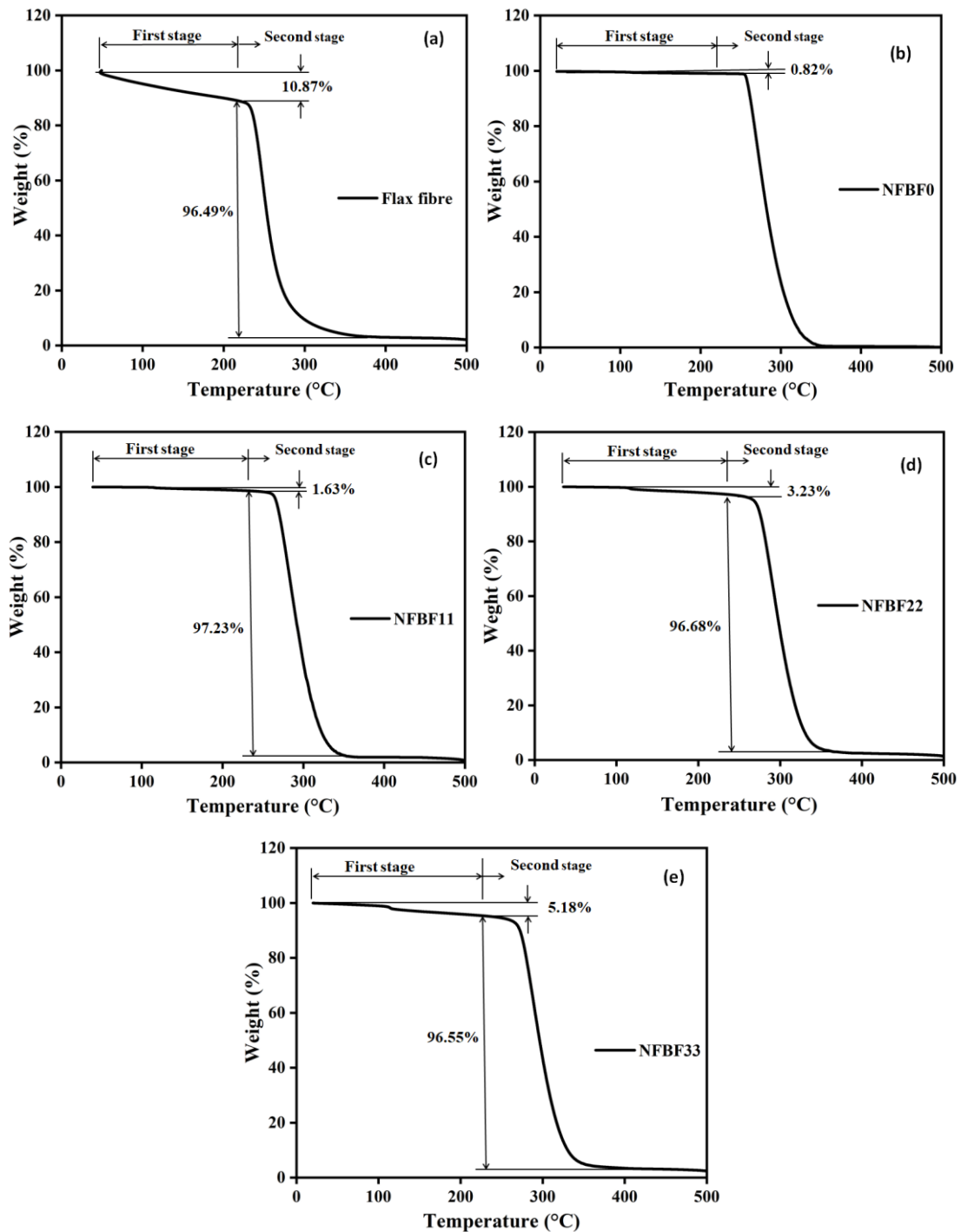


Figure 4.3 Thermogravimetric analysis of (a) Flax fibre, (b) PLA (c) NFBF11, (d) NFBF22 and (e) NFBF33 composites.

Degradation temperature for different percentage of weight loss of flax fibre, PLA and NFBF/PLA composites are reported in Table 4.3. Results in Table 4.3, illustrate that thermal degradation temperature of flax fibre reinforced PLA composites

increases with increase in fibre content compared to pure PLA. NFBB22 and NFBB33 reinforced composites showed nearly the same thermal degradation temperature around (319° C) which is higher than pure PLA and flax fibre. From Table 4.3, it is also observed that the residual mass percentage increases with the amount of fibre reinforcement with the PLA polymer. The NFBB33 composite has the highest residual mass (char) of about 5.01%. The temperature of degradation and residual mass percentage of NFBB/PLA composites depend on interfacial characteristics with polymer, surface condition and nature of fibres (Kumar et al. 2013).

Table 4.3. Effect of thermogravimetric temperature on weight loss of PLA and NFBB/PLA composites

Material	Weight loss %					Residual mass at 350 °C (%)
	10%	20%	40%	60%	80%	
Flax fibre	198.84	237.01	247.08	256.56	272.22	4.08
PLA	260.75	266.23	276.05	286.58	301.47	1.49
NFBB11	270.20	276.02	286.24	297.58	311.73	2.58
NFBB22	274.98	281.81	292.62	303.54	319.86	4.11
NFBB33	270.97	279.52	290.44	301.77	319.15	5.01

These results represent that the thermal stability of the composites is enhanced with the reinforcement of the NFBB. This is due to good interfacial bonding between fibre and matrix. The previous investigations reported that good fibre-matrix bonding improves the uniform heat transfer in the composites and thus results in higher thermal stability of the composites (Hong et al. 2017). Jang et al. (2012) and Khuntia and Biswas (2020) also reported thermal stability of the composites is increased with the natural fibre reinforcement compared to the neat polymer matrix.

4.5 Heat deflection temperature

HDT is the temperature required to achieve a deflection of 0.25 mm for an applied load of 0.455 MPa. HDT provides a maximum temperature limit for a material used in thermal applications. HDT behaviour of the pure PLA and NFBB/PLA composites is shown in Figure 4.4. Figure 4.4 shows, pure PLA has a HDT value of 54.80° C and it

is increased with fibre reinforcement. It is also observed that, as the fibre content increases the HDT value of the composites also increases proportionately. Increase in fibre content from 11% to 33% increases HDT value also from 88.66° C to 127.67° C, which is 61.78% to 132.97% higher than the pure PLA. Flax fibres are bad conductors of heat (Kymäläinen and Sjöberg 2008), reinforcement of these fibres enhances the thermal stability of the composites (Khuntia and Biswas 2020). Due to this reason HDT of the NFBF/PLA composites is improved. Also, the previous investigations reported that good fibre-matrix bonding improves the uniform heat transfer in the composites which also results in higher thermal stability of the composites (Hong et al. 2017). The NFBF33 composite showed significant enhancement in HDT, due to better enhancement in the modulus (stiffness) of the composites which reduces the creep rate under given load (Liu et al. 2005, 2007). This enhancement in HDT is attributed to the strong fibre-matrix interfacial strength as observed previously by other researchers (Awal et al. 2015; Huda et al. 2006; Singh et al. 2008). The findings of the NFBF strengthened PLA composite (high HDT values) results suggests that NFBF/PLA composites can be used in applications which require operating temperature higher than pure PLA.

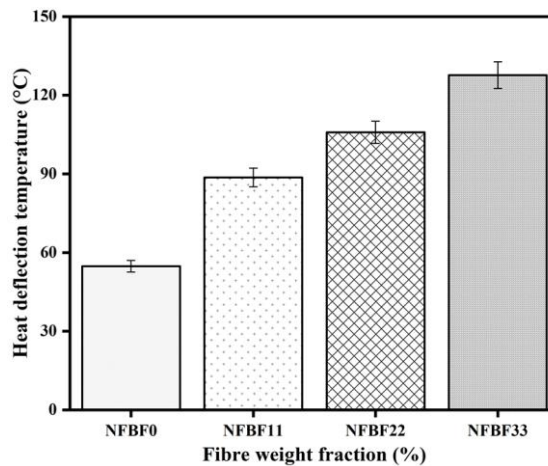


Figure 4.4 Heat deflection temperature of PLA and NFBF/PLA composites

4.6 Thermal deflection study

Effect of increase in temperature on transverse deflection of a beam like specimen made of PLA and NFBF/PLA composites under different heating conditions is discussed in this section. Before presenting the results associated with different

studies carried out, sample deflection curves of PLA and NFBF/PLA are given in Figure 4.5. This is done to understand the general trend in thermal deflection of PLA and NFBF/PLA beams with increase in temperature.

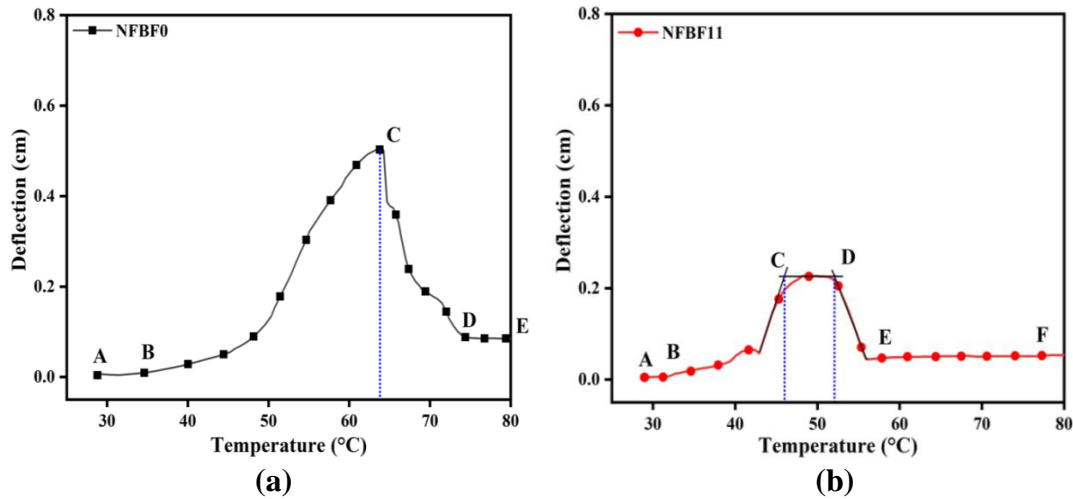


Figure 4.5 Thermal deflection curves of PLA (NFBF0) and NFBF/PLA composites

For this, thermal deflection of pure PLA and NFBF/PLA composite beams under case-1 heating is considered and the results presented in Figure 4.5. One can clearly observe from Figure 4.5 that the thermal deflection trends of the pure PLA and NFBF/PLA beams are totally different from each other and this can be explained by dividing the curves as shown in Figure 4.5. In stage A-B there is no major change in the deflection with increment in temperature for both the PLA and NFBF/PLA beams. This indicates that the beams provide some resistance against heating initially. In stage B-C, for PLA beam the deflection increases exponentially with increase in temperature and reaches maximum deflection at point C that is 63° C. Maximum deflection of the pure PLA is noticed near the glass transition temperature (67° C). At this temperature, gap between molecules increases and the material experiences transition from solid state to rubbery state (Shrivastava 2018). However, for NFBF/PLA composite beams the rate of increase in deflection amplitude is less compared to PLA beam. Reduction in the thermal deflection of the composites can be attributed to the enhancement of Young's modulus and reduction in co-efficient of thermal expansion due to the NFBF reinforcement.

In stage C-D, with further increment in temperature, the beam deflects in opposite direction drastically for PLA beam. Glass transition temperature (T_g) of PLA,

NFBF11, NFBF22 and NFBF33 composites is 67° C, 65.4° C, 65.8° C and 68.1° C respectively. When the temperature is less than T_g , the molecular chains cannot move around due to less energy. However, the energy increases with increase in temperature and allows the molecular chains to move around each other at T_g . As a result of this, the material changes from rigid state to flexible state with significant reduction in strength. It is also well known that there is no significant variation in storage modulus with increase in temperature till T_g . The increase in deflection of PLA beam with increase in temperature till T_g can be attributed to two factors. One is increase in the energy to allow the polymer chain to move around each other and another factor is thermal stress which increases with the temperature. The expression for thermal stress is $\sigma_{th} = E\alpha\Delta T$; E -Young's modulus, α -co-efficient of thermal expansion and ΔT is the temperature rise above ambient temperature. Thermal stress increases with increase in ΔT and also increases the deflection of the beam till T_g . Beyond, T_g , the deflection of the beam reduces suddenly due to significant reduction in the storage modulus which causes a significant reduction in the thermal stress. In the case of NFBF/PLA composite beams there is no significant change in deflection with increase in temperature in region C-D. This can be ascribed to the action of viscoelastic stresses developed due to heating. This stresses holds the beam in the maximum deflected position for some time even though there is an increase in temperature. Due to the combined effects of visco-elastic behaviour, nature of heat transfer, Young's modulus and effective co-efficient of thermal expansion the thermal deflection behaviour of NFBF/PLA beams is entirely different than the PLA beam. Also the action of viscoelastic stresses developed due to heating holds the beam in the maximum deflected position for some time even with increase in temperature.

In stage D-E there is no much variation in deflection with further increment in temperature. However, the beam deflects in opposite direction drastically due to the release of the developed viscoelastic stresses. Beyond this stage there is no noteworthy change in deflection with increment in temperature. This clearly shows that the crept viscoelastic behaviour due to an increase in temperature, results in change in thermal deflection curves for PLA and NFBF/PLA composites.

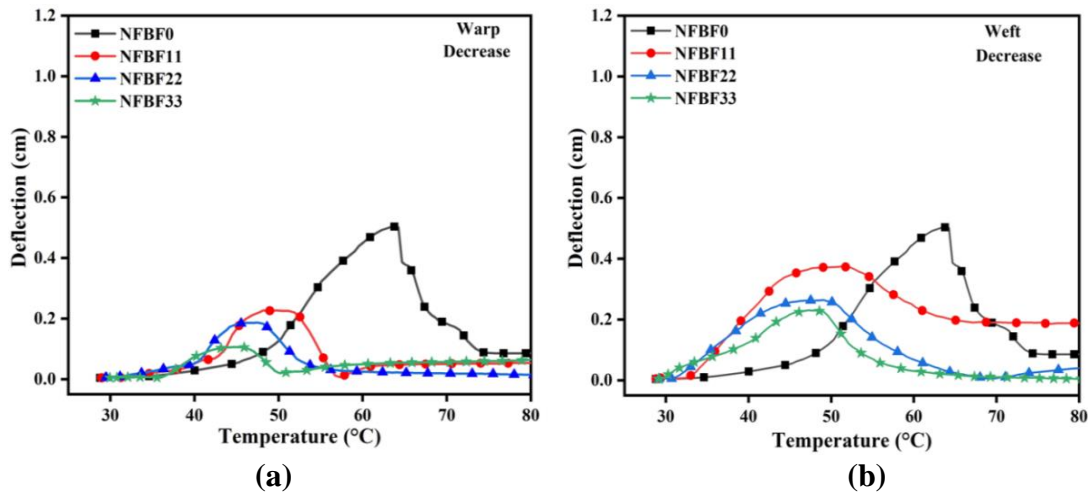


Figure 4.6 Thermal deflection curves for decrease case in (a) warp direction and (b) weft direction loading of PLA and NFBF/PLA composites

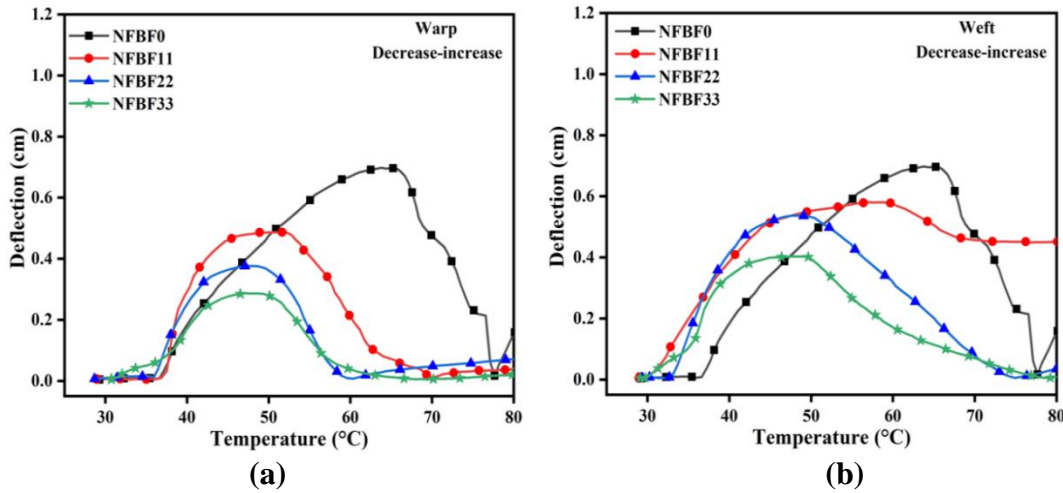


Figure 4.7 Thermal deflection curves for decrease-increase case in (a) warp direction and (b) weft direction loading of PLA and NFBF/PLA composites

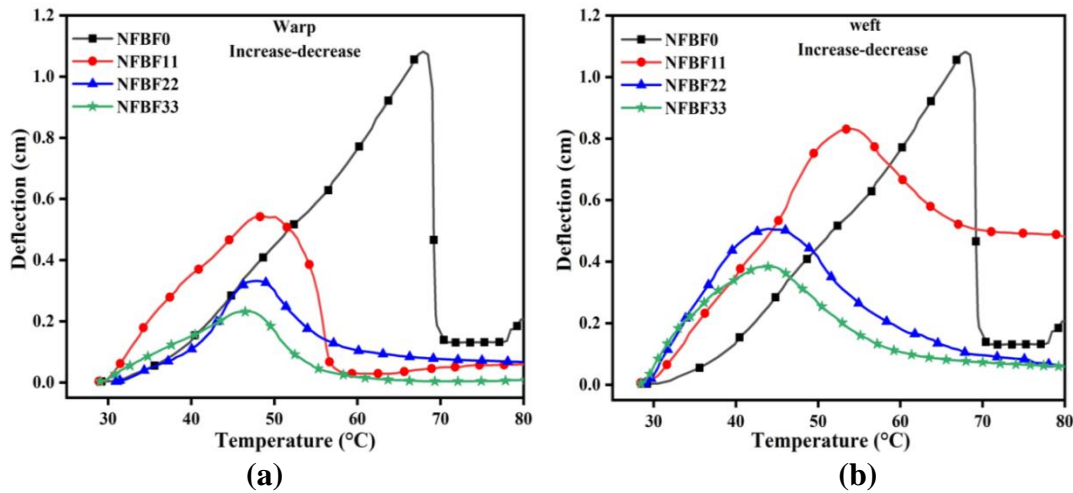


Figure 4.8 Thermal deflection curves for increase-decrease case in (a) warp direction and (b) weft direction loading of PLA and NFBF/PLA composites

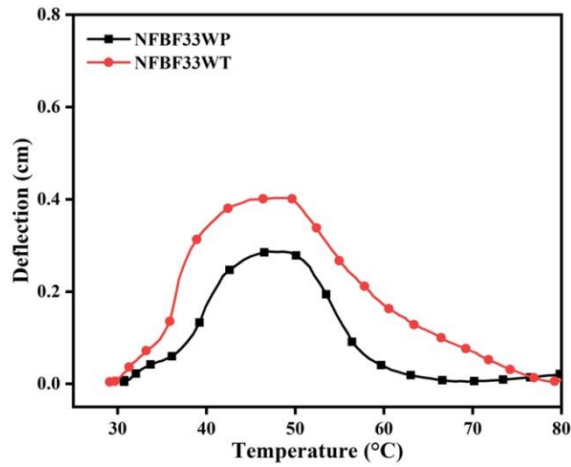


Figure 4.9 Comparison of deflection of NFBF/PLA composite beam under warp and weft direction heating in case 2

Thermal deflection test is conducted on pure PLA (NFBF0) and NFBF/PLA composites manufactured with 3 weight fractions (11%, 22% and 33%) of natural fibre and are represented as NFBF11, NFBF22 and NFBF33 respectively. This test is conducted in both the directions (warp and weft) of the NFBF/PLA composites and the test results are presented in graphs as shown in Figure 4.6, Figure 4.7 and Figure 4.8 for the different heating conditions as explained in section 2.12. The peak values of the PLA and NFBF/PLA composites are reported in Table 4.4. From, Figure 4.6 to Figure 4.8, it is evident that deflection behaviour of the PLA beam with increase in temperature is entirely different from the NFBF/PLA composites. Deflection of PLA beam is lower than that of NFBF/PLA beams in the temperature range of 30 - 50° C beyond that the deflection of the PLA beam is greater than the composite beams. Deflection of the composite beams reduces with increase in natural fibre content and less deflection is observed for NFBF33 composite beam. The same trend is observed for both warp and weft direction heatings. However, deflections of composite beams are high for the weft direction heating compared to the warp direction heating. This is because of lower stiffness and strength of the NFBF/PLA composite along the weft direction. Similarly, the width of region C-D corresponding to composite beams for the weft direction heating is greater than that of the warp direction heating. Basically the region C-D represents viscoelastic behaviour of the composites; the composite is relatively less stiff along weft direction as observed in terms of higher deflection. So, the viscoelastic stresses are high for the weft direction heating which is reflected as

larger C-D region. This decrease in viscoelastic stresses is observed with increase in fibre content also for both warp and weft direction heating. This clearly indicates that increase in structural stiffness due to fibre content reduces viscoelastic stresses. Same trend in thermal deflection of the beams with increase in temperature is observed under case-2 heating also. However, deflection of the beams under case-2 is higher compared to case-1 heating. This is due to heating of beam at both the ends under case-2 heating. Variation in deflection with increase in temperature of PLA beam under case-3 heating is slightly different compared to other cases. There is a sudden drop in deflection after reaching the peak due to the heating of the beam at the middle under case-3 (Figure 2.13c). There is no clear C-D region in the deflection curve of NFBBF/PLA beams under case 3 heating as observed in the other cases.

From Figure 4.6 to Figure 4.8, it is observed that the deflection of the pure PLA is high for all the cases compared to the NFBBF/PLA composites. It is also observed that the natural fibre reinforcement decreases the deflection and it is further decreasing with the increase in fibre content for both warp and weft direction heating of the NFBBF/PLA composites. This can be clearly seen from Figure 4.10 and Figure 4.11, where the PLA specimen has higher deflection and NFBBF/PLA specimens have relatively less deflection. It is observed that among the different cases studied the NFBBF33 composite showed lower deflection. NFBBF33 composite under warp direction heating showed 79%, 59% and 78% reduction in deflection compared to pure PLA for case-1, case-2 and case-3 respectively. Reinforcement of fibre enhances the strength and stiffness of the PLA and these properties are further enhanced with the increase in fibre weight percentage (Bodros et al. 2007; Graupner et al. 2009; Plackett et al. 2003; Porras et al. 2016). Hence, the deflection of the fibre reinforced composites reduces as compared with the pure PLA. In Figure 4.6 to Figure 4.8 the NFBBF/PLA composites under the weft direction heating showed higher deflection compared to the warp direction heated composites. Reason for this is the fabric used for the reinforcement has more number of yarns in warp direction (10 yarns/cm) and less number of yarns in weft direction (6 yarns/cm). Due to more number of yarns present in the warp direction the NFBBF/PLA composites have higher strength and stiffness under warp direction loading. Hence, it provides more resistance against the

deflection which results in lower deflection for warp direction heating compared to the weft direction heating as clearly seen in Figure 4.9. The NFBF33 composite under warp direction heating showed 54%, 29% and 53% lower deflection compared to NFBF33 composite under weft direction heating for case-1, case-2 and case-3 respectively.

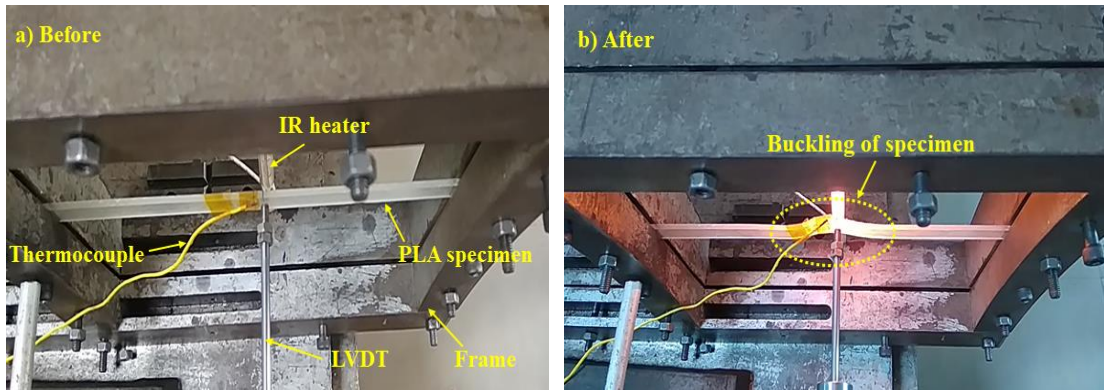


Figure 4.10 Images of PLA specimen under case 3 heating a) before test, b) after test

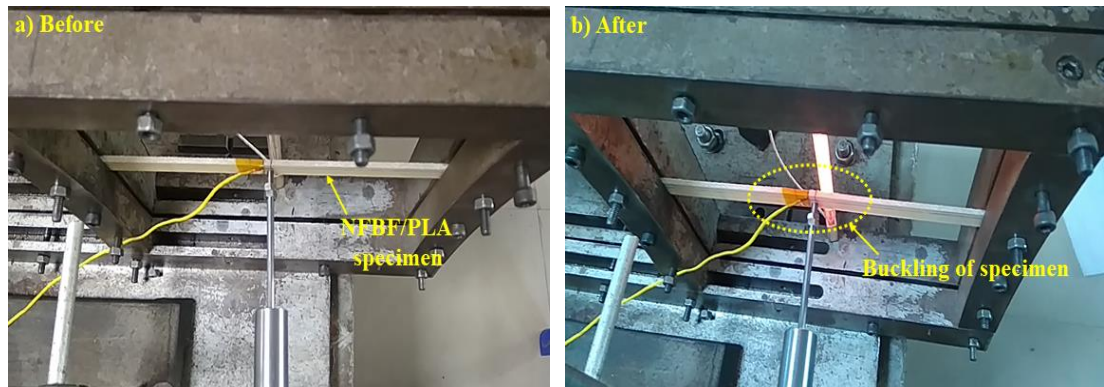


Figure 4.11 Images of the NFBF/PLA composites under case 3 heating a) before test, b) after test

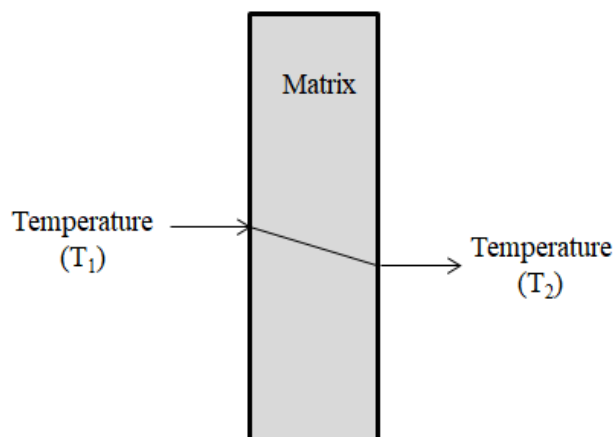


Figure 4.12 Heat transfer in pure PLA

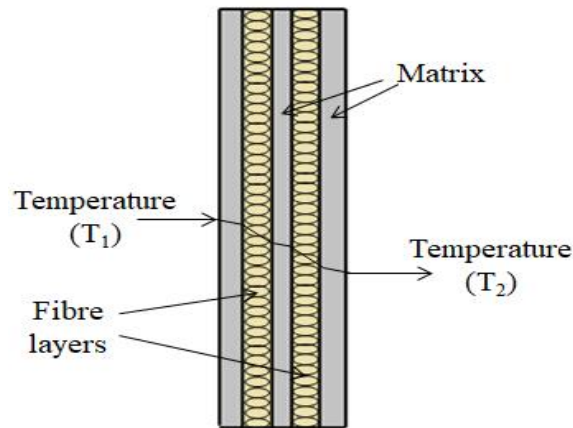


Figure 4.13 Heat transfer in NFBF/PLA composite

From Figure 4.6 to Figure 4.8, it is also observed that along with the deflection of the composites, temperature corresponding to peak deflection also reduced for the NFBF/PLA composites compared to pure PLA. Temperature distribution in the PLA and NFBF/PLA composites depends on the nature of heat transfer and thermal conductivity of the material. This can be explained with the help of Figure 4.12 and Figure 4.13 which shows heat transfer of PLA and NFBF/PLA composites respectively. Figure 4.12 shows the cross section of pure PLA, which has same thermal conductivity throughout the material. Because of this reason heat transfer takes place easily in the PLA beams. However, for NFBF/PLA composites, heat transfer of the material reduces because of change in thermal conductivity and physical properties of the fibre and matrix materials. Natural fibre is a bad conductor of heat; hence it provides the resistance to faster heat transfer rate (Kymäläinen and Sjöberg 2008). The thermal resistance property of the composites further enhanced with the increase in fibre content. Because of this reason there are drops in temperature as shown in Figure 4.13. The NFBF/PLA composite has PLA and NFBF layers in sequence. When the temperature is applied on the surface of the composites, the heat transfer takes place first through PLA layer where small temperature drop takes place and when it approaches NFBF layer, the natural fibre provides some thermal resistance due to porous structures. Hence at this point reduction of temperature for the composite is more compared to pure PLA. Increase in the number of natural fibre layers increases the heat resistance proportionately which results in increased temperature drop. This temperature drop between the interfaces of the

composite constituents is called as interfacial thermal resistance (ITR) (Pietrak and Wi 2015). The NFBF33 composite showed highest resistance to heat transfer, hence 26% to 30% reduction in temperature corresponding to the peak deflection is noticed compared to pure PLA temperature and according to the heating cases.

To check this thermal resistance behaviour of the composites a time study is done for the pure PLA and NFBF/PLA composites. This study is about to find the time needed to reach the ideal temperature (80° C) for PLA and NFBF/PLA composites and the results are presented in Figure 4.14. This study showed that the pure PLA required lesser time to reach the ideal temperature and natural fibre reinforced composites required more time to reach the same. This ideal temperature reaching time is proportional to the natural fibre content. To reach the ideal temperature, pure PLA required 61 seconds and mean while NFBF33 reinforced PLA composites in warp direction loading required maximum time which is recorded as 72 seconds. These time results also show the stability of the composites to sustain the temperature load better than pure PLA.

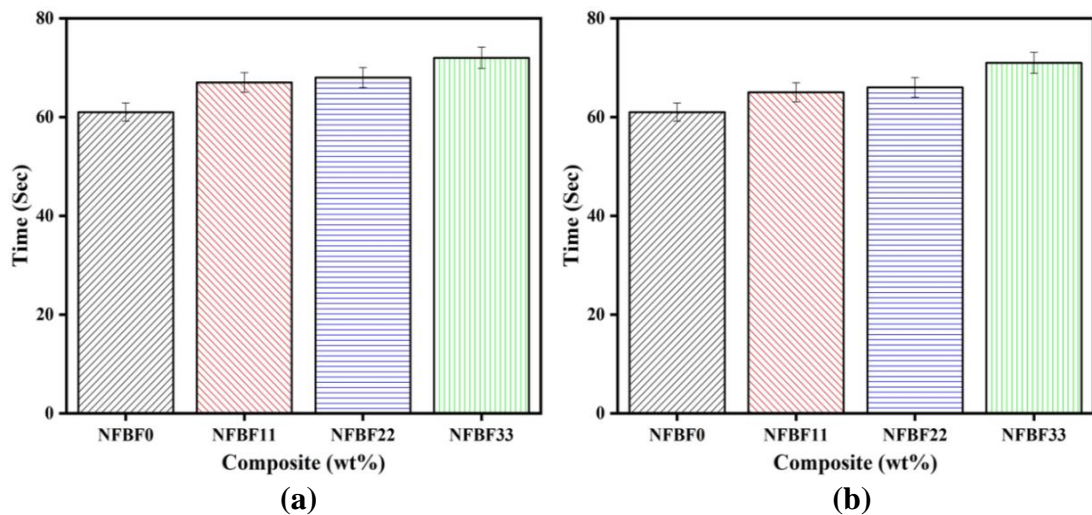


Figure 4.14 Time required attaining 80 °C surface temperature for PLA and NFBF/PLA composites under (a) warp and (b) weft direction loading

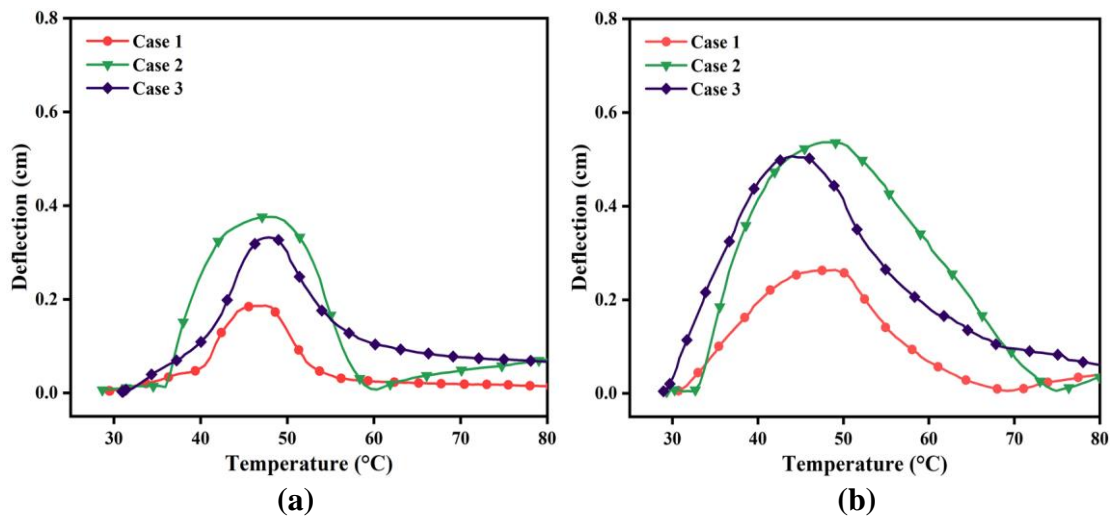


Figure 4.15 Heating profile effect on deflection of NFBF22/PLA under (a) warp and (b) weft directions heating

Effect of temperature profile on deflection behaviour of NFBF22/PLA composite beam under warp and weft heating is shown in Figure 4.15. Figure 4.15a shows that the deflection of the NFBF22 reinforced PLA composites is lower for case 1, higher in case 2 and medium for case 3 for both warp and weft direction heatings. In case 1 the temperature load (heating source) is applied near to the fixed end (Figure 2.13a). In this condition specimen stiffness is higher near to the fixed end hence it will give more resistance to the applied load due to this the deflection of the composite specimen is less. In case 2 the specimen is heated at both ends (Figure 2.13b). Because of this the composite specimen gives the more deflection. In case 3 heat is applied at the centre of the testing specimen (Figure 2.13c) where the stiffness of the composite specimen is less and hence the beam undergoes higher deflection than the case 1. Same trend in deflection is observed in weft direction loading of the NFBF22/PLA composites (Figure 4.15b) also. This test results are helpful for the application of automobile and other interior applications where the material should maintain the lower inside temperature compared to outside environment by providing resistance to heat transfer.

Table 4.4 Peak values of the deflection and temperature of pure PLA and NFBB/PLA composites

Case	Composite	Orientation	Deflection (cm)	Temperature (°C)
Case-1	NFBB0	-	0.503 ± 0.020	63.443 ± 3.17
	NFBB11	Warp	0.226 ± 0.013	48.184 ± 1.92
		Weft	0.375 ± 0.018	51.381 ± 3.59
	NFBB22	Warp	0.186 ± 0.005	47.563 ± 1.90
		Weft	0.262 ± 0.020	47.526 ± 2.37
	NFBB33	Warp	0.105 ± 0.006	44.742 ± 2.13
Weft		0.229 ± 0.011	47.180 ± 1.88	
Case-2	NFBB0	-	0.698 ± 0.055	63.770 ± 3.82
	NFBB11	Warp	0.478 ± 0.028	52.780 ± 2.11
		Weft	0.580 ± 0.029	57.031 ± 3.42
	NFBB22	Warp	0.375 ± 0.028	47.089 ± 2.35
		Weft	0.536 ± 0.042	47.571 ± 3.29
	NFBB33	Warp	0.286 ± 0.032	47.091 ± 2.85
Weft		0.402 ± 0.024	47.606 ± 1.90	
Case-3	NFBB0	-	1.082 ± 0.086	67.917 ± 4.075
	NFBB11	Warp	0.540 ± 0.032	50.168 ± 2.50
		Weft	0.826 ± 0.066	54.873 ± 3.19
	NFBB22	Warp	0.331 ± 0.029	47.854 ± 2.87
		Weft	0.505 ± 0.035	48.940 ± 2.95
	NFBB33	Warp	0.232 ± 0.019	47.136 ± 2.35
Weft		0.491 ± 0.029	48.021 ± 2.92	

4.7 Conclusion

Flammability results revealed that the flame retardance property of the NFBB composites is enhanced up to 75.41% with reference to the PLA. DSC and TGA results showed enthalpy (ΔH_m), percentage crystallinity (X_c) and thermal stability or thermal degradation temperature properties are enhanced for the NFBB/PLA composites compared to pure PLA. TGA also presented the residual mass (char) of the composites increased due to the fibre reinforcement. The NFBB33 composite has

the highest residual mass (char) of about 5.01%. HDT of the NFBBF/PLA composites improved from 61.78% to 132.97% for 11 to 33% fibre content compared to pure PLA.

Thermal deflection study is performed for both warp and weft direction heating conditions under three different types of temperature variations. The thermal deflection of the composites reduced with the reinforcement of the NFBBF due to improved stiffness of the composites. Due to the enhanced thermal resistance 26% to 30% of reduction in peak amplitude is noticed for NFBBF/PLA composites. Warp direction heated composites showed better thermal resistance and reduced deflection over weft direction heated composites. The warp direction heated NFBBF33 composite beam showed lowest deflection, which is 59% to 79% less compared to pure PLA and 29% to 54% less compared to weft direction heated NFBBF33 beam for case-1, case-2 and case-3 respectively. It is also noticed from the time study that the sustainability temperature is improved for the NFBBF/PLA composites and NFBBF33 achieved highest temperature sustainability of 72 seconds.

5 WATER ABSORPTION, THICKNESS SWELLING AND BIODEGRADABILITY OF COMPOSITES

In this chapter water absorption and thickness swelling effects on flexural properties of the NFBF/PLA composites are discussed. Flexural test is performed on the prepared composites before and after the water absorption test. Influences of fibre reinforcement, variation in fibre mass and different loading directions (warp and weft) of composites on water absorption and flexural properties are also analysed.

Biodegradability is the transformation of materials by bacteria or other living organisms into water, carbon dioxide and biomass due to biological activity, such as enzymatic action (Chan et al. 2018). In the present work, compost soil burial test is performed to study the biodegradability characteristics of the composites. Followed by this the weight loss and tensile strength of the composites are studied to analyse the biodegradability as a function of burial time. Biodegradability of PLA and its composites are characterised for possible use in packaging, construction and automotive interior applications as shown in Figure 5.1.

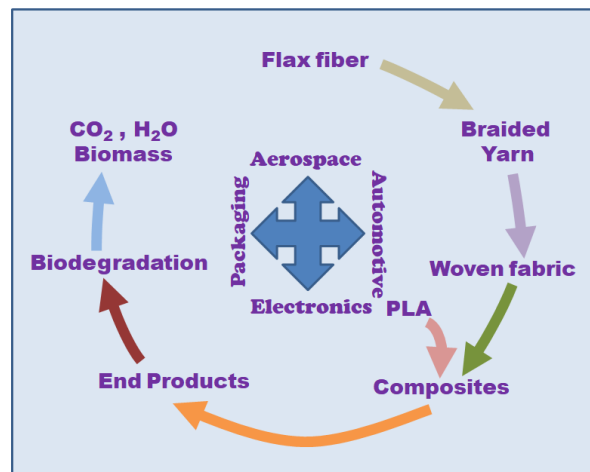


Figure 5.1 Schematic of manufacturing of braided flax yarn woven reinforced PLA composites

Pure PLA (NFBF0), NFBF/PLA composites with 22 wt.% (NFBF22) and 44 wt.% (NFBF44) of the fibre content having a thickness of 1.5 mm (Morales et al. 2017) are considered for this study.

5.1 Water absorption

For many applications of wood-plastic products water sensitivity is an important criterion. Water absorption and thickness swelling characteristics of NFBF/PLA composites at different loading levels of fibres immersed in distilled water at room temperature along warp and weft directions are shown in Figure 5.2 and Figure 5.3 respectively. Increase in fibre weight percentage enhances the water absorption and thickness swelling characteristics. Pure PLA do slightly absorb water of 0.3% and due to this reason 0.66% of thickness swelling is observed. The NFBF33 composite absorbed highest amount of water of about 4.55% and 5.78% for the warp and weft direction immersion respectively. This results in higher thickness swelling of these composites of about 2.75% and 2.92% respectively. Natural fibres are tubular porous structures, reinforcement of these fibres creates more water residence sites which increases the water absorption by capillary action. Natural fibre reinforced polymer composites water absorption depends on fibre permeability, fibre orientation, fibre loading, surface protection, exposed surface area, diffusivity, void content, temperature and individual components hydrophilicity (Ashori and Nourbakhsh 2009). Figure 5.2 and Figure 5.3 also clearly shows the effect of fabric orientation on water absorption and swelling behaviour of the composites. Higher amount of water absorption is observed for the composites immersed along the weft direction compared to the composite immersed along the warp direction. When NFBF/PLA specimen (127 mm × 13 mm × 3 mm) immersed longitudinally in the water, water absorption of the composites is high along the width direction compared to the longitudinal direction due to the exposure of more surface area. When the composites immersed along the weft direction of the composite, warp direction will be the width side of the test specimen. Hence, it absorbs more water due to the presence of more number of yarns along the warp direction. Similarly, when the warp direction composite is immersed, weft direction will be the width side of the test specimen. Due to this reason the water absorption of the composites is less for the warp direction immersion. Due to this reason the water absorption and thickness swelling percentage is higher for weft direction immersion compared to warp direction immersion. This

justifies the effect of fibre loading, exposed surface area and fibre orientation on water absorption.

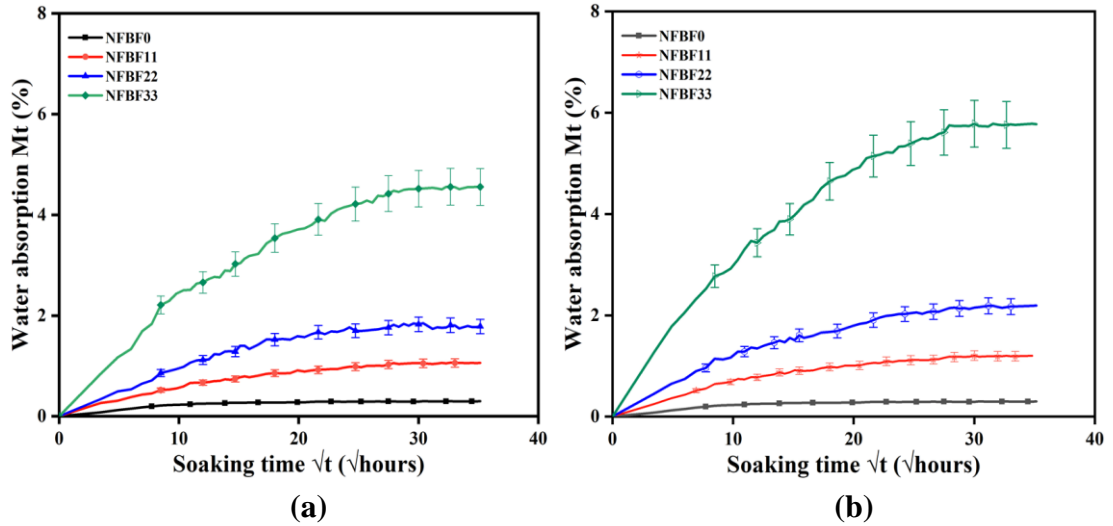


Figure 5.2 Water absorption of PLA and NFBF/PLA composites under (a) warp and (b) weft direction loading

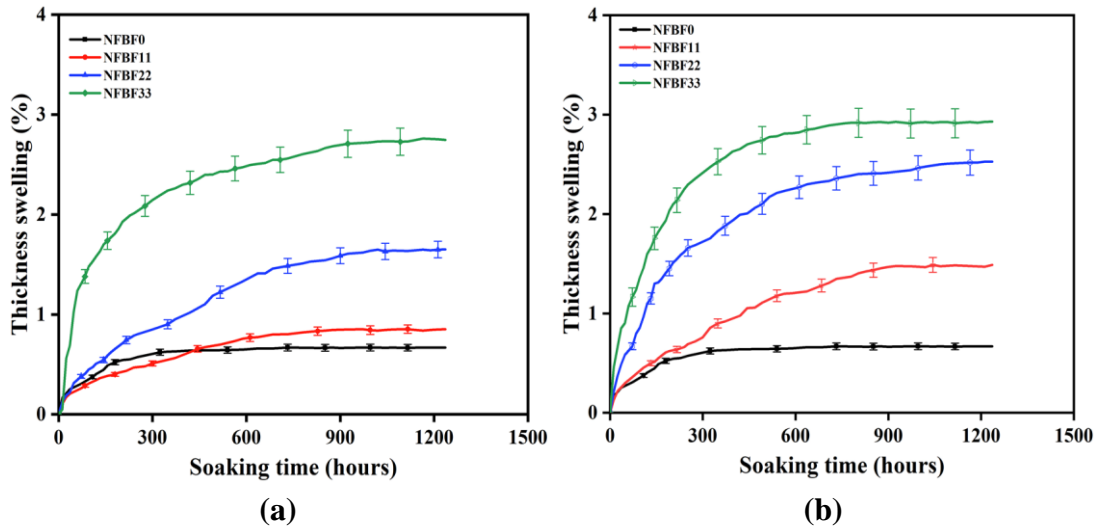


Figure 5.3 Thickness swelling of PLA and NFBF/PLA composites under (a) warp and (b) weft direction loading

5.1.1 Transport coefficients

The kinetic parameter, diffusion coefficient (D) is calculated from Equation (5.1):

$$D = \pi \left(\frac{kh}{4M_{\infty}} \right)^2 \quad (5.1)$$

where, k is the original slope of the water absorption curve (M_t) as opposed to the square time root (\sqrt{t}) and h represents initial thickness of the composite specimen (Almansour et al. 2017). The coefficient of diffusion characterises the potential of water molecules to pass through the polymer sections. Table 5.1 shows the diffusion coefficient for pure PLA and NFBF/PLA composites. The diffusion coefficient is significantly high for NFBF/PLA composites compared to pure PLA. The diffusion coefficient increases with increase in fibre content and the present results are in agreement with results reported by other authors (Arbelaiz et al. 2005; Espert et al. 2004).

Table 5.1 The maximum moisture uptake, diffusion coefficient and permeability of pure PLA and NFBF/PLA composites

Type of Sample	Fabric Direction	Saturation moisture uptake M_t (%)	Diffusion coefficient $D \times 10^{-8}$ (m^2/s)	sorption coefficients $S_c \times 10^{-3}$ (g/g)	Permeability coefficient $P \times 10^{-12}$ (m^2/s)
NFBF0	-	0.30	0.34	0.48	1.63
NFBF11	Warp	1.08	1.31	1.70	22.27
	Weft	1.20	1.49	2.03	30.24
NFBF22	Warp	1.84	1.41	2.85	40.18
	Weft	1.99	1.94	3.08	59.75
NFBF33	Warp	4.57	1.47	6.28	92.31
	Weft	5.78	1.77	8.23	145.67

Permeability of water in the composites depends on the water absorption capability of the natural fibre. Because in the natural fibre reinforced composites the permeability of water occurs through sorption. Hence, to calculate the permeability, sorption coefficient (S) is commonly used. Sorption coefficient (S) for equilibrium water absorption of the composites is calculated using Equation 5.2 (Nosbi et al. 2010).

$$S = \frac{M_{\infty}}{M_p} \quad (5.2)$$

where, M_{∞} is the equilibrium moisture uptake mass and M_p is the coupon mass before sorption test. The coefficient of permeability (P) is the net impact of the coefficient of diffusion (D) and coefficient of sorption (S) as given in Equation 5.3,

$$P = D \times S \quad (5.3)$$

The results of S and P of pristine PLA and NFBF/PLA composites on the water absorption behaviour are presented in Table 5.1. From Table 5.1, it is clear that NFBF33 composite has the highest permeability than pure PLA and the other composites. Reason for this trend is the same as explained in the water absorption section.

5.1.2 Effect of water absorption on flexural properties

Flexural strength and flexural modulus of the NFBF/PLA composites along warp and weft direction loading with and without water absorption are presented in Figure 5.4 to Figure 5.7. From Figure 5.4 and Figure 5.5, it is observed that flexural strength and modulus of the NFBF/PLA composites are enhanced due to NFBF reinforcement and these properties further increases with the increase in the fabric content. The NFBF33 composite showed highest strength and modulus of about 92.3 MPa and 4.5 GPa respectively, which are 42.88% and 52.07% higher than pure PLA. Flexural strength and modulus of NFBF/PLA composites for weft direction loading are less due to the presence of less number of yarns along the loading direction. Flexural strength of the NFBF/PLA composite decreases with the increase in water uptake percentage and it is further decreased with the increase in braided fabric content. Due to the water absorption, the decrease in flexural strength and modulus observed for pure PLA is 9.59% and 3.13% and for the NFBF33 composite (for warp direction loading) the corresponding values are of about 23.23% and 26.89% respectively. This can be attributed to the weak fibre matrix interface due to water absorption, hence there is a decrease in flexural properties after water uptake (Dhakal et al. 2007). Natural fibres are hydrophilic in nature, a large number of hydrogen bonds formed between the polymer and cellulose macromolecules with the many hydroxyl groups (-OH) present in the fibre structure (Sombatsompop and Chaochanchaikul 2004). Presence of high hydroxyl groups (-OH) in natural fibres leads to poor resistance to moisture and weakens the fibre-matrix bonding and dimensional variance in composite materials, leading to a reduction in mechanical properties (Diamant et al. 1981).

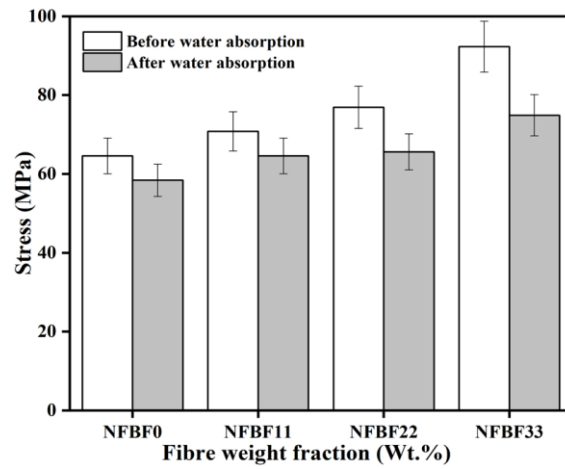


Figure 5.4 Flexural stress of PLA and NFBF/PLA composites for warp direction loading

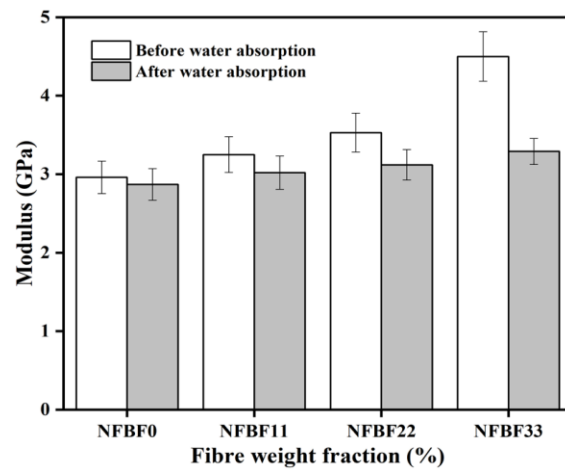


Figure 5.5 Flexural modulus of PLA and NFBF/PLA composites for warp direction loading

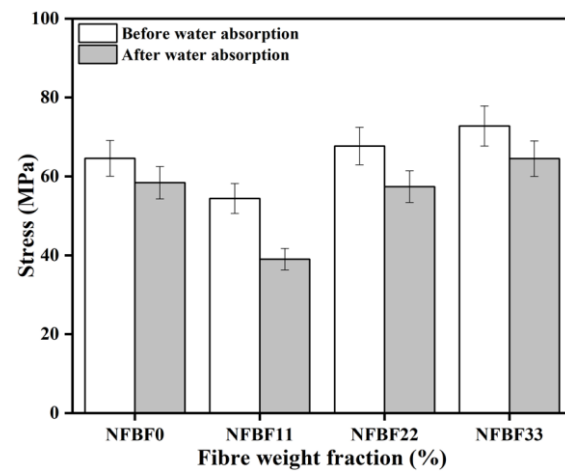


Figure 5.6 Flexural stress of PLA and NFBF/PLA composites for weft direction loading

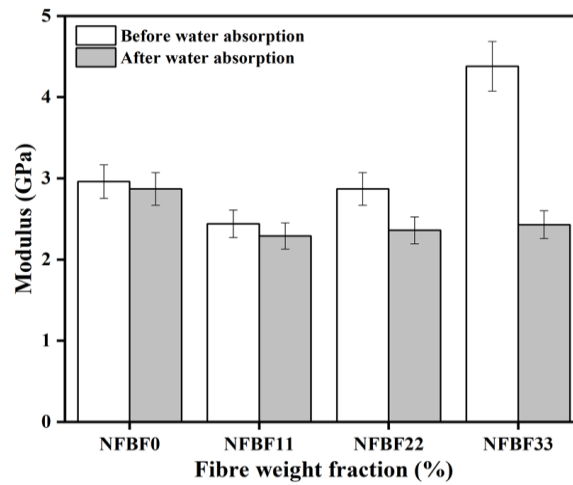


Figure 5.7 Flexural modulus of PLA and NFBF/PLA composites for weft direction loading

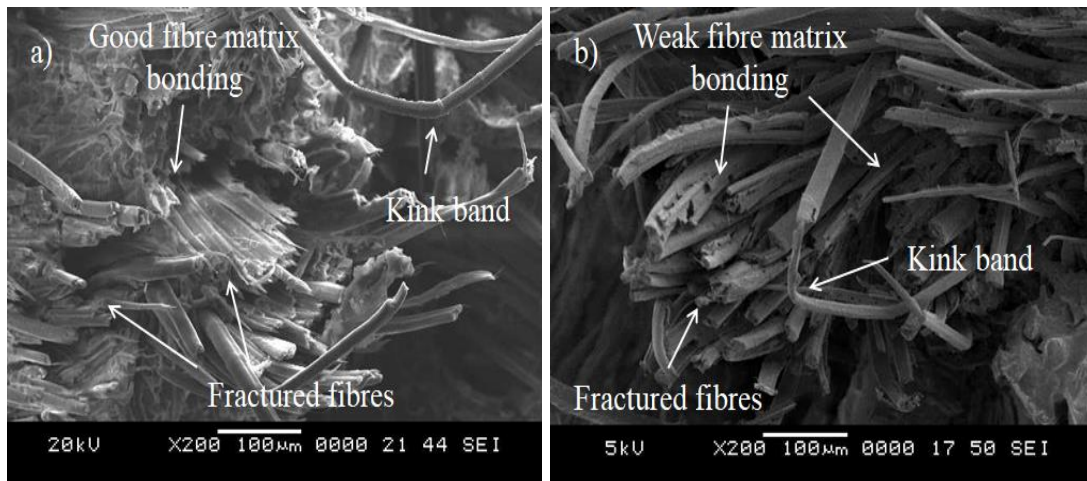


Figure 5.8 SEM images of the fractured surface of NFBF/PLA composites a) before water absorption, b) after water absorption

Microstructure images of the fractured surfaces of the NFBF/PLA composites before and after the water absorption tests are given in Figure 5.8. Fractured fibres, kink bands and also the strong interfacial adhesion between fibre-matrix are observed on the fractured surface of the composite before the water absorption test as seen in Figure 5.8. However, fractured surface of the NFBF/PLA composite, after the water absorption test, is totally different which clearly shows the degradation of the fibre-matrix interfacial bonding due to the water absorption as seen in Figure 5.8b. Good interfacial adhesion facilitates effective stress transfer capacity across the natural fibre and PLA, results in significant enhancement in flexural strength and modulus. In fact, after water absorption process significant amount of lignin and hemicellulose has

been leached out which results in the reduction of flexural strength and modulus of the composites after the water absorption test.

Table 5.2 Comparison of water absorption results of NFBF/PLA composites with other natural fibre/PLA composites

Composite	Fibre Structure	Fibre weight (%)	Immersion time (days)	Weight gain (%)	Reference
Flax/PLA	3D braided woven fabric	33	52	5.78	Present
Flax/PLA	Random fibres	50	21	60	(Shanks et al. 2005)
Flax/PLA	Woven 2×2 twill	40	30	12	(Siengchin et al. 2013)
Flax/PLA	Woven 4×4 hopsack	40	30	13	(Siengchin et al. 2013)
Flax/PLA	Commingled yarns	40	1	17	(Linganiso et al. 2014)
Flax/PLA	Nonwoven fabrics	40	1	38	(Linganiso et al. 2014)
Flax/PLLA	Unidirectional fabrics	50	60	14	(Duigou et al. 2015)
Flax/PLA	Unidirectional fabrics	34	30	16	(Foruzanmehr et al. 2016)

Weight gain percentage of present NFBF/PLA composite as a result of water absorption test is compared with other types of flax/PLA composites reported in literature as shown in Table 5.2. From Table 5.2, one can observe that the water absorption of the NFBF/PLA composites is lower than that of other PLA composites which also indicates that 3D braided fabric reinforcement enhances water resistance capability of PLA composites compared to other forms of reinforcement. The hydrophilicity of the natural fibre and PLA can increase the water absorption and this water acts as plasticiser or hydrolysis agent. This results in deterioration of the composites (Yew et al. 2005).

5.2 Biodegradability study

Influences of wt.% of braided yarn fabric and burial time on weight loss of PLA and its composites are shown in Figure 5.9.

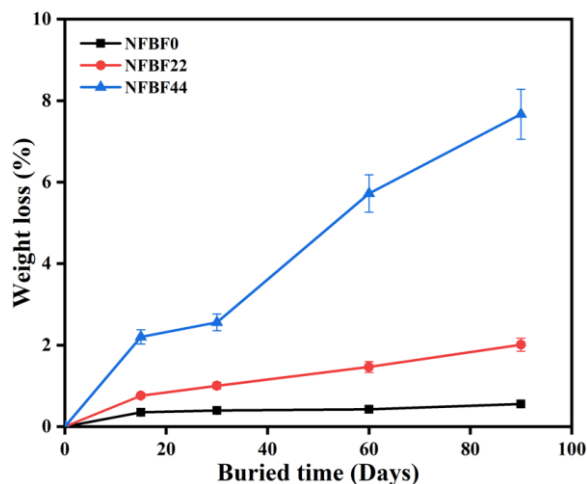


Figure 5.9 Percentage weight loss of PLA and NFBF/PLA composites as a function of burial time

Percentage loss of weight for pristine PLA and NFBF/PLA composites increases with the increase in the incubation time. A more significant increase in percentage weight loss is noticed for NFBF/PLA composites compared to pure PLA. This indicates that the reinforcement of fabric with braided flax fibre accelerates the biodegradation of the PLA. The pure PLA polymer does not show much degradation after 15 days of incubation time and the similar trend is also noticed by Yussuf et al. (2010). Pure PLA sample showed a weight loss of about 0.56% for 90 days of soil burial. Due to its hydrophobic nature, the moisture absorption rate is low (Islam et al. 2010a). Hence pure PLA polymer degrades very slowly in soil (Ohkita and Lee 2005). On the other hand NFBF is easily biodegradable in the compost soil due to micro-organisms (such as fungi and bacteria). Figure 5.9 indicates that the biodegradation features of the composites are enhanced due to the NFBF reinforcement. The reason for this is the presence of hydrophilic groups in the natural fibre (flax fibre) of the composites, which facilitates the easy absorption of the micro-organisms and moisture from the compost. Due to moisture absorption swelling of the natural fibre takes place which intern develop the matrix micro-cracks on the composite surfaces (Islam et al. 2010a). Also, this process weakens the surface of the fibre-matrix adhesion property of the composites as shown in Figure 5.16 and Figure 5.17. This results in a greater exposed area for micro-organisms and water with the PLA (Huang et al. 2018). This is responsible for the increase in the percentage loss of weight for the composite with an

increased burial time. Figure 5.9 shows for 22 wt.% of NFBB reinforcement the weight loss is 3.01% and 44 wt.% of NFBB reinforced composites showed a much higher amount of weight loss of about 7.66%. An increase in NFBB content increases the cellulose content of the fibre and this leads to increased moisture absorption of the composite. The moisture absorption has a synergetic effect on the rate of biodegradability (Yussuf et al. 2010). Because of this reason loss of weight is high for the NFBB44 composites compared to the NFBB22 composites.

Infrared spectra analysis is performed to examine the biological impact on the chemical structure of the native and deteriorated composites. Figure 5.10 presents the FTIR spectra of NFBB44 composites before and after the biodegradation test. The FTIR spectrums of the composites before and after biodegradation test are compared to study the appearance and change of the transmittance peaks. The peaks at 2880.41-2999.31 cm^{-1} corresponds to C-H (Alkane group) strong vibrational stretching. Peaks between 1084.92-1186.27 cm^{-1} assigned to stretching of ester bonds (Razak et al. 2014). The 1186.27 cm^{-1} can be attributed to C-O in PLA and 1084.92 cm^{-1} is attributed to C-O in cellulose (Jiang et al. 2019). The carbonyl aldehydes in lignin and acetyl ester in the hemicellulose are carbonyl groups and observed due to stretching peak in the spectra at 1631.55 cm^{-1} for composites before biodegradation (Cantero et al. 2003; Hamdan et al. 2010). After the biodegradation test this peak does not exist due to the dismissal of hemicellulose and lignin. A strong and sharp peak is observed at 1755.24 cm^{-1} co-related to C=O (carbonyl) stretching of acetyl groups of natural flax hemicellulose. Biodegradation contributes to a more extreme peak at about 1755.24 cm^{-1} due to esterification reaction (Cantero et al. 2003). Peaks at 3435.81-3683.19 cm^{-1} related to O-H stretching bonds. A shift in this peak represents the level of hydrogen bonding and the frequency with higher level denotes the fibre is free from bonding (Gunning et al. 2013). FTIR spectra results support the biodegradation of NFBB filled PLA biocomposites.

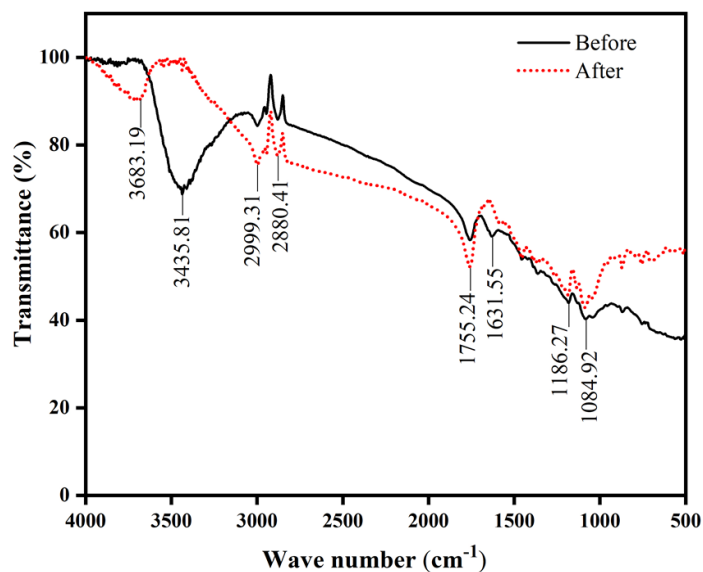


Figure 5.10 FTIR spectra of NFBF44 composites before (0 day) and after (90 days) biodegradation test

SEM images of the pristine PLA and NFBF/PLA composites before and after the soil incubation test are shown in Figure 5.11a and Figure 5.11b respectively. Surfaces of PLA and its composites are clean and smooth before the soil incubation. However, after 90 days of the incubation test, the surfaces are appeared with pores and groves due to the erosion of the matrix. Micro-cracks are observed on the composites surfaces which are formed due to the swelling of natural fibre as a result of water absorption. In composites, the resin surface is degraded first resulting in exposure of fibres to the environment. The fibre breakage, peeling and gap between fibre bundles are observed in NFBF44 composite as shown in Figure 5.11b (enlarged). This is the evidence of enhanced degradation of fibre-rich composites by absorbing more water and microorganisms.

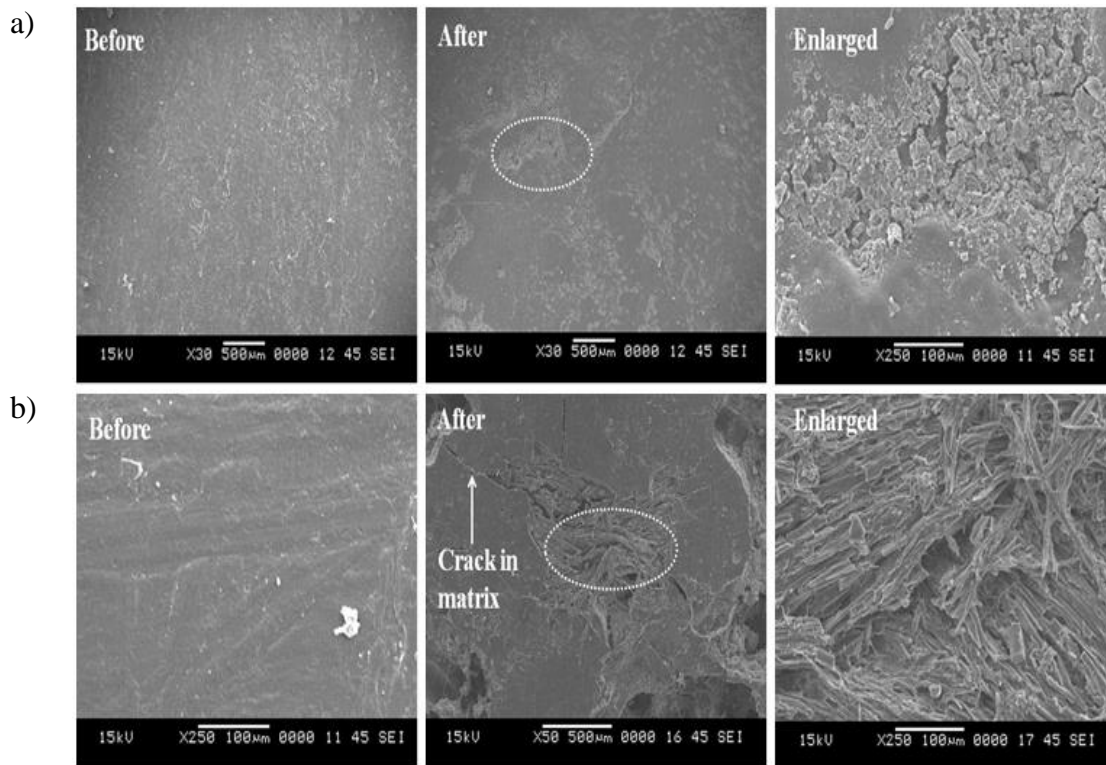


Figure 5.11 SEM photomicrographs of pure PLA and NFBF/PLA composites before and after (90 days) biodegradation test a) PLA, b) NFBF44%

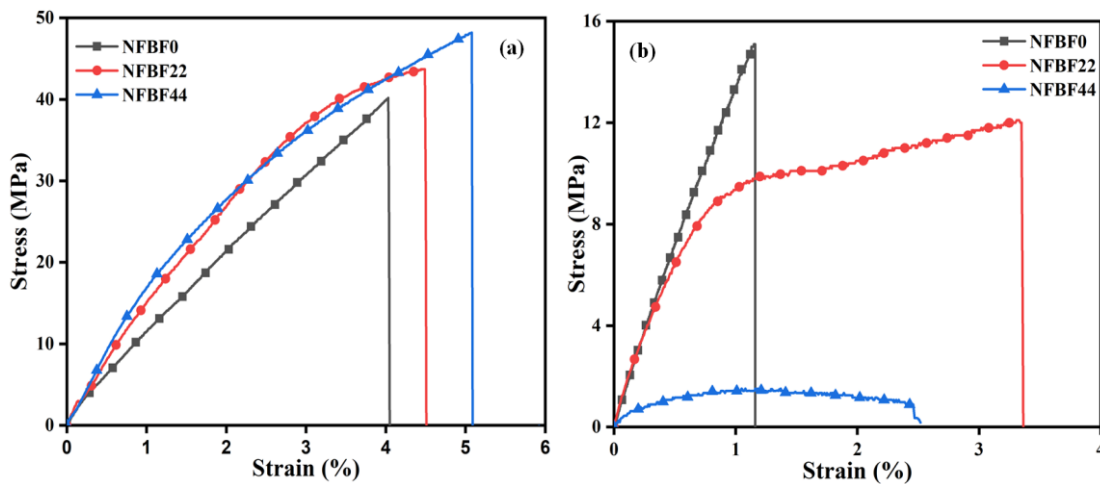


Figure 5.12 Stress-strain curves of PLA and NFBF/PLA composites (a) before and (b) after the biodegradation test

Figure 5.12(a) represents the stress-strain curves of the pure PLA and NFBF/PLA composites before the biodegradation test. Tensile stress and Young's modulus of 40 MPa and 1.37 GPa respectively are observed for pure PLA. The PLA polymer tensile strength and percentage strain are increased due to the reinforcement of NFBF.

Oksman et al. (2003) noticed that the increase in long heckled flax fibre (reinforced in the form of handmade roving architecture) content results in decrement of tensile strength of the heckled flax fibre composites. However, in the present study increase in strength with increase in NFBF content is observed. It may be due to the architecture of the fibre reinforcement which improved the fibre-matrix bonding (Figure 5.15) and enhanced stress transfer from PLA polymer to strong flax fibres. Khondker et al. (2006) study also revealed that the reinforcement of braided jute/PLA yarn enhanced the mechanical properties by improving the wettability of matrix over fibre bundles, matrix fusion and interfacial-adhesion characteristics. The NFBF44 composite showed the highest strength and modulus of 48 MPa and 1.61 GPa and these values are 20% and 17.51% high compared to pure PLA. Kumar et al. (2010) performed a tensile study on the flax woven fabric/PLA composites fabricated by compression molding method and reported a tensile strength of 21 MPa. Similarly, Adomavičiūtė et al. (2015) studied flax weft knitted fabric/PLA composites and observed an ultimate strength of 28 MPa. Compared to these composites tensile strength of the present NFBF/PLA composite is high (48 MPa). Improved fibre-matrix adhesion, architecture of reinforcement fibre and wettability of the fibre bundles might be reason for tensile strength enhancement of flax braided/PLA composites. Rajesh and Pitchaimani (2017b) also concluded that the mechanical properties of the jute braided yarn composites is better than conventional yarn composites. Figure 5.12(b) shows the tensile stress-strain curves of PLA and its composites after the bio-degradation test (90 days). From Figure 5.12(b), it is observed that there is a decrease in the tensile properties of the composites due to the biodegradation. There is a significant change in the stress-strain curves of the NFBF/PLA composites due to the biodegradation. This may be due to a decrease in strength of the reinforced fibre and reduction in fibre-matrix bonding after 90 days of soil incubation, as seen in Figure 5.11(b).

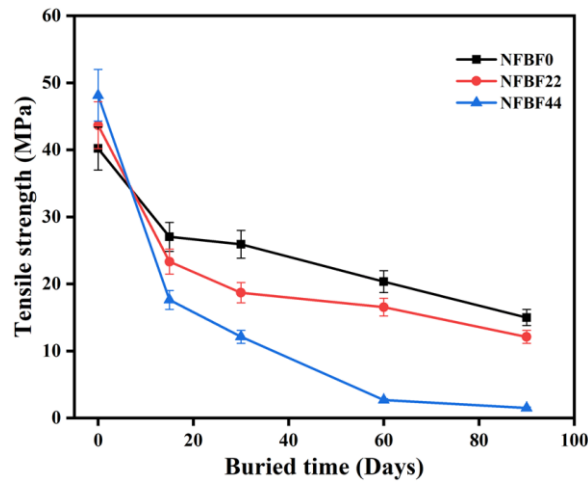


Figure 5.13 Effect of compost soil burial on tensile strength of the PLA and NFBF/PLA composites

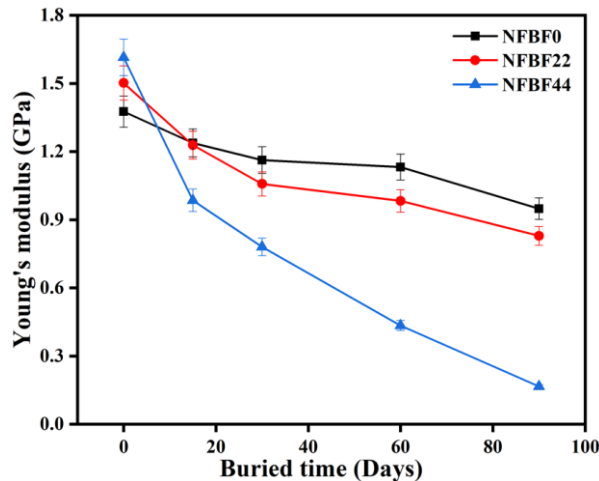


Figure 5.14 Effect of compost soil burial on Young's modulus of the PLA and NFBF/PLA composites

Reduction in tensile strength and Young's modulus of PLA and NFBF/PLA composites as a function of burial time are shown in Figure 5.13 and Figure 5.14 respectively. The strength and modulus of the PLA and its composites are high before the soil burial test. From Figure 5.13, it is clear that the tensile strength of neat PLA and NFBF/PLA composites decreased rapidly from 0 to 15 days, and there is a gradual decrease from 15 days to 90 days. This is due to the moisture absorption of the PLA and its composites. Reduction in tensile properties of the NFBF44 composites can be explained using SEM images shown in Figure 5.15 to Figure 5.17. From Figure 5.15 it can be observed that the fibre and matrix have good interfacial bonding and fibres are in a good circular shape (original shape). So these composites

are capable to sustaining relatively higher load. Figure 5.16 shows the fungal growth on the composites which also shows matrix, lignin and cellulose leached out of surfaces of the fibres after 30 days soil burial test. Figure 5.16 also indicates the initiation of fibrillation of the fibres which represents the initiation of deterioration of the composite. Due to this reason, composites are unable to sustain the higher loads and hence composites showed lower tensile properties. After 60 days of soil burial test (Figure 5.17) the fibres are further fibrillated and fungal growth started on the fibres. Crawford et al. (2017) study shows that fungal growth significantly affects the tensile properties and dry mass of natural fibre composites. They also reported that the effect depends on the exposure condition, time, fibre type and fibre architecture (length scale of fibres). Because of these reasons, the load-bearing capacity of the composites decreased further. Significant reduction in strength and modulus of the NFBF/PLA composites with an increase in filler content is observed for 90 days of incubation. The NFBF44 composite experienced a higher reduction in tensile strength and modulus of about 96% and 89% respectively compared to its before degradation results. The main chemical compositions of a natural fibre are cellulose and lignin. The biodegradation of cellulose and lignin includes random chain scission of the bonded β -1, 4-glucosidic and side chains of the phenyl propane (Kim et al. 2006; Ochi 2008) and this results in degradation of fibre strength, hence reduces the strength and modulus of the composite.

Weight loss measurement, change in FTIR spectra, reduction in tensile properties (strength and modulus) and SEM micrographs confirm the severe biodegradation of the composites due to the NFBF reinforcement.

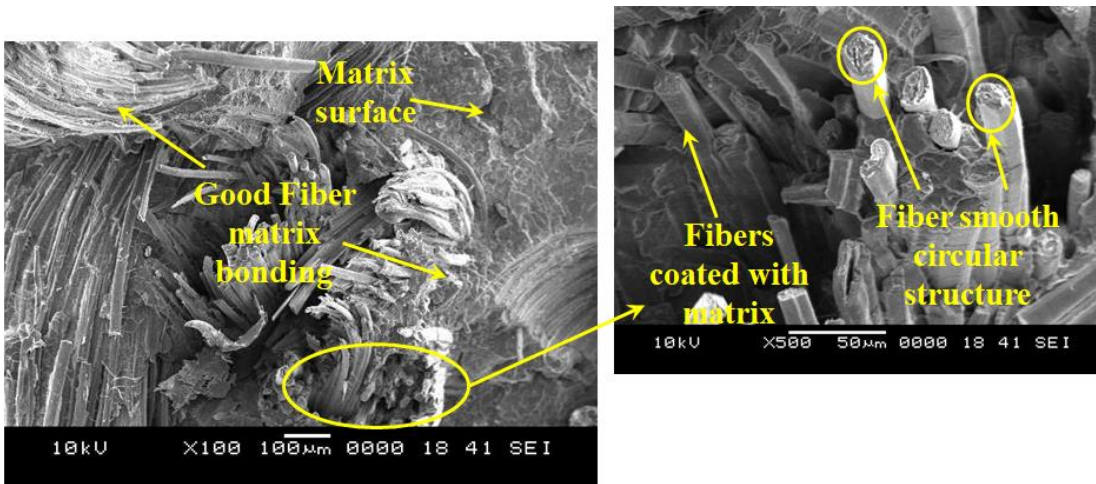


Figure 5.15 SEM micrograph of the tensile fractured surface of the NFBF44 composite before biodegradability

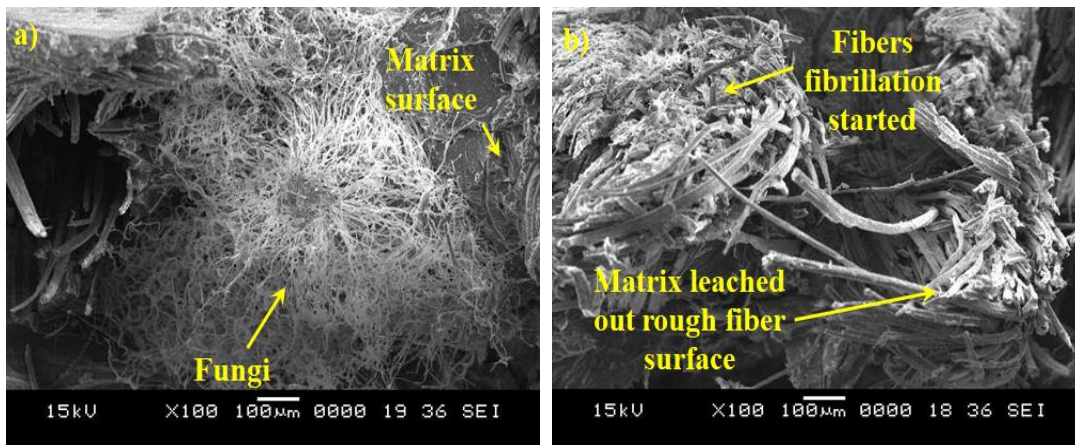


Figure 5.16 SEM micrographs of the tensile fractured surface of the NFBF44 composite after 30 days of soil burial test

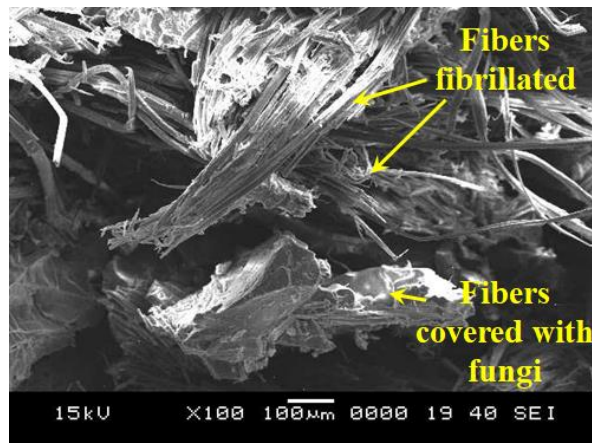


Figure 5.17 SEM micrographs of the tensile fractured surface of the NFBF44 composite after 60 days of soil burial test

Table 5.3 Comparison of biodegradability results of NFBF/PLA composites with other natural fibre/PLA composites

Composite	Fibre Structure	Fibre volume / weight (%)	Soil type	Number of days	Weight loss (%)	Reference
Flax/PLA	3D braided woven fabric	44	Compost	90	7.66	Present
Flax/PLA	Nonwoven	20	farmland soil	90	25	(Kumar and Yakubu 2010)
Flax/PLA	Woven	30	farmland soil	90	20	(Kumar and Yakubu 2010)
Flax/PLA	Unidirectional fibre	30	Compost	56	10	(Bayerl et al. 2014)
Flax/PLA	Short fibre	30	Compost	56	5	(Bayerl et al. 2014)
Flax/PLA	Long fibre	30	Compost	56	4	(Bayerl et al. 2014)

Weight loss of NFBF/PLA composites as a result of the biodegradability test is compared with other types of flax/PLA composites reported in the literature as shown in Table 5.3. The nature of fibre reinforcement (short and random, continuous long and woven shape) significantly influences the biodegradability of the composite material. Weight loss associated with the present NFBF/PLA composite is less compared to the composites with other forms of reinforcement of flax fibre. Kumar and Yakubu (2010) performed a biodegradability investigation on nonwoven and woven flax fibre-filled PLA composites (40 mm × 20 mm × 0.65 mm) prepared by compression molding method. Biodegradation test is conducted in a farmland soil at room temperature (25 ± 5° C). The test results show, biodegradation of the nonwoven flax is 25% for 20% of fibre content for 90 days farmland soil burial. The woven flax composite degradation is 20% for 30% fibre content for 90 days of farmland soil burial. According to the literature, for higher fibre content, the biodegradability of the composites should be high (Gunti et al. 2016; Saeed et al. 2018). However, biodegradability of the woven composites is poor due to the resistance provided by the fabric against microbial attack. This slows the biodegradation process of composites (Behera et al. 2012). Bayerl et al. (2014) conducted a biodegradability

experiment on short, long and unidirectional flax fibre reinforced composites (15 mm × 15 mm × 3 mm) in the compost soil environment at 40° C. They prepared the flax/PLA composites using the compression molding method. As observed from Table 5.3, the biodegradability of the unidirectional flax fibre composite has maximum weight loss and the long fibre composite has lower weight loss. These studies shown that biodegradation of the composite is influenced by the nature of fibre reinforcement. Before biodegradation of the composites hydrolysis of the ester linkage occurs (Harnnecker et al. 2012). Good fibre-matrix adhesion causes slow moisture absorption (hydrolysis) of composites (Yatigala et al. 2018). This slows the biodegradation process of the composites. Hence, the lower biodegradability (7.66%) for 44 wt.% of fibre at 90 days soil incubation period in compost soil is associated due to the architecture of the reinforcement material (fibre) and improved interfacial bonding between fibre and matrix. The less weight loss suggests that the braided fabric composites can be used in applications such as food packaging and bio-medical which requires a slow degradation rate.

5.3 Conclusion

The water absorption and thickness swelling behaviour of neat PLA and braided yarn PLA composites are investigated. The effect of water absorption on flexural properties of PLA and its composites is also analysed. The reinforcement of braided yarn fabric enhances the flexural strength and modulus of the PLA. The NFBF33 composite under the warp direction loading showed maximum flexural strength and modulus of 92.3 MPa and 4.5 GPa respectively, which are 42.88% and 52.07% higher than pure PLA. The water absorption and thickness swelling of the composites are enhanced due to the fibre reinforcement and increases with the fibre content. Flexural properties of the composites decreased due to the water absorption. The diffusion coefficient and permeability coefficients are high for NFBF composites compared to pure PLA.

Effect of braided yarn fabric reinforcement on biodegradability behaviour has been investigated and compared with the results reported in the literature. Tensile strength and modulus of PLA composites are improved due to the reinforcement of braided yarn textile fabric. Biodegradability study revealed that the reinforcement of more

number of NFBF layers increases the degradation rate. However, it is less compared to the other forms of natural fibre reinforcement. The surface contact area with short fibre reinforcement is much higher than that of the NFBF reinforcement which reduces the fibre- water molecule interaction.

6 TRIBOLOGICAL BEHAVIOUR AND FRACTURE TOUGHNESS OF COMPOSITES

6.1 Introduction

Literature survey reveals that short and random oriented natural fibre composites are mostly studied by several researchers to analyse the wear characteristics. Furthermore, wear studies on biodegradable woven natural fibre composites are also very limited. The present work focuses on the analysis of tribological properties of flax braided yarn fabric reinforced PLA composites. Wear study carried out on pin-on-disc wear test set-up to analyse the influences of number of fabric layers, applied loads and sliding velocities on wear properties of braided woven fabric PLA composites is presented.

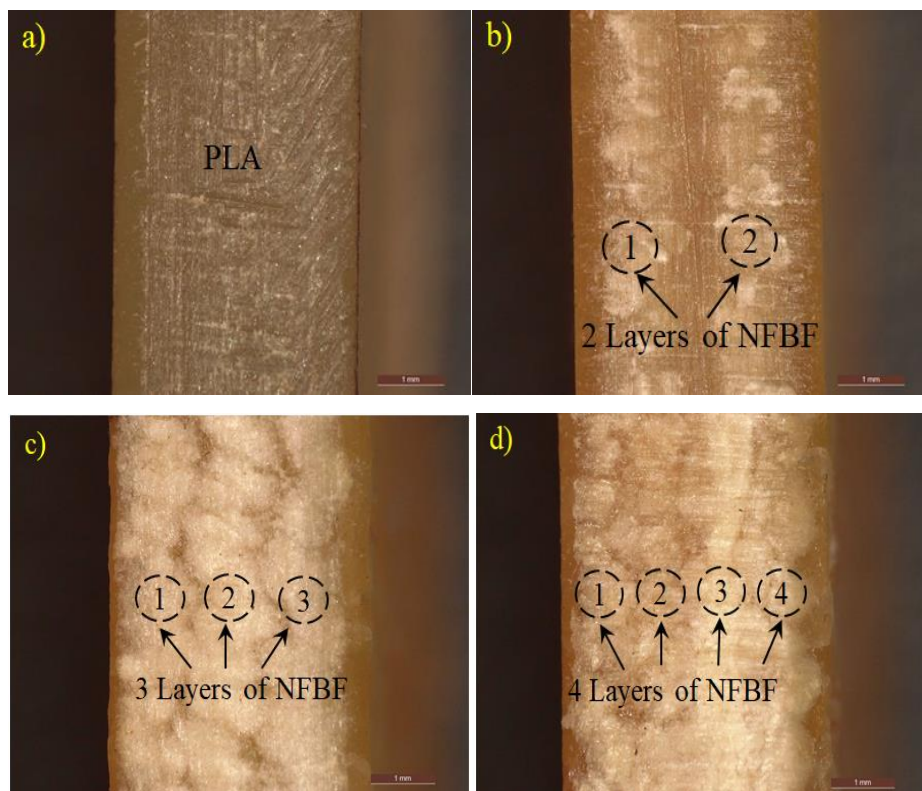


Figure 6.1 Cross-sectional views of PLA and NFBF/PLA composites with different number of fabric reinforcement.

In this study, two, three and four number of natural fibre 3D braided yarn fabrics are reinforced with PLA and according to their fibre weight fraction (18, 26 and 35 wt.%)

the composites are designated as NFBBF18, NFBBF26 and NFBBF35 respectively. These composite results are compared with the pure PLA (NFBBF0). Micrographs of cross-sectional views of PLA and NFBBF/PLA composites with different numbers of fabric layer reinforcement are shown in Figure 6.1. The number of layers present in the composites can be clearly seen from these graphs. The prepared PLA and NFBBF 18 (2 layers of NFBBF) have nearly same thickness of 3.9 to 4 mm and the composites prepared with 3 layers (NFBBF26) and 4 layers (NFBBF35) have the thickness in the range of 4 to 4.1 mm.

6.2 Density

Density (theoretical and experimental) and void content results of PLA and NFBBF/PLA composites considered for the wear study are reported in Table 6.1. The presence of void content will impact the mechanical and physical characteristics of the composites (Jawaid et al. 2011). There is a possibility of air entrapment during reinforcement of the braided fabric with polymer matrix. It is observed that the pure PLA has less void content and it increases with the reinforcement content. Also NFBBF35 composite has higher void content of 2.256%. The natural fibres are porous structures and the 3D braided fabrics are loosely packed structures, so the void content increased with fibre content respectively. Layerwise reinforcement of the 3D braided fabric increase the voids. However, the percentage void content of 3D braided fabric composites analysed are well within the limit.

Table 6.1 Density and void content of the PLA and NFBBF/PLA composites

Composite	Theoretical density (g/cm ³)	Experimental density (g/cm ³)	Void content (%)
NFBBF0	1.240	1.233±0.0007	0.564
NFBBF18	1.263	1.239±0.0025	1.883
NFBBF26	1.274	1.252±0.0023	1.726
NFBBF35	1.285	1.256±0.0020	2.256

6.3 Wear studies

Influence of fabric loading on frictional force and height loss of the PLA and NFBBF/PLA composites under 30 N normal applied load and 3 m/s sliding speed is presented in Figure 6.2. Adhesion and deformation are the two predominant mechanisms which make contributions to friction between polymer composite and steel friction and these mechanisms are depends on the applied load, chemical, mechanical and geometrical properties (El-Tayeb 2008; Zsidai et al. 2002). Figure 6.2(a), represents the frictional force versus sliding distance and it indicates that the frictional force of the NFBBF/PLA composites is greater than the neat PLA. PLA polymer is a soft material and has lower surface roughness. However, the reinforcement of the NFBBF to the PLA, increases the surface roughness of the composites. Hence, increase in frictional force is observed for NFBBF/PLA composites and there is a significant increase in the friction force with increase in the fibre content. Figure 6.2(b) represents the height loss of the pure PLA is gradually increasing with respect to sliding distance up to 2000 m. From 2000 - 2500 m sliding distance, height loss in the specimen increases drastically. This is due to rise in surface frictional temperature, which causes the softening of the PLA specimen and film generation (El-Sayed et al. 1995; Gill and Yousif 2008). Frictional temperature further increases as the sliding distance increases and leads to plastic flow of the PLA specimen. This softening and film generation of PLA acts as lubricant between specimen and counter surface. The gradual increase in height loss is observed for the NFBBF/PLA composites also, but it is less compared to the PLA. The increase in NFBBF content in the composites results in reduction of the height loss of the NFBBF/PLA composites. This also clearly indicates that roughness and strength of the PLA is increased due to the NFBBF reinforcement. Natural fibres are tubular structures and bad conductors of heat (Kymäläinen and Sjöberg 2008). Use of these fibres as the filler materials in composites reduces the softening and film generation. Hence the NFBBF/PLA composite shows a lower height loss compared to PLA.

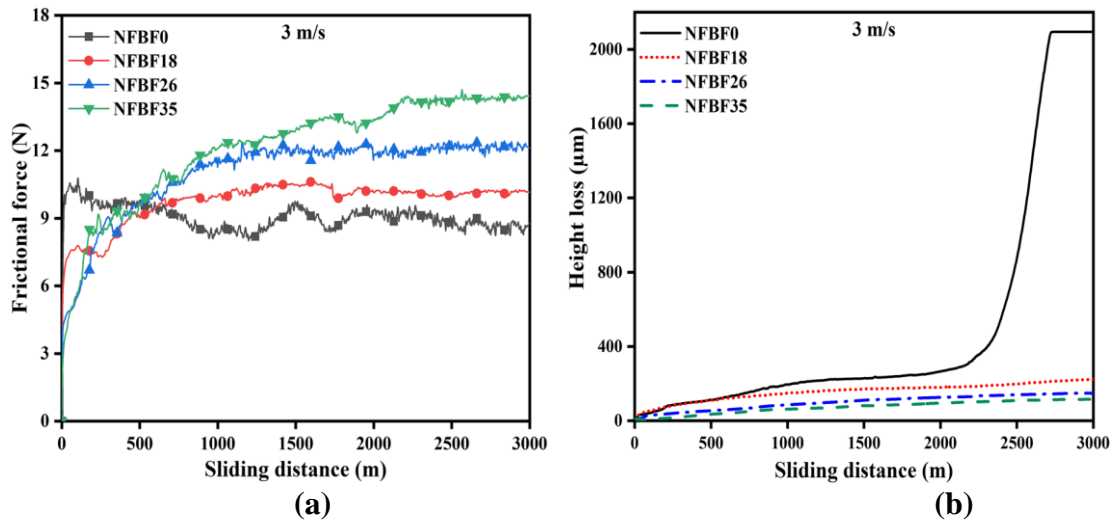


Figure 6.2 (a) Frictional force and (b) Height loss of PLA and NFBF/PLA composites under 30N load

6.3.1 Coefficient of friction

Effect of applied load and sliding velocity on co-efficient of friction of PLA and NFBF/PLA composites for a 3000 m sliding distance is presented in Figure 6.3. Enhancement, reduction or stabilization of the friction co-efficient relies on the development of polymer thin film, which bring change in the ploughing friction because of interface geography (El-Tayeb et al. 2006). For PLA and NFBF/PLA composites the friction co-efficient increased with higher sliding speed for 10 N applied load. However, for the higher velocity (3 m/s) and applied normal load (30 N) co-efficient of friction is reduced. This can be attributed to softening effect of the material due to the increase in temperature between the counter surface and specimen. For the first two velocities (1 and 2 m/s), the NFBF/PLA composites showed the same trend as that of PLA. But, for 3 m/s speed, the softening and film generation takes place at the contact surfaces of PLA. This reduces the friction between the specimen and counter surface and results in lower coefficient of friction. Observation of Figure 6.3(b-d), shows that the co-efficient of friction is high for the NFBF/PLA composites compared to pure PLA.

Coefficient of friction increases with applied load for the sliding velocity values 1 m/s and 2 m/s irrespective of the material as seen in Figure 6.3. For PLA and its composites, significant increase in coefficient of friction with increase in applied load

is observed for sliding velocity of 1 m/s. This increased rate can be clearly observed in PLA composites for 10 N and 20 N loads compared to 30 N load. Reduction in coefficient of friction is observed for 30 N load at a sliding speed of 3 m/s in all the cases.

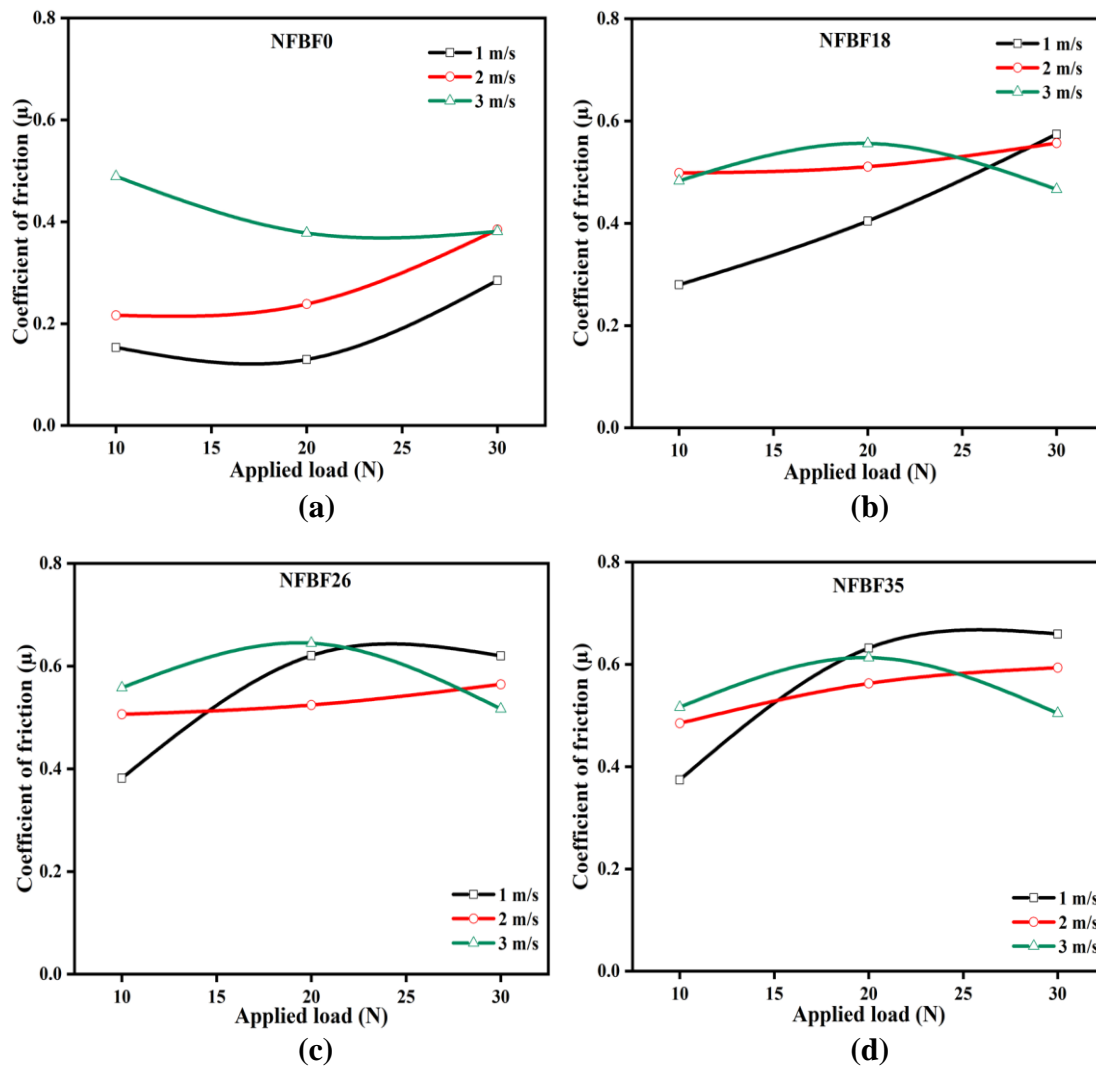


Figure 6.3 Coefficient of friction versus applied load for NFBF/PLA composites of (a) NFBF0 (PLA), (b) NFBF18, (c) NFBF26, and (d) NFBF35.

Coefficient of friction increases with an increase in load and sliding speed irrespective of temperature rise up to certain extent. However, the higher speed (3 m/s) and higher applied load (30 N) increases temperature between the specimen and counter surface. This builds the thermal gradient along the thickness of the specimen and develops thermal stress in the specimen. The thermal stress weakens the fibre-matrix bonding

and fibres get loose and shear off effectively because of axial thrust created by the sliding of pin which can be clearly seen from Figure 6.11 (b, c and d). Because of continuous sliding the fibre detachment occurs which reduces the coefficient of friction. The coefficient of friction also reduces with smooth back film transfer due to sliding in the presence of fibres (Yousif 2008).

6.3.2 Wear rate

Figure 6.4, indicates that the wear rate of the braided fabric PLA composites is less compared to PLA specimen. This also indicates that the braided fabric reinforcement reduces the wear rate of PLA significantly. Significant increase in wear rate of PLA is observed for higher sliding velocity as shown in Figure 6.4(a). In Figure 6.4(a), wear rate of PLA increased for higher sliding velocity. In case of higher velocity (3 m/s), the friction and temperature between the PLA specimen and sliding surface increases, leading to a polymer thin film generation. PLA is a temperature sensitive material, due to the increase in temperature PLA starts to soften and resulting in the plastic deformation. Hence, there is a significant increase in wear rate of PLA for the higher values of sliding velocity and applied load.

The wear rate of NFBBF/PLA composites (Figure 6.4b) reduced significantly due to the reinforcement of NFBBF with PLA. This is due to enhanced surface roughness and wear resistance property of the NFBBF/PLA composites. The fibre and polymer rub together during sliding process, matrix material is supported by the fabric and protects the polymer from being removed easily (Yousif and EL-Tayeb 2007). Good interfacial bonding between fibre-matrix helps to distribute the applied load evenly between fibre and matrix system and hence enhancement in the wear resistance property of the composites. Wear resistance of the NFBBF/PLA composites (Figure 6.4b to d), increases with fibre content in the composite.

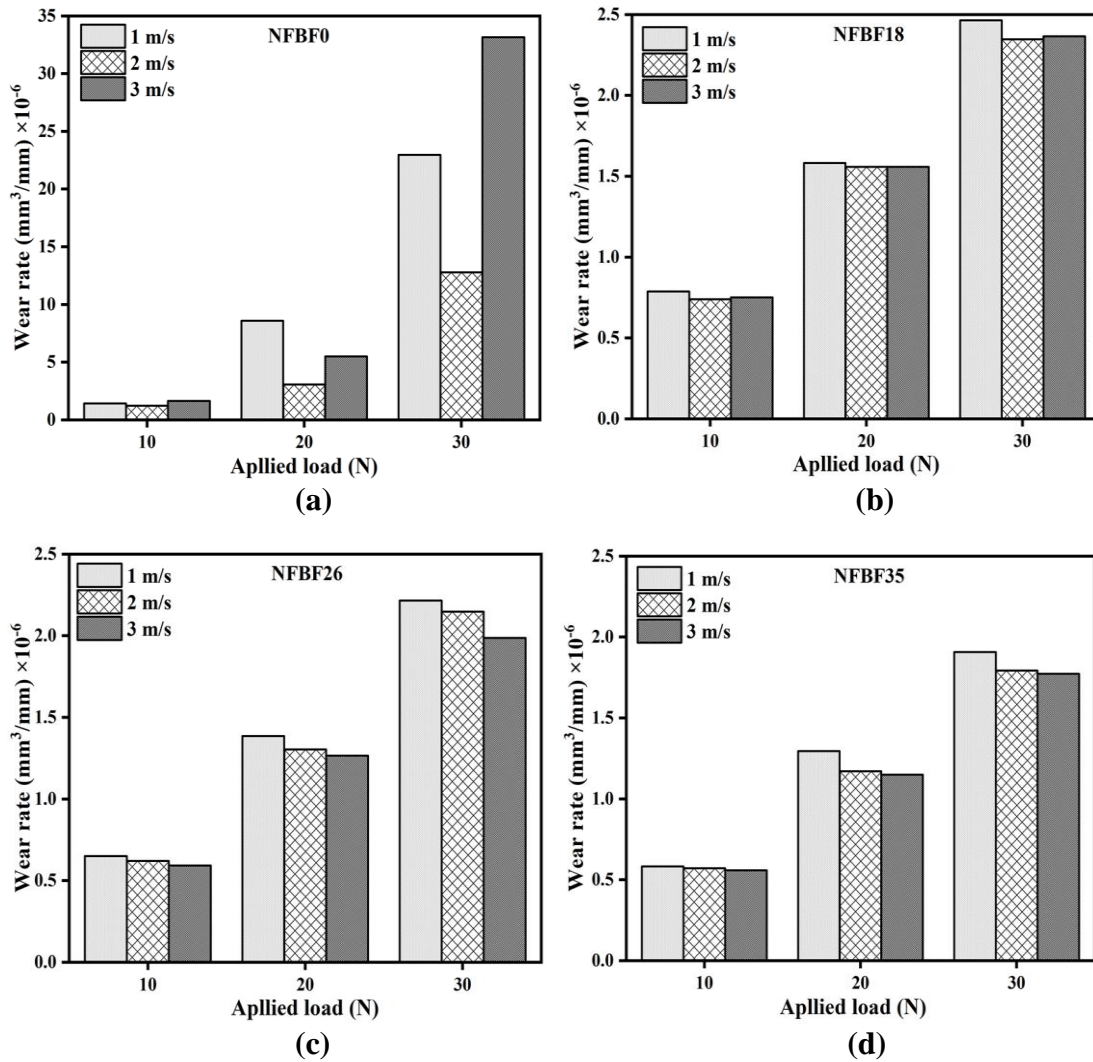


Figure 6.4 Effect of load and speed on wear rate for NFBF/PLA composites (a) neat PLA, (b) NFBF of 18 wt. %, (c) NFBF of 26 wt. %, and (d) NFBF of 35 wt. %

Observation of Figure 6.4 shows that the wear rate of the pure PLA and NFBF/PLA composites increases with increase in applied normal load (10 N to 30 N) for all the sliding velocities studied. NFBF0 showed an increase-decrease-increase trend for all applied loads and velocities. Maximum wear rate is observed when 30 N load is applied with a sliding velocity of 3 m/s. At this condition, the temperature reaches maximum due to this plastic deformation of the PLA occurs, which results in maximum wear rate. The NFBF18 composite under 10 N and 30 N load at velocities 1 m/s, 2 m/s and 3 m/s showed increase-decrease-increase trend and for 20 N load under 2 m/s and 3 m/s showed similar trend in wear rate. This indicates that the wear rate of the PLA is reduced with NFBF reinforcement for all applied normal loads at a

3 m/s sliding velocity compared to pure PLA. This is further decreased with an increase in fibre weight percentage. Reason can be explained as follows, initially for lower weight percentage of fibre the back transfer of fibre film is less hence the reduction in wear rate is less for the NFBF/PLA composite compared to pure PLA. When the weight fraction of the fibre is high, back transfer of fibre film is high and this film acts as a shield and protects the specimen from further damage. The exposure of non-abrasive fibrous materials on the counter surface also causes reduction in the wear rate.

6.3.3 Specific wear rate

Specific wear rate results of the pure PLA and NFBF/PLA composites are shown in Figure 6.5 to Figure 6.7 for three different sliding velocities. The specific wear rate increases with an increase in applied load for PLA and NFBF/PLA composites irrespective of fibre content and sliding velocities. Similar behaviour is observed by Yousif and El-Tayeb (2008) for the oil palm reinforced composites. The effect of the load applied on the specific wear rate is more clearly articulated in pure PLA than the NFBF/PLA composites. From Figure 6.5, the increase in specific wear rate of the pure PLA is less for 10 N to 20 N applied load and sudden increase is observed for the 30 N applied load. For 30 N applied load PLA specimen lost its dimensional stability and got distorted due to high axial repeated thrust. This happens due to the softening and polymer film generation of the pure PLA.

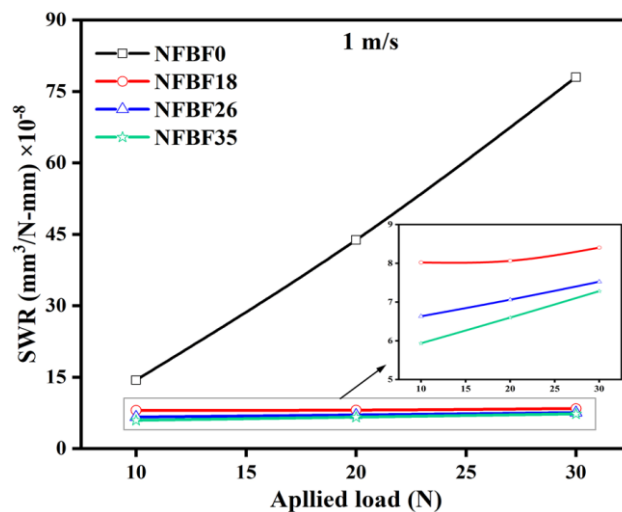


Figure 6.5 Specific wear rate versus applied load for 1 m/s of PLA and NFBF/PLA composites

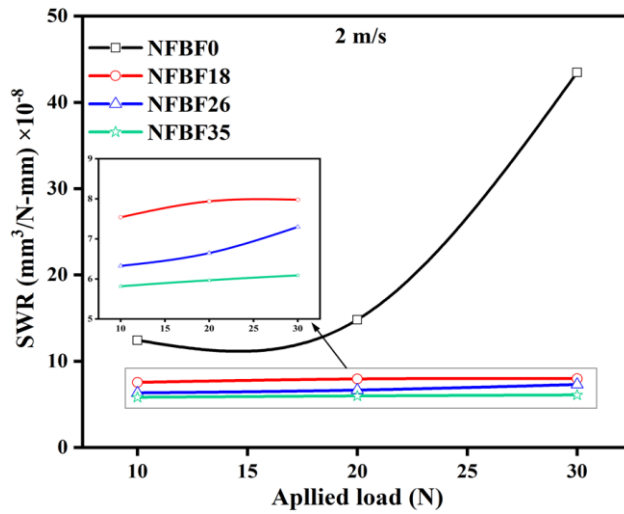


Figure 6.6 Specific wear rate versus applied load for 2 m/s of PLA and NFBF/PLA composites

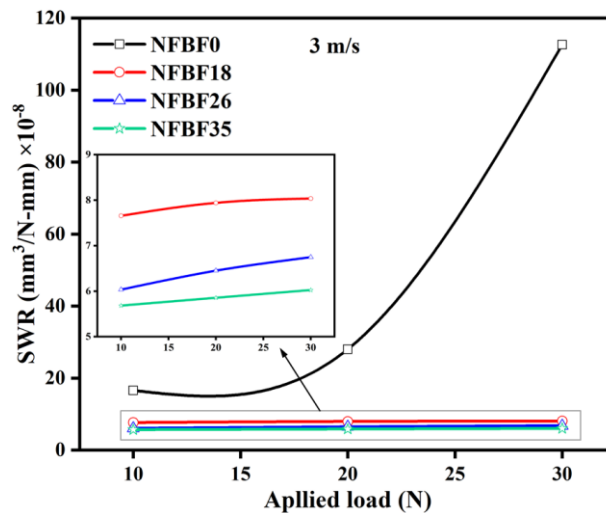


Figure 6.7 Specific wear rate versus applied load for 3 m/s of PLA and NFBF/PLA composites

The NFBF/PLA composite showed lower specific wear rate results compared to pure PLA. This represents the enhancement in the wear property of the PLA with NFBF reinforcement. During the sliding process, applied load is transferred from matrix to the reinforced fibre which depends on the strong interfacial bonding between the fibre and matrix. This protects the easy removal of PLA polymer from the composites and also prevents the fibre pull out during the sliding. This in turn enhances the wear properties of the composites. Yousif (2008) and Yousif and El-Tayeb (2007) also reported that the wear resistance of the composites is enhanced by good interfacial bonding between fibre and matrix. The wear resistance of the composites is further

enhanced with the increase in fibre content. The NFBF35 composite showed a highest wear resistance compared to pure PLA and other composites as seen in Figure 6.5 to Figure 6.7.

Effect of NFBF reinforcement on specific wear rate (SWR) of PLA is shown in Figure 6.8 for the sliding velocity of 1 m/sec and applied load of 10 N. For initial sliding distance, SWR of the pure PLA and its composites is high then SWR reduces drastically with further increase in sliding distance. At a distance of about 3000 m PLA and NFBF/PLA composites showed lowest SWR values. This indicates that material removal rate is less for the higher sliding distances. This may be due to the generation of transfer film on the counter surface. Pure PLA showed high SWR due to generation of high interface temperature and undergoes a softening process which increases the material removal rate. In the case of NFBF/PLA composites the material removal rate is less for higher sliding distances. The strong fibre-matrix bonding prevents the fibre pull out and the presence of fibres at the sliding interface reduce the softening process of the resin (Yousif et al. 2010).

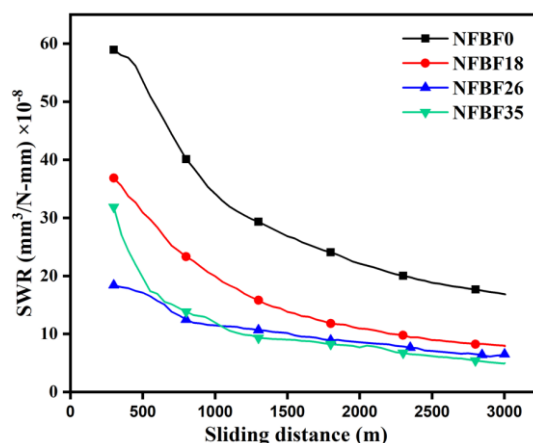


Figure 6.8 Specific wear rate versus sliding distance for PLA and NFBF/PLA composites at 1 m/s sliding velocity and 10 N applied load

The comparison of minimum and maximum values of SWR of pure PLA with NFBF/PLA composites are presented with percentage variation in Figure 6.9. Pure PLA is considered as base material for the comparison purpose and the percentage reduction is shown down head arrows. For pure PLA $12.43 \times 10^{-8} \text{ mm}^3/\text{N-mm}$ is recorded as minimum specific wear rate for 10 N applied load and 2 m/s velocity. Whereas, the maximum specific wear rate of $112.62 \times 10^{-8} \text{ mm}^3/\text{N-mm}$ is measured

for 30 N load and 3 m/s velocity. The great degree of reduction in SWR for pure PLA is observed as a result of NFBF reinforcement. From Figure 6.9 it can be seen that the NFBF35 composite received lower SWR compared to pure PLA for both minimum and maximum values. The NFBF35 composite showed 54.29% and 94.95% reduction for minimum and maximum SWR compared to pure PLA. This proves the reinforcement of NFBF with PLA enhanced the friction and wear properties of the PLA polymer.

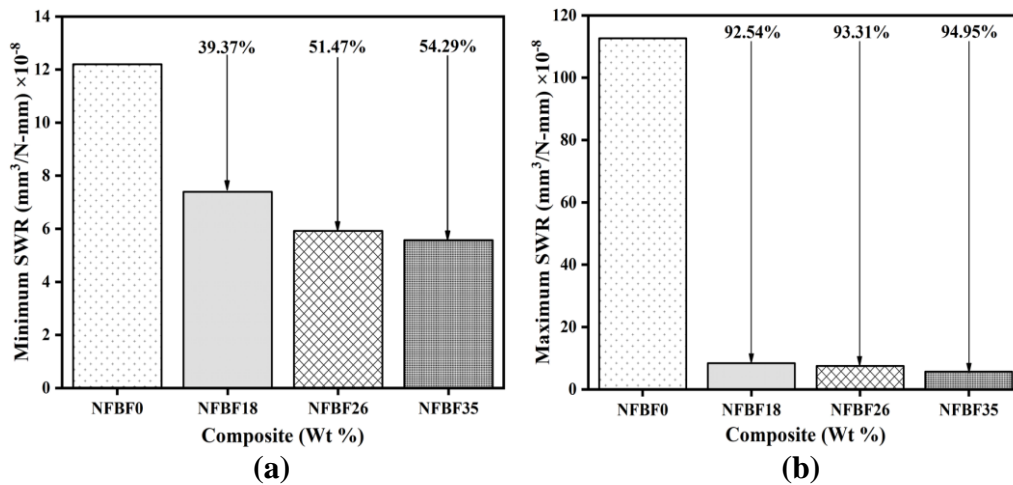


Figure 6.9 Percentage variation of specific wear rate minimum and maximum values of PLA and NFBF/PLA composites

6.3.4 Worn surface morphology

SEM micrographs of worn surfaces of the PLA and NFBF/PLA composites samples tested for wear parameters under 10 N applied load at 1 m/s are presented in Figure 6.10. SEM image taken on worn surface of the PLA sample (Figure 6.10a), shows a parallel grooves in the sliding direction and the surface also appeared to be rough. SEM image taken on worn surface of the NFBF18 composite sample Figure 6.10(b), shows the presence of exposed fibre as a result of micro-cutting and micro-ploughing processes. However, strong fibre-matrix interfacial bonding is observed in the NFBF26 and NFBF35 composites as seen in the corresponding SEM images shown in Figure 6.10(c) and Figure 6.10(d). This facilitates the equal distribution of stresses in the fibre and matrix and increases resistance to any composite damage. Hence, the wear performance of NFBF reinforced PLA composites are improved. Small cracks in fibres are seen from Figure 6.10(d) which is due to the side shear forces.

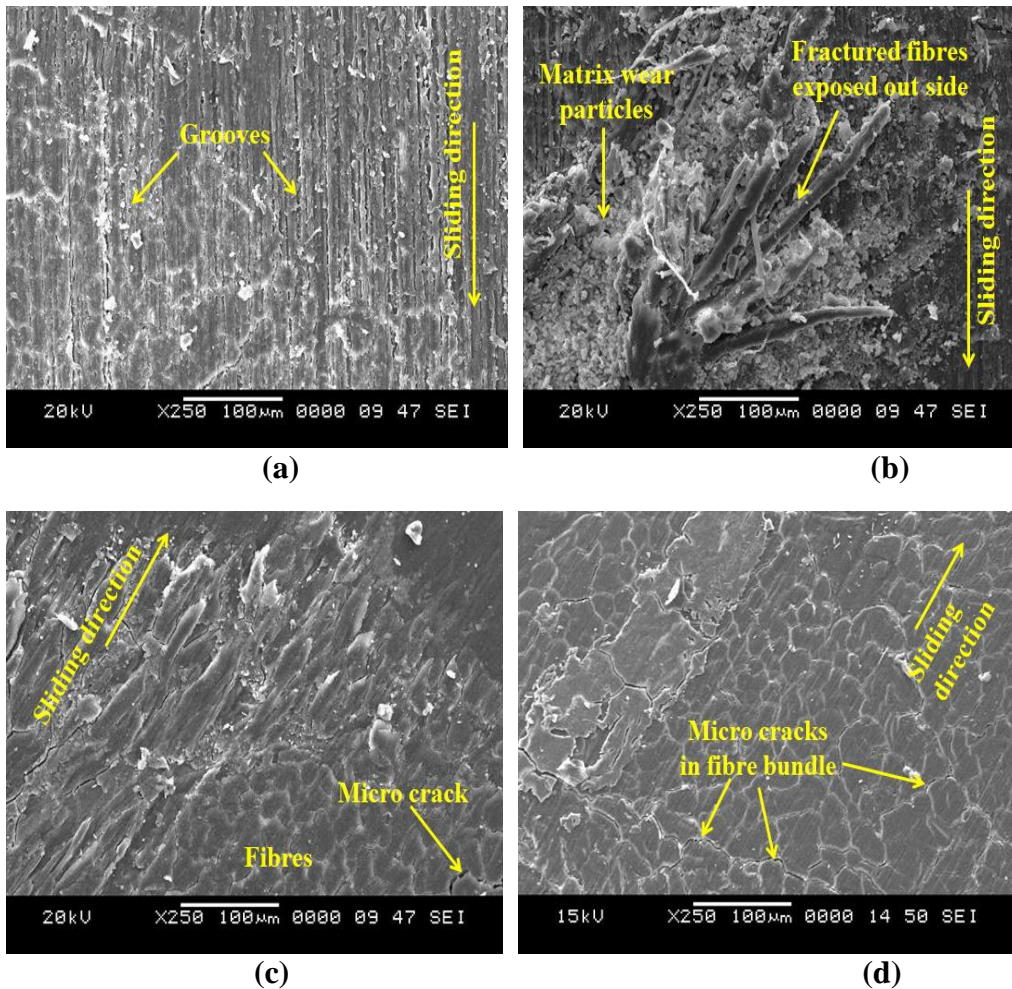


Figure 6.10 SEM images of worn surfaces of pure PLA and NFBF/PLA composites for 10 N applied normal load and 1 m/s velocity (a) NFBF0, (b) NFBF18, (c) NFBF26 and (d) NFBF35

Figure 6.11 indicates SEM micrographs taken from worn surfaces of the pure PLA and NFBF/PLA composites under a load of 30 N applied at 3 m/s. Fibre pull out, deformed and bent fibres, fibre-matrix debonding, plastic deformation, film formation and deformation debris are the different modes of wear mechanism (Rashid et al. 2017). PLA is a soft material, rubbing of this material with hard steel generates frictional heat which leads to further softening of the PLA. Moreover, the increase in applied load also increases the frictional heat which results in plastic flow of the material as seen in Figure 6.11(a). Figure 6.11(b), shows three damage features, such as fibre fracture, fibre peeling and fibre bend along the sliding direction. For higher load and speed the composites with the lower fibre content are unable to sustain the load and stresses developed during the sliding process leading to fibre fracture and

fibrillation of fibres. Natural fibres are relatively soft and non-abrasive materials in addition to that the ability to bend and deform in sliding forms a thin back transfer film. This helps to reduce the mechanical interlocking between the pin and disc, it results to a decrease in the friction co-efficient (El-Tayeb 2008). Figure 6.11(c) and Figure 6.11(d) shows a gap between the polymer and fibre due to the debonding. In the course of sliding, this could take place due to high shear stress associated with the thermochemical loading. Frictional heat between contact surfaces rises during wear testing and it causes a partial softening of the material constructed on a thin film layer (Omrani et al. 2016). This layer behaves as a layer of protection and prevents the mechanical interlocking. Because of this reduced friction co-efficient and increased wear resistance are observed for NFBF26 and NFBF35 composites.

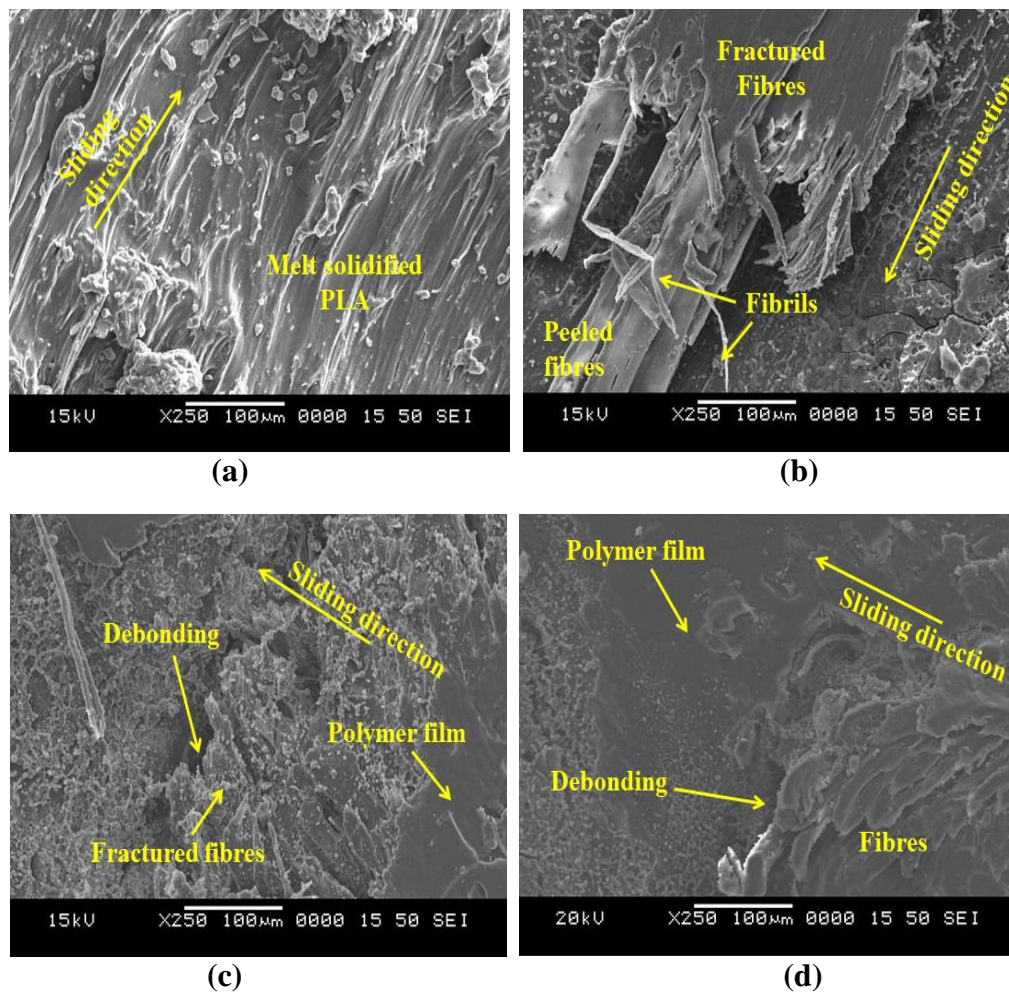


Figure 6.11 Worn surfaces SEM micrographs of pure PLA and NFBF/PLA composites for 30 N applied load and 3 m/s velocity of (a) NFBF0, (b) NFBF18, (c) NFBF26 and (d) NFBF35

SEM images of wear debris of pure PLA and NFBF/PLA composite for 30 N applied load at a 3 m/s velocity for 3000 m sliding distance are displayed in Figure 6.12. Figure 6.12(a) shows the pure PLA wear debris and its softening and plastic flow behaviour. Figure 6.12(b) shows the fibre wear debris of the NFBF35 composite. It is known that the wear debris particles fills the gap between the sliding interface and rolls in the interface. Furthermore, it will not abrade composite due to the lubricating aspect of the fibres, which leads to the reduction of the friction coefficient. In turn, this reduces the material removal rate of the composites.

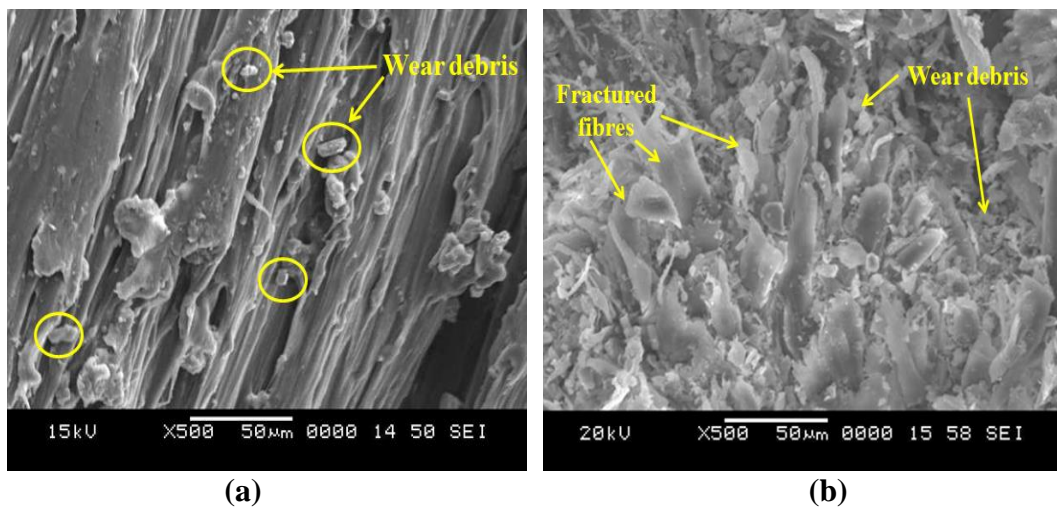


Figure 6.12 Wear debris micrographs of (a) NFBF0, (b) NFBF35

6.4 Plane strain fracture toughness

Plane strain fracture toughness experiment carried out on PLA and NFBF/PLA composites using single-edge-notch-bend (SENB) specimens is presented in this section. This experiment is carried out with different load of fibre and results are compared with the pristine PLA. Finally the fracture toughness results are compared with the other natural fibre reinforced PLA composites available in the literature.

6.4.1 Tensile properties

Stress-strain curves of PLA and NFBF/PLA composites are shown in Figure 6.13, while ultimate tensile stress and Young's modulus of PLA and NFBF/PLA composites are shown in Figure 6.14. It can be observed from Figure 6.13 that PLA has a linear deformation and for the NFBF/PLA composites the deformation behaviour is non-linear due to reinforcement. It is also observed that the strength and

strain percentage of the NFBF/PLA composites are higher compared to PLA (NFBF0). Tensile strength and modulus of the pure PLA are enhanced due to the reinforcement of the NFBF as seen in Figure 6.14. Kumar et al. (2010) studied flax fabric reinforced PLA composites and reported ultimate tensile strength and tensile modulus of 21 MPa and 0.137 GPa for 30% weight fraction of the fibre. It is clear that tensile properties of NFBF/PLA composites are better than the flax woven PLA composites studied by Kumar et al. (2010) due to the architecture of the yarn used to make the fabric used in the present work. Rajesh and Jeyaraj (2017b) also shown that the reinforcement of flat braided yarn woven fabric composites enhances the mechanical properties of the composites compared to random-short fibre and conventional woven fabric composites for same fibre weight percentage.

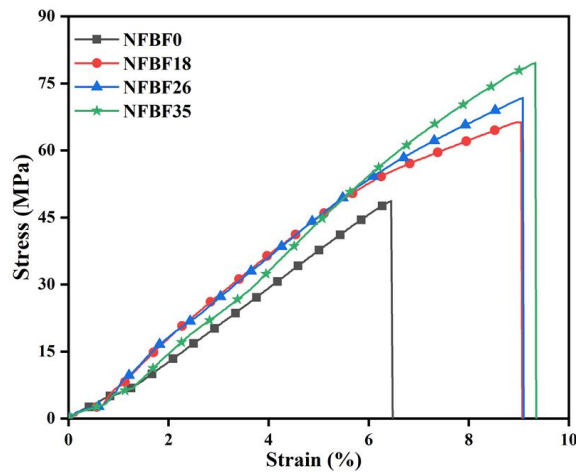


Figure 6.13 Stress-strain curves of PLA and NFBF/PLA composites

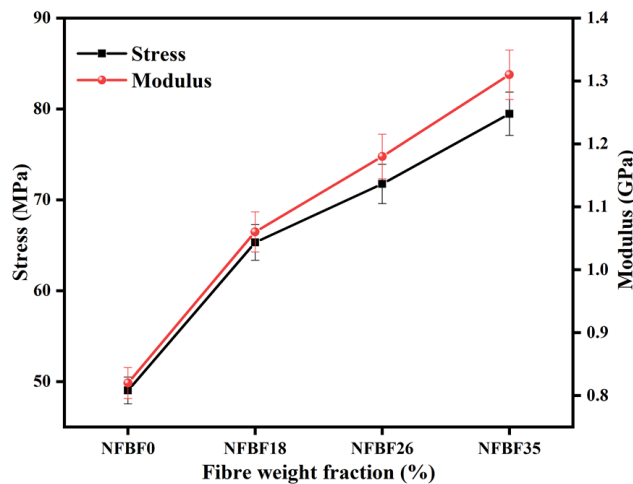


Figure 6.14 Ultimate tensile stress and modulus of the pure PLA and NFBF/PLA composites

The enhancement of the tensile properties due to reinforcement can be attributed to good fibre-matrix interfacial bonding, which results in better stress transfer from PLA matrix to flax fibres. Composites with low fibre weight fraction are unable to transfer much stress which leads to lower strength of the composites. However, for the composites with higher weight percentage of the fibre are able to transfer much stress, hence received higher stress. The average values of ultimate stress and modulus of the PLA specimens are 49.02 MPa and 0.82 GPa respectively. Ultimate stress and modulus increases with increase in fibre content and maximum stress and modulus of 79.47 MPa and 1.31 GPa respectively observed for NFBF35 composites which are 62.11% and 59.75% high compared to pure PLA results.

6.4.2 Fracture toughness

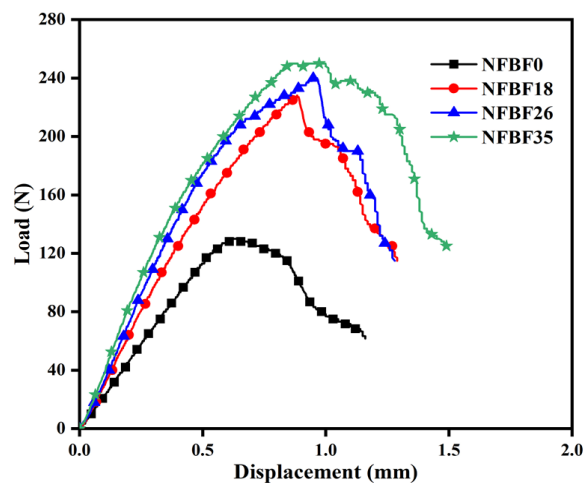


Figure 6.15 Typical load versus displacement curves of PLA and NFBF/PLA composites

Typical load versus displacement curves of PLA and NFBF/PLA composites are shown in Figure 6.15. It can be observed that the deformation of the load-displacement curve is linear for pure PLA. However, for the NFBF/PLA composites initially the deformation is linear followed by a non-linear deformation is noticed before the maximum load attainment. Due to plastic deformation and crack propagation in the PLA and NFBF/PLA composites reduction in load is noticed after maximum load attainment. After peak load there is a gradual decrease in load vs. displacement of the PLA, this shows that after crack initiation pure polymer underwent gradual crack propagation. But in the case of composites load-

displacement curves are relatively compliant nature. Due to fibre reinforcement the crack-propagation becomes a slow progressive process. From Figure 6.15, it can be seen that the NFBF reinforcement enhanced the load bearing capacity and it further enhanced with increase in fibre weight percentage. This can be attributed to the good fibre-matrix adhesion which improves load transfer from the matrix to the reinforcement hence improves the properties. Area under the curve of the NFBF/PLA composites is increased compared with the pure PLA, this might be due to increased strain percentage with the fibre reinforcement which can be seen from Figure 6.13.

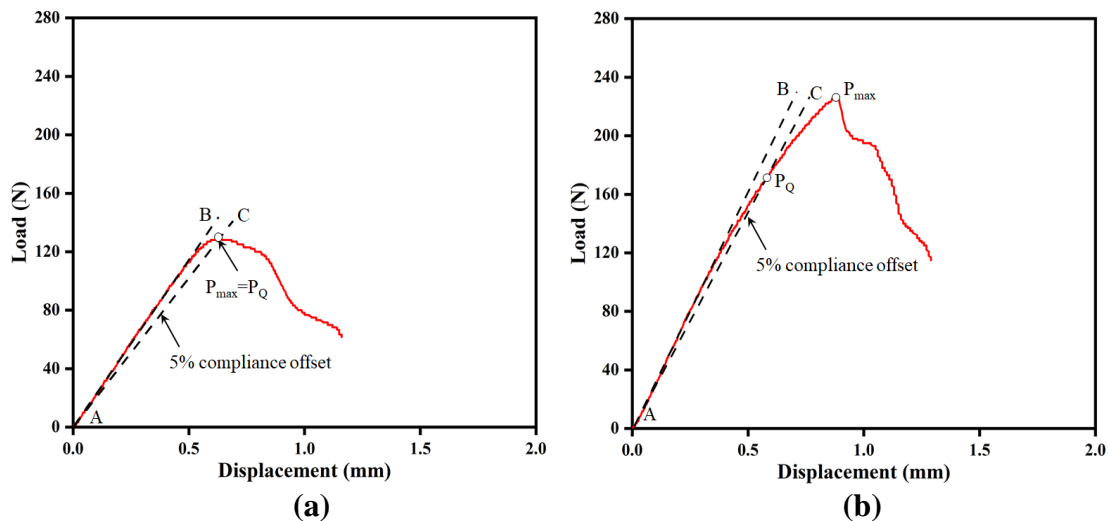


Figure 6.16 Measurement of P_Q from load versus displacement curve for (a) pure PLA and (b) NFBF18 composite

Measurement of P_Q from load versus displacement curve for PLA and NFBF/PLA composites is shown in Figure 6.16. From Figure 6.16, it can be seen that, line AC is drawn 5% offset from the original load displacement curve tangent as outlined in the standard (“Standard Test Methods for Plane-Strain Fracture Toughness and Strain Energy Release Rate of Plastic Materials 1” n.d.). In Figure 6.16a, measured maximum load (P_{max}) of the pure PLA sample, lies between the two lines (AB and AC), hence P_{max} is considered as P_Q . Similarly in Figure 6.16b the maximum load (P_{max}) of the NFBF/PLA composite lies outside the lines (AB and AC), hence the intersection point of line AC and load versus displacement curve is considered as P_Q . Similar load-displacement behaviour is noticed for all the NFBF/PLA composite samples. Measured P_Q value is used to calculate the K_Q given in Equation 2.16.

Figure 6.17 represents the fracture toughness (K_{IC}) values of PLA and NFBBF/PLA composites for different fibre weight fraction. The reinforcement of braided yarn fabric showed enhancement in the fracture toughness compared to PLA and it increases with increase in the fibre content. Similar observations are reported by Mustapha et al. (2015), Alvarez et al. (2006) and Agopyan and John (1992). The fracture toughness of the fibre reinforced composites depends on the fibre bridging between the two crack sides (Mustapha et al. 2015). This fibre bridging in the crack requires higher load and strain energy for crack propagation which depends on the architecture of the fibre for the woven composites. Sawpan et al. (2011) observed 36.4% enhancement in K_{IC} due to improved fibre bridging and load bearing capacity of the long natural fibre composites compared to the typical short-random oriented natural fibres. Rajesh and Jeyaraj (2016) showed that the load bearing capacity of the braided fabric composites improved with the enhancement in the storage modulus compared to knitted and woven fabric composites. Due to improved fibre bridging and load bearing capacity of the flax fibre braided composites, K_{IC} values are enhanced compared to other short-random natural fibres, long fibres and woven mat composites as shown in Figure 6.20. Mechanical properties of the fabric reinforced composites depends on the fibre yarn and matrix properties, weaving or braiding architectures, yarn spacing and fibre content (Huang 2000). Pristine PLA showed K_{IC} value of 3.10 MPa-m^{1/2} and it is further increased due to NFBBF reinforcement. NFBBF35 composite showed maximum K_{IC} of about 5.32 MPa-m^{1/2}, it is 71.61% greater than the value corresponds to pure PLA.

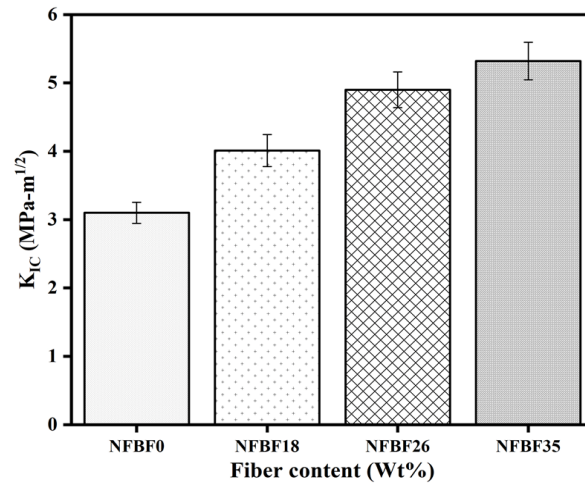


Figure 6.17 K_{IC} of PLA and NFBF/PLA composites for different fibre weight percentage

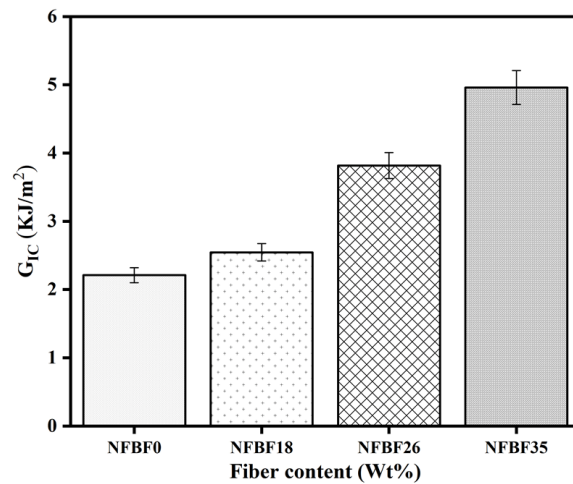
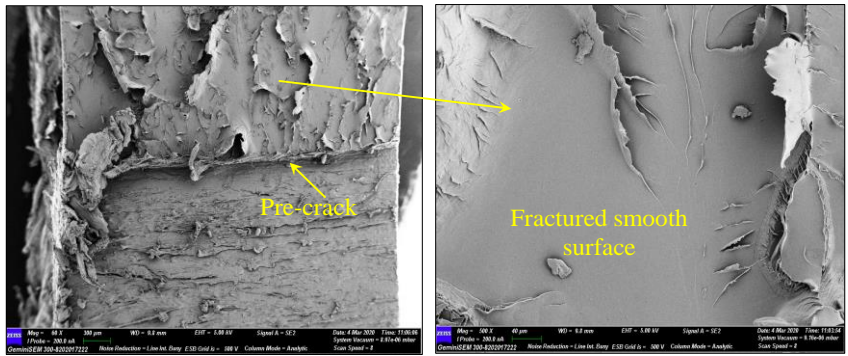


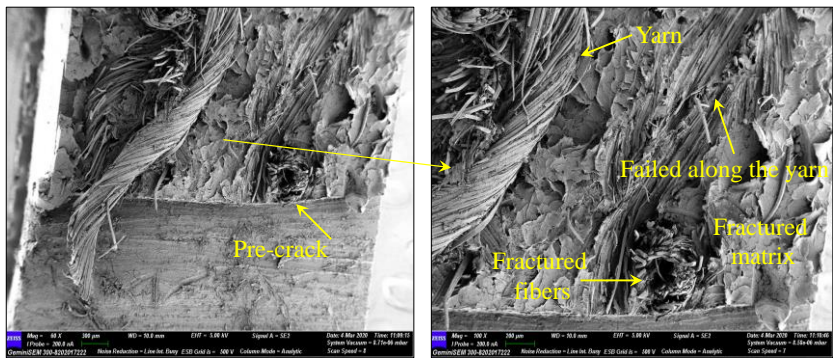
Figure 6.18 G_{IC} of PLA and NFBF/PLA composites for different fibre weight percentage

Effect of increase in weight fraction of the fabric on the strain energy release rate (G_{IC}) of the composites is shown in Figure 6.18. From Figure 6.18, it is clear that the strain energy release rate increases significantly with increase in fibre weight fraction. The NFBF35 composite has a strain energy release rate of 4.96 KJ/m², while it is 2.21 KJ/m² for the pure PLA sample. It can be observed that the NFBF reinforcement significantly improved the strain energy by 15% to 124% (2.54 KJ/m² to 4.96 KJ/m²) as compared with the virgin PLA sample value. This enhancement in the strain energy might be due to toughening effect linked to the reinforcement of flax fabric with the neat PLA polymer (Kumar et al. 2019).

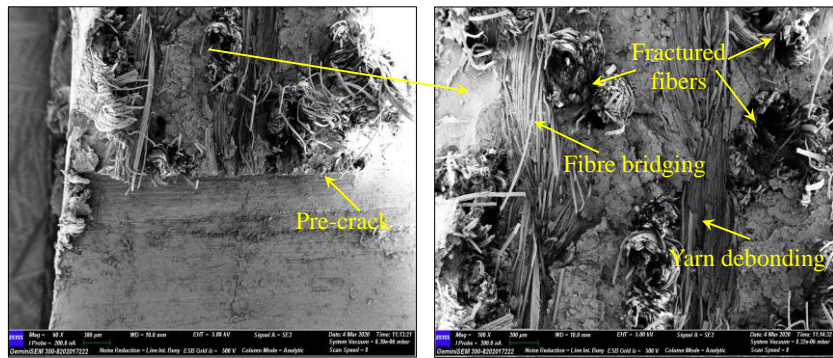
Figure 6.19 shows SEM images taken on the fractured surfaces of the PLA and NFBBF/PLA composites. It shows the morphology of the specimens and fibre morphology in the composite structures. PLA is a glassy semi crystalline polymer, because of its inherent chemical composition and atomic structure, is very brittle (Song et al. 2011). Because of its brittle nature there is a reduction in elongation at break which can be seen from Figure 6.13. Figure 6.19a represents the brittle like region on the fractured surface of the neat PLA, this might be the reason for significant shortage of toughness mechanism. The literature study also indicates that the toughness of the PLA decreases due to its brittle nature (Zhou et al. 2016). The NFBBF reinforcement improves the elongation at break and load bearing capacity of the PLA polymer. Due to this there is an enhancement in the K_{IC} values of the composites. Figure 6.19b-d shows a rougher surface and river pattern formed on the matrix due to yarn pull out. This indicates that the failure of the composites occurs along the yarn due to stress concentration surrounding the braided yarn which further results in yarn de-bonding. This is the reason for the crack deflection mechanism and plastic deformation which improves fracture durability during deformation by increasing the crack propagation duration. Higher fibre content and reduced PLA quantity can be seen in Figure 6.19d, which improves the load bearing capacity of NFBBF35 composite. This in turn enhances fracture toughness of NFBBF35 composite. At the same time, lower fibre content and higher PLA quantity can be seen in Figure 6.19b, which results in lower fracture toughness of NFBBF18 composite as initial crack propagation occurs easily at matrix rich region. The enhancement in the modulus of the PLA with the NFBBF reinforcement plays an important role in preventing the crack propagation. Fibre pull-out, fibre-bridging and fibre fracture are the energy absorbing events of the cellulose fibres which are involved in the enhancement of the K_{IC} (fracture toughness) values of the polymer matrix (Alamri and Low 2012; Wang et al. 2007).



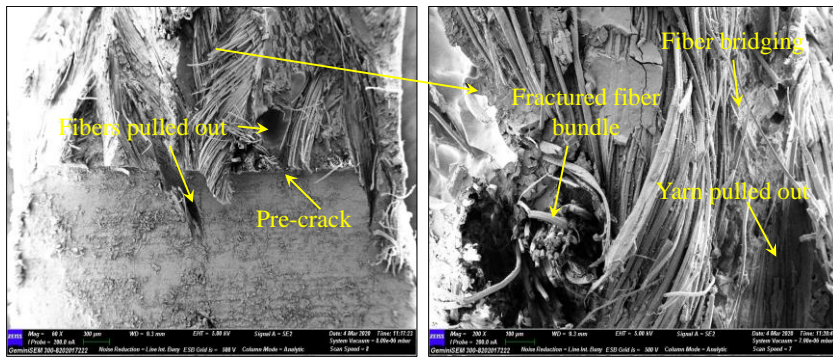
(a)



(b)



(c)



(d)

Figure 6.19 SEM micrographs of fractured surfaces of SENB specimens a) pure PLA, b) NFBF18, c) NFBF26 and d) NFBF35 composites

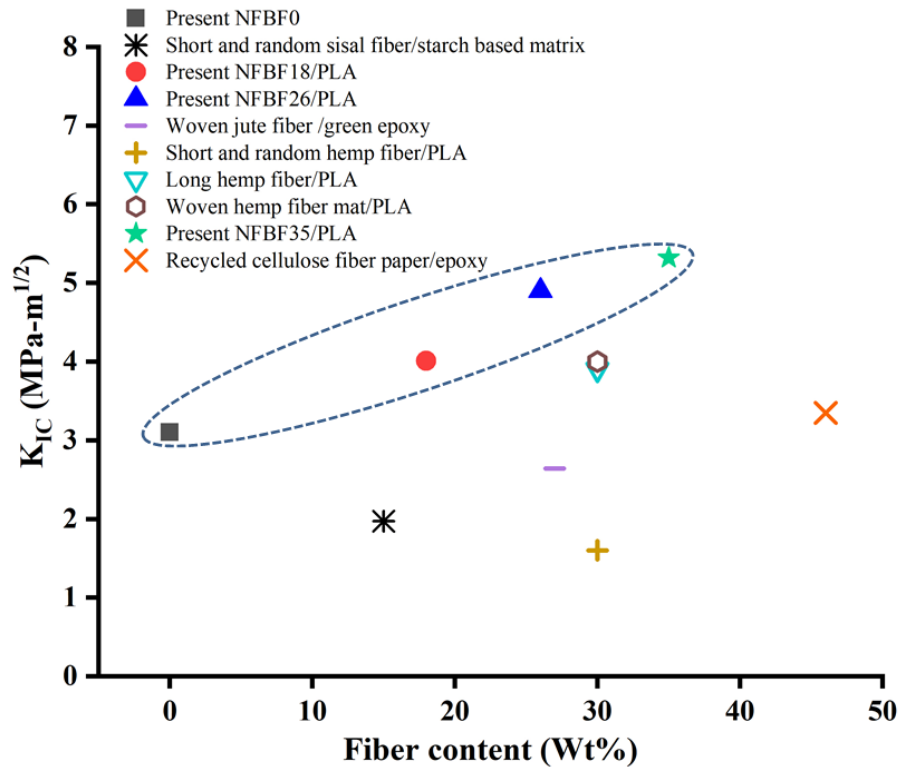


Figure 6.20 Fracture toughness (K_{IC}) plotted against fibre content from available literature studies

Figure 6.20 presents the comparison of K_{IC} values of NFBF/PLA composites with different natural fibre reinforced PLA composites reported in literature. From Figure 6.20, it can be observed that fracture toughness (K_{IC}) of NFBF/PLA composites is high compared to other types of natural fibre reinforced PLA composites. Architecture of the fibre reinforcement and good fibre-matrix interfacial bonding may be reason for fracture toughness enhancement. Sawpan et al. (2011) observed that the reinforcement of natural fibre in the form of short and random fibre K_{IC} value is decreased compared to neat PLA and it is further decreased with the increase in fibre content. It is due to the higher stress concentration associated with the short fibre ends and poor matrix bonding (Sawpan et al. 2011). Fracture toughness of the PLA composites is enhanced with the reinforcement of long hemp fibre (Islam et al. 2010a). This may be due to reduced stress concentration and higher aspect ratio of the long fibres provides better resistance to bending and crack propagation. K_{IC} value is further increased with the reinforcement of hemp fibre in the form of woven mat preforms (Islam et al. 2010b). The interlocking nature of the fibre in the woven mat

requires higher load for deformation or bending. Textile composites provide high energy absorption under compressive loads and high degree of interweaving of fibre yarns in the material microstructure presents obstacle to macroscopic crack propagation (Xie et al. 2006). Hence it shows higher fracture toughness. From this comparison study, it can be concluded that the architecture of the reinforcement fibre influences the plane-strain fracture toughness (K_{IC}) of the composites. In the case of braided composites yarn segments needs more strain energy to begin crack propagation compared to standard fabric composites (Ren et al. 2010). Due to this there is an enhanced fracture toughness is observed for flax fibre braided PLA composites.

6.5 Conclusion

The friction and wear characteristics of the NFBBF/PLA composites subjected to dry sliding have been investigated. The influence of different fibre weight fraction is analysed for various loads and sliding velocities. It is found that, the NFBBF reinforced PLA composites offers great degree of coefficient of friction and wear rate. The reinforcement of NFBBF in PLA enhanced frictional force and reduced the height loss of the composite specimen. Wear rate and specific wear rate of the pure PLA and NFBBF/PLA composites increases with increase in applied normal load. NFBBF reinforcement reduces specific wear rate of PLA and about 95% reduction for the NFBBF35 composite. These findings may be useful for light weight bearing applications, for example non-biodegradable plastic washers, bushings and window roller bearings can be replaced with these biodegradable natural fibre reinforced PLA composites. SEM micrographs of NFBBF/PLA composites have shown good fibre-to-matrix interfacial bonding. This facilitates composite to avoid easier de-bonding and this contributes to an improved wear resistance property for the composites. Fibre fracture, fibre peeling, de-bonding and micro-cracks are observed as the common wear failure mechanisms of the NFBBF/PLA composites.

Tensile strength and modulus of the PLA are enhanced with the reinforcement of NFBBF and these are further enhanced with the increase in fabric content up to 62.11% and 59.75% respectively. Similarly K_{IC} and G_{IC} values are also improved with the

reinforcement of braided yarn fabric. Pristine PLA showed K_{IC} and G_{IC} of 3.10 MPa- $m^{1/2}$ and 2.21 KJ/ m^2 . Whereas, the NFBF35 composite showed maximum K_{IC} and G_{IC} values of about 5.32 MPa- $m^{1/2}$ and 4.96 KJ/ m^2 respectively. SEM analysis indicated the good fibre-matrix bonding, fibre fracture and fibre bridging, which are helps to improve the tensile strength, modulus and fracture toughness of the composites. Fracture toughness study shows higher K_{IC} values for NFBF/PLA composites compared to other types of natural fibre reinforced composites. This is due to architecture of the reinforcement fibre used. These composites are being developed for potential applications in the housing and automobile interiors such as telephone stand, seat back and door trim.

7 BUCKLING AND FREE VIBRATION PROPERTIES

Several research studies published on natural fibre reinforced PLA composites are related to prediction of tensile, flexural, impact and compression properties. However, the characterization of buckling and free vibration of PLA and its composites under axial compression is not studied so far. It is important to find the mechanical buckling and free vibration behaviour of braided flax fibre PLA bio-composites for automotive, aerospace marine and biomedical applications. Objective of the present work is to find the mechanical buckling and dynamic properties of the braided flax fibre fabric PLA bio-composites under axial-compressive loads. Effect of fibre content on buckling and free vibration response is also investigated.

7.1 Density and void content

Theoretical and experimental densities of the PLA and NFBBF/PLA composite samples are calculated in order to analyse the porosity content and the results are given in Table 7.1. The porosity (void content) of the composite samples influence the physical and mechanical properties of the composites (Jawaid et al. 2011). Observation by Table 7.1 shows that the experimental density of the virgin PLA polymer samples is lower than the theoretical density. This is due to the air entrapment while manufacturing the PLA polymer samples. The difference between theoretical and experimental densities increases with the number of NFBBF layers. This is attributed to the porous and moisture sensitivity nature of the natural fibres (Sanjay et al. 2016; Weidong and Yan 2012). Fabrics are loosely packed structures and reinforcement of fabrics in layer sequencing methods also may increase the void content. However, the void content of the present composites is within the acceptable range.

Table 7.1 Density and void content of the composites

Material	ρ_{th} (g/cm ³)	ρ_{exp} (g/cm ³)	ϕ_v (%)
NFBF0	1.2400	1.2385±0.001	0.120
NFBF11	1.2695	1.2569±0.002	0.992
NFBF22	1.2849	1.2613±0.005	1.836
NFBF33	1.2964	1.2649±0.017	2.429

7.2 Buckling under axial compression

Buckling behaviour of the PLA and NFBF/PLA composite specimens is investigated by applying a uni-axial compressive force through the universal testing machine (UTM). The NFBF/PLA composites are developed with different numbers of fabric layers as 0, 1, 2 and 3 (The maximum number of layers is limited to three due to the 3 mm thickness constraint associated with the test specimen) to analyse the effect of fibre loading on axial buckling behaviour of the PLA composites. Figure 7.1 represents the axial load vs. displacement curves of the PLA and its composites and these are plotted using the data collected from UTM through the data-acquisition-system.

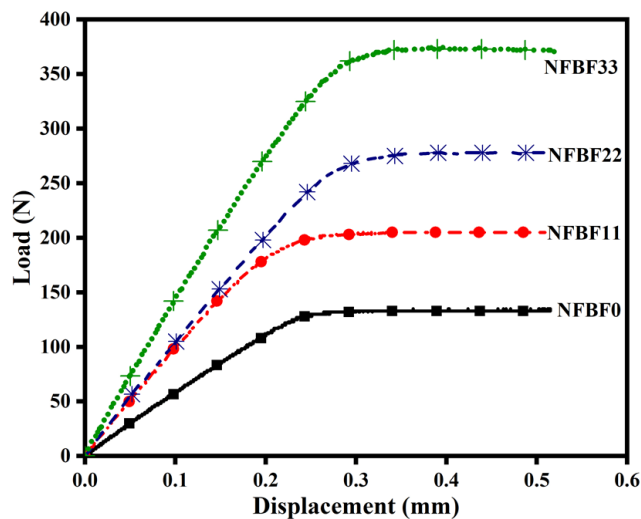


Figure 7.1 Axial load vs. displacement curves of samples according to NFBF content

Influence of number of layers of NFBF reinforcement on the load vs. displacement curve of the NFBF/PLA composites is given in Figure 7.1. It is also noticed that the neat PLA samples are buckled earlier than NFBF filled composites due to the lowest

stiffness associated with it. The critical buckling load estimated through DTM and MBC methods are presented in Figure 7.2. During the experiment, it is noticed that buckling mode shapes of the PLA and its composites are showed typical global buckling mode shapes and all specimens buckling mode shapes have zero deflection at the fixed ends and maximum deflection at the centre as depicted in Figure 7.3b. It is also observed that none of the NFBF/PLA composites are failed due to the delamination between fibre and matrix or between fabric layers as evident from Figure 7.3b. This can be attributed to the lower compressive strength associated with the composite laminas compared to the wrinkling strength of the composite (Fleck and Sridhar 2002).

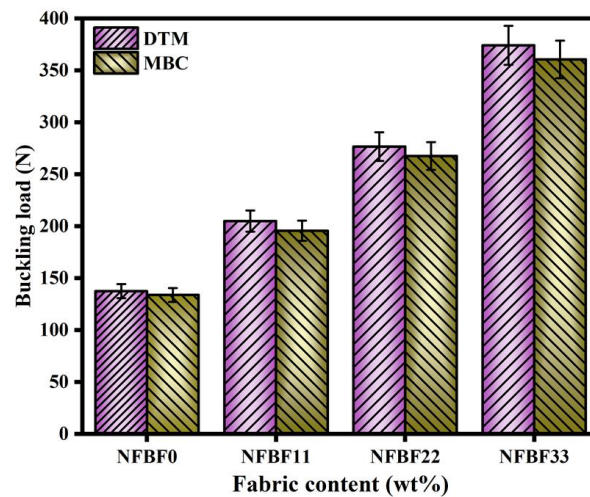


Figure 7.2 Critical buckling load of PLA and its composites obtained from DTM and MBC techniques.

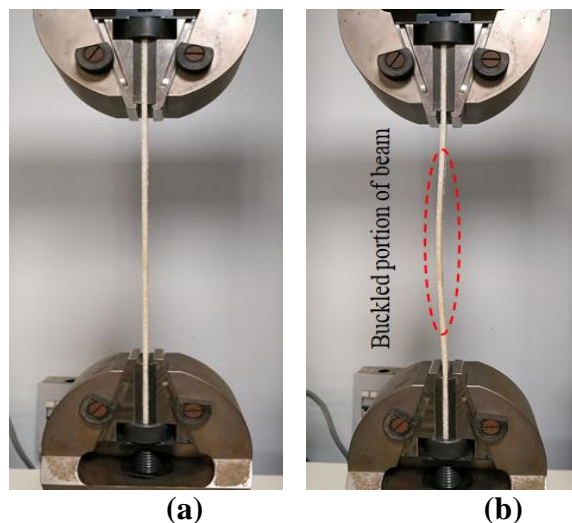


Figure 7.3 NFBF/PLA composite specimen representative images (a) before and (b) after buckling test

From Figure 7.1 and Figure 7.2 it is noticed that the compressive load sustainability of the PLA polymer is increased due to the NFBF reinforcement. It is also observed that the buckling strength of the composite increases with number of layers of reinforcement. This can be attributed to the enhanced strength and stability of the PLA polymer due to the reinforcement which led to improved load transfer between the polymer matrix and natural fibre. Neat PLA sample showed minimum critical-buckling load (P_{cr}) of 137.50 N. Meanwhile the composite reinforced with NFBF33 registered the highest critical-buckling load (P_{cr}) of 374.19 N. Bozkurt et al.(2019) carried out the buckling analysis on glass fibre filled epoxy composites and reported a critical buckling load of 341.75 N for composite specimens of 200 mm \times 20 mm \times 2.4 mm (length \times width \times thickness) with a gauge length of 155 mm. Axial-buckling study on kevlar/epoxy beam is carried out by Ozbek (2021) on composite specimens of 225 mm \times 20 mm \times 4.05 mm with a gauge length of 180 mm and obtained the critical buckling load (P_{cr}) as 405 N. Based on these studies, it can be suggested that the present NFBF/PLA composites can be used as the alternative for the synthetic polymer and synthetic fibre reinforced (glass/epoxy and kevlar/epoxy) composites. The critical-buckling load of the NFBF33 composite is 172.13% high compared to the virgin PLA value. Waddar et al. (2019) carried out an axial buckling study on sandwich composites of syntactic foam core and sisal fabric/epoxy skin using a specimen of 210 mm \times 12.5 mm \times 4 mm. The axial compressive test results showed that neat epoxy has a critical buckling load of 237.67 N and sisal/syntactic foam/epoxy sandwich composite has 514.43 N respectively. This study also shows that the reinforcement of syntactic foam as core and sisal fabric as skin enhanced the critical buckling load (P_{cr}) of 116.44% compared to neat epoxy value. From this study, it is noticed that the neat epoxy polymer has a higher buckling load-bearing capacity compared to neat PLA. Also, the reinforcement of sisal fabric skin and syntactic foam core showed an improvement of 116.44%. This percentage enhancement is lower than the present NFBF/PLA composites (172.13%). This can be attributed to good fibre matrix interfacial adhesion, higher stiffness and strength associated with the braided yarn fabric compared to conventional yarn fabric (sisal fabric) composites. Rajesh and Pitchaimani (2017b) experimentally proved that the reinforcement of braided yarn fabric significantly enhances the mechanical properties

of the composites compared to short fibre composites and conventional yarn fabric composites. Khondker et al.(2006) study also revealed that the braiding technique improves the interfacial bonding of fibre-matrix, fibre bundles (yarns) wettability and matrix fusion. Present PLA composites developed by reinforcing braided yarn also showed good fibre matrix bonding and matrix distribution inside the fibre bundle (yarn) as shown in Figure 7.4. Good interfacial bonding between fibre and matrix increases the load sharing capacity between the interface of matrix and fibre and this property enhances the compressive performance of the composite (Jin et al. 2016). Due to this reason, present NFBF/PLA composites showed better performance under axial-compressive load compared to the PLA.

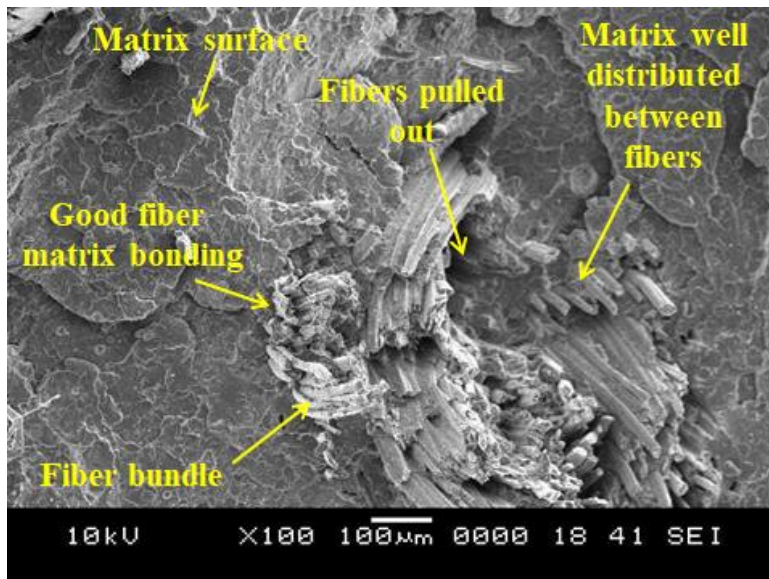


Figure 7.4 SEM micrograph presenting fibre matrix bonding of NFBF11 composite

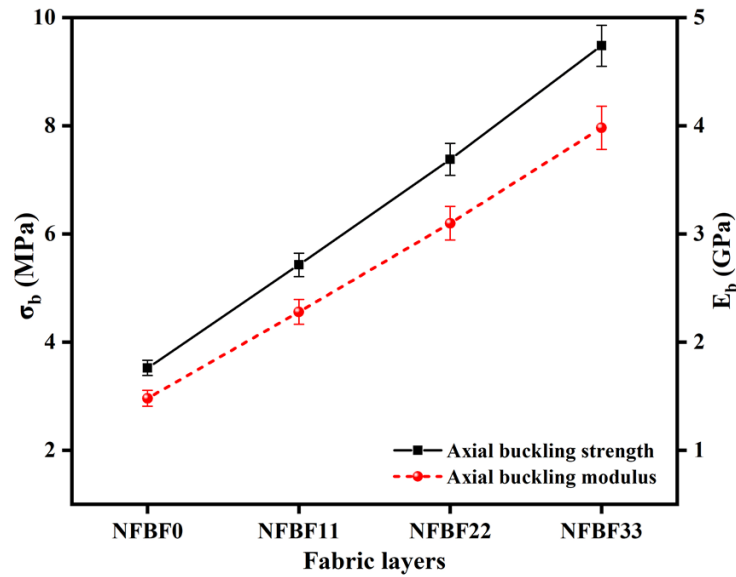


Figure 7.5 Buckling strength and modulus of the PLA composites with different fabric content

The buckling strength of PLA and NFBF/PLA composites is calculated as the product of critical buckling load and the cross-sectional area of the test specimen (i.e. $\sigma_b = P_{cr} / A$). Similarly, the axial compression (buckling) modulus (E_b) is calculated using stress-strain (i.e. $E_b = \sigma_b / \varepsilon$) relation. Calculated strength (σ_b) and modulus (E_b) results of neat PLA and its composites are shown in Figure 7.5. Axial buckling strength and modulus of the virgin PLA is 3.52 MPa and 1.48 GPa respectively. Buckling strength and modulus of the PLA specimen is increased with number of NFBF layers of reinforcement. It is noteworthy that a similar trend of enhancement in mechanical properties (compressive strength and modulus) are observed by different researchers (Jirawattanasomkul et al. 2019; Pei et al. 2016; Yan and Chouw 2015). The composite filled with 3 layers of braided yarn fabric (NFBF33) showed the highest strength (9.47 MPa) and modulus (3.98 GPa) compared to virgin PLA and other composites.

7.3 Free vibration response under axial compressive load

Neat PLA and NFBF/PLA composites analysed for the buckling behaviour is considered for the free vibration study under axial compression. The natural frequencies of first three bending modes are obtained by increasing the compressive load in the step of 30 N. A light-weight sensor is pasted on the composite specimen at

a distance of 30 mm from the bottom fixed end as shown in Figure 2.21 and to excite the composite beam at the different marked positions roving impact-hammer technique is used. From this, frequency response functions (FRF's) are obtained using DEWE-Soft software which uses FFT to convert time-domain signals into frequency domain signals. Figure 7.6 represents a typical FRF curve of the NFBF11 composite beam.

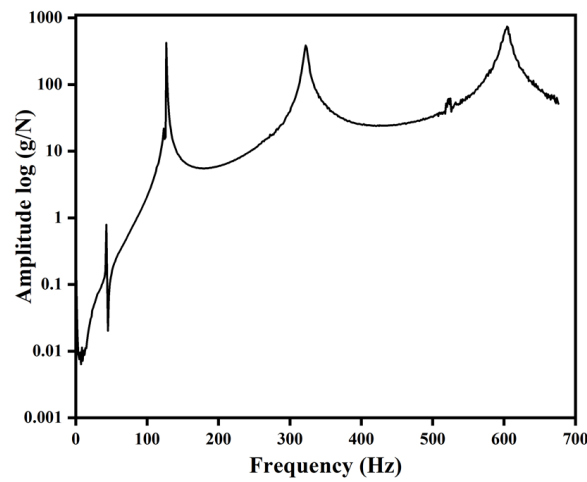


Figure 7.6 Representative frequency response function of NFBF11 composite sample

Natural frequencies obtained at different loading for first three bending modes are presented in Figure 7.7. The natural frequency of NFBF/PLA composite beams is always high compared to pure PLA samples. This can be attributed to higher stiffness and strength associated with the NFBF/PLA composites. Further, the natural frequency of all the samples (PLA and NFBF composites) reduces with the increase in the magnitude of the axial compressive load. To measure free vibration response accurately and efficiently under a particular axial-compressive load, it is important to maintain the constant axial-compressive load for a certain time period and this is achieved by controlling the UTM program with a constant incremental load (30 N). First bending mode natural frequency of the composite beams approaches the minimum value when the load is near the P_{cr} and it suddenly increases just after crossing P_{cr} value. Axial-compressive load on the composite beams develops the compressive membrane stresses, which reduces the laminate stiffness. Due to this reason, the natural frequency of the composite reduces in the pre-buckling region. In the post-buckling region, significant amount of geometric deformation takes place, at

this point, composite laminate gains structural stiffness. This stiffness gain in turn enhances the natural frequency of the composite beam in the post-buckling region. Previous findings of composite beams and columns are also reported similar trend (Mirzabeigy and Madoliat 2016; Rajesh and Pitchaimani 2017c; Waddar et al. 2019; Wu et al. 2015).

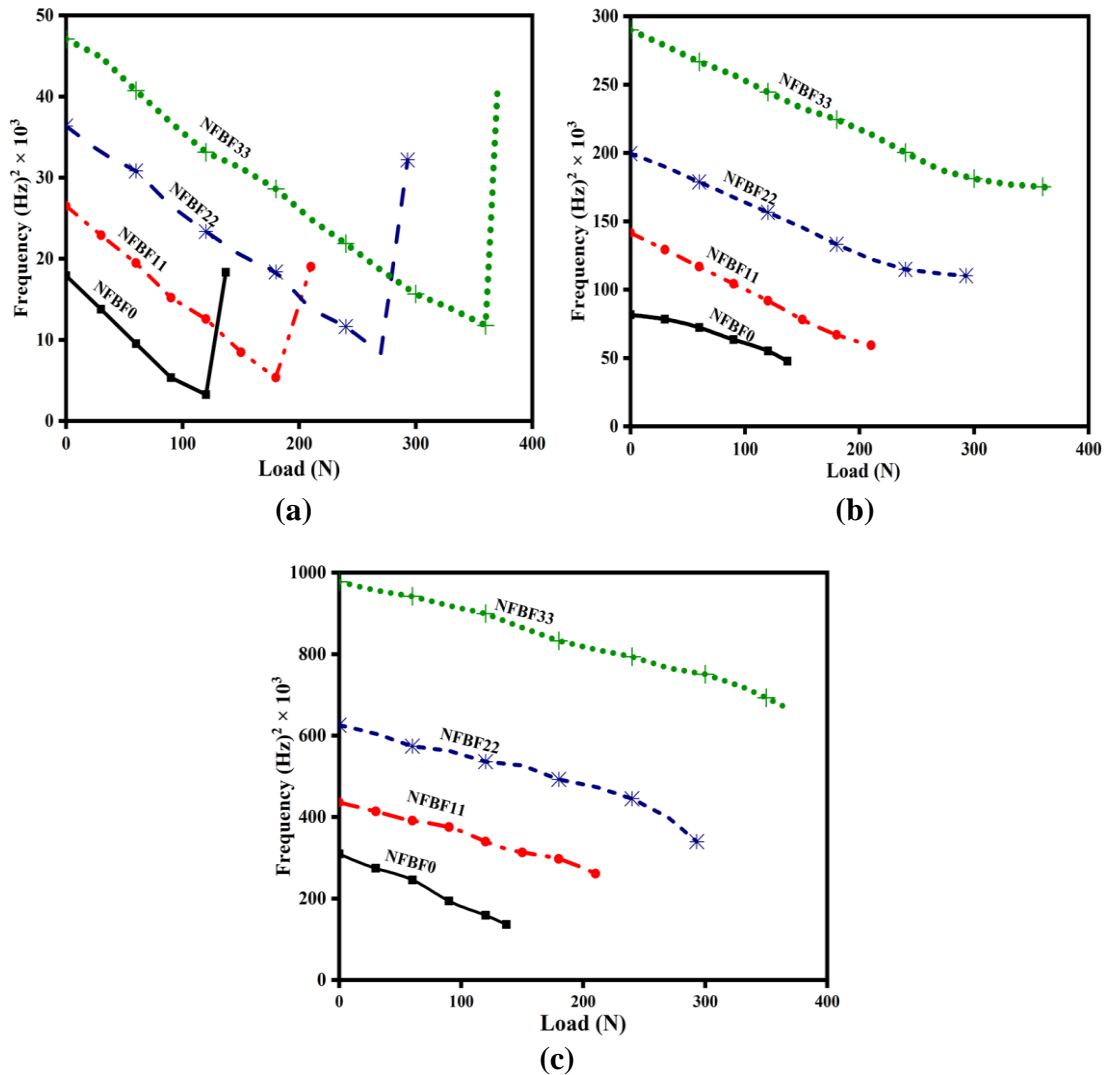


Figure 7.7 Influence of increase in axial-compressive load on natural frequencies of (a) 1st, (b) 2nd and (c) 3rd modes

7.4 Property comparison plots

Comparison of the critical buckling load associated with the present NFBF/PLA composites with the buckling load of similar composites available in literature is given in Figure 7.8. The comparison is done in terms of density of the different

7.5 Conclusion

Buckling and free vibration responses of NFBF/PLA biocomposites are investigated experimentally. Density results reveal that the density of PLA polymer increases with the reinforcement of natural fibre fabric. NFBF/PLA composites exhibited global buckling mode shape without interlaminar delamination of laminas and wrinkling of the fabric. Natural frequency and critical buckling load (P_{cr}) are enhanced with the filler content. The NFBF33 showed the highest critical buckling load and frequency compared to other counterparts. Natural frequencies of the composites reduced in the axial compression load. For the fundamental mode, before critical-buckling load, the natural frequency is minimal and after critical-buckling load exponential increase is noticed due to gain in geometrical stiffness of composite specimen. Property plot of critical buckling versus density of available references shows NFBF/PLA biodegradable composites have better specific-properties than natural fibre filled synthetic polymer composites and the NFBF33/PLA composite presented competitive buckling strength with neat epoxy/sisal fabric sandwich composites.

8 SUMMARY AND CONCLUSIONS

8.1 Summary

Comprehensive study has been carried out to analyse the mechanical, thermal, biodegradability, wear, fracture, buckling and free vibration properties of the natural fibre braided yarn woven fabric reinforced PLA bio-composites. In the present study, 3D braided yarn is prepared by solid braiding method and followed by this plain woven fabric is prepared in handloom weaving machine. The prepared fabric is used as filler material in PLA polymer. Before preparation of the composites, PLA and NFBBF/PLA sheets are prepared by solution casting method. Using these sheets composites are prepared by using film stacking and hot press compression molding method. PLA composites are fabricated with different weight fraction of natural fibre 3D braided yarn woven fabric according to the nature of test.

Mechanical properties such as tensile, flexural and impact properties of the braided yarn fabric composites are compared with the virgin PLA composites and other similar composites available in literature. In order to understand the thermal deflection behaviour of the composites thermal deflection test is conducted at different non-uniform heating conditions. Effect of water absorption and thickness swelling on mechanical properties of the composites is studied by performing flexural test before and after water absorption test. Biodegradability characteristics of the present NFBBF/PLA composites are studied through the compost soil incubation test. Wear behaviour of the present NFBBF/PLA composites is investigated by carrying out the wear test on pin-on-disc tribometer at different applied load and speed combinations. Fracture toughness of the present composites is evaluated based on the SENB test. Finally, static and free vibration responses of a beam like structure made of the present composites, under the axial edge compression are studied.

8.2 Conclusion

The important conclusions are summarised as;

Mechanical properties of the composites

- Tensile strength and modulus of braided yarn woven fabrics are reduced compared to braided yarn. The tensile properties of the fabric are found to be better for the warp direction loading compared to the weft direction loading.
- The reinforcement of NFBF enhanced the tensile, flexural, impact and interlaminar shear strength properties of the composites.
- Warp direction loaded composites showed good mechanical properties compared to weft direction loaded composites.
- Comparative study on the mechanical properties of present NFBF/PLA composites with similar composites shows that the properties of the present composites are better in most of the cases.

Thermal buckling behaviour under nonuniform thermal heating

- Flammability results revealed that the flame retardance property of the NFBF/PLA composites is enhanced up to 75.41% for 33 wt.% of NFBF reinforcement.
- DSC results showed enthalpy (ΔH_m) and percentage crystallinity (X_c) are enhanced significantly due to the NFBF reinforcement.
- TGA analysis also revealed that the NFBF reinforcement improves the thermal properties of the composites.
- The residual mass (char) of the composites is increased with the fibre reinforcement. The NFBF33 has the highest residual mass (char) of about 5.01%.
- The thermal deflection of the composites reduced remarkably with the reinforcement of the NFBF due to improved stiffness of the composites and at the same time thermal resistance property also improved compared to pure PLA.

- Warp direction loaded composites showed better thermal resistance and reduced deflection over weft direction loaded composites.
- Critical temperature and deflection of the beam significantly vary with the heating source position.
- The time study showed that the temperature sustainability is improved for the NFBBF/PLA composites.

Water absorption and biodegradability

- The water absorption and thickness swelling of the NFBBF/PLA composites are increased with the increase in fibre content.
- Significant reduction in the flexural properties of the NFBBF/PLA composite is observed due to the water absorption.
- The diffusion coefficient and permeability coefficients are high for the NFBBF/PLA composites compared to pure PLA.
- Biodegradability study revealed that the bio-degradation rate of the present NFBBF/PLA composites is lower than the PLA composites with other typical forms of natural fibre reinforcement.

Wear and fracture toughness properties

- The reinforcement of NFBBF in PLA enhanced frictional force and reduced the height loss of the composite specimen.
- NFBBF reinforcement reduces specific wear rate of PLA and about 95% reduction is observed for the NFBBF35 composite.
- SEM micrographs of NFBBF/PLA composites have shown good fibre-to-matrix interfacial bonding. Fibre fracture, fibre peeling, de-bonding and micro-cracks are observed as the common wear failure mechanisms of the NFBBF/PLA composites.
- K_{IC} and G_{IC} values of the NFBBF/PLA composites are enhanced due to the NFBBF reinforcement and the NFBBF35 composite showed a maximum K_{IC} and G_{IC} of about 5.32 MPa-m^{1/2} and 4.96 KJ/m² respectively.

- Fracture toughness study shows that the values of K_{IC} of the NFBF/PLA composites are much higher than the other natural fibre reinforced PLA composites values reported in the literature.

Buckling and free vibration

- Natural frequency and critical buckling load (P_{cr}) of the NFBF/PLA composites increase with the number of NFBF layers reinforcement.
- Natural frequency of the NFBF/PLA composites reduces, with increase in the magnitude of the edge compressive load and the reduction is highly significant for the fundamental mode near the buckling load.
- NFBF/PLA composites presented global buckling mode shape without interlaminar delamination of laminas and wrinkling of fabric.
- Property plot of critical buckling load versus density of available references shows NFBF/PLA biodegradable composites have better specific-properties than the other similar composites reported in the literature.

SCOPE FOR FUTURE WORK

In this research, mechanical, thermal, biodegradability, wear, fracture and buckling studies are carried out for different weight fraction of braided yarn fabric composites. The interlaminar fracture toughness of braided yarn fabric PLA composites can be addressed. The life cycle study under different environmental conditions (such as sunlight and rain) can be analysed. Effect of chemical treatment on flax fibre surface of the braided yarn fabric composites can be studied. To replace the non-degradable switch boards, circuit boards and other electronics applications, electrical conductivity and co-efficient of thermal expansion tests can be conducted.

REFERENCES

- Adomavičiūtė, E., Baltušnikaitė, J., Jonaitienė, V., and Stanys, S. (2015). "Formation and properties of textile biocomposites with PLA matrix reinforced with Flax and Flax/PLA weft knitted fabrics." *Fibres Text. East. Eur.*, 23(3), 45–50.
- Agopyan, V., and John, V. M. (1992). "Durability evaluation of vegetable fibre reinforced materials." *Build. Res. Inf.*, 20(4), 233–235.
- Ahmed, J., Zhang, J., Song, Z., and Varshney, S. K. (2009). "Thermal properties of polylactides." *J. Therm. Anal. Calorim.*, 95(3), 957–964.
- Akbaş, Ş. D. (2019). "Post-buckling analysis of a fiber reinforced composite beam with crack." *Eng. Fract. Mech.*, 212, 70–80.
- AL-Oqla, F. M., Salit, M. S., Ishak, M. R., and Aziz, N. A. (2015). "A Novel Evaluation Tool for Enhancing the Selection of Natural Fibers for Polymeric Composites Based on Fiber Moisture Content Criterion." *BioResources*, 10(1), 299–312.
- Alamri, H., and Low, I. M. (2012). "Characterization of Epoxy Hybrid Composites Filled with Cellulose Fibers and Nano-SiC." *J. Appl. Polym. Sci.*, 126(S1), E222–E232.
- Alavudeen, A., Rajini, N., Karthikeyan, S., Thiruchitrambalam, M., and Venkateshwaran, N. (2015). "Mechanical properties of banana/kenaf fiber-reinforced hybrid polyester composites : Effect of woven fabric and random orientation." *Mater. Des.*, 66, 246–257.
- Alimuzzaman, S., Gong, R. H., and Akonda, M. (2015). "Three-Dimensional Nonwoven Flax Fiber Reinforced Polylactic Acid Biocomposites." *Polym. Compos.*, 35(7), 1244–1252.
- Alix, S., Philippe, E., Bessadok, A., Lebrun, L., Morvan, C., and Marais, S. (2009). "Effect of chemical treatments on water sorption and mechanical properties of flax fibres." *Bioresour. Technol.*, 100(20), 4742–4749.
- Almansour, F. A., Dhakal, H. N., and Zhang, Z. Y. (2017). "Effect of water absorption on Mode I interlaminar fracture toughness of flax / basalt reinforced vinyl ester hybrid composites." *Compos. Struct.*, 168, 813–825.
- Alvarez, V. A., Ruscekaite, R. A., and Vazquez, A. (2003). "Mechanical Properties and Water Absorption Behavior of Composites Made from a Biodegradable Matrix and Alkaline-Treated Sisal Fibres." *J. Compos. Mater.*, 37(17), 1575–1588.
- Alvarez, V., Vazquez, A., and Bernal, C. (2006). "Effect of Microstructure on the Tensile and Fracture Properties of Sisal Fiber/Starch-based Composites." *J. Compos. Mater.*, 40(1), 21–35.
- Aly, N. M. (2017). "A review on utilization of textile composites in transportation

towards sustainability A review on utilization of textile composites in transportation towards sustainability.” *IOP Conf. Ser. Mater. Sci. Eng.*, 042002.

Anuar, H., Razali, M. S., Saidin, H. A., Fazlina, A., Hisham, B., Nur, S., Mohd, E., and Ali, F. (2016). “Tensile Properties of Durian Skin Fibre Reinforced Plasticized Polylactic Acid Biocomposites.” *Int. J. Eng. Mater. Manuf.*, 1(1), 16–20.

Arao, Y., Fujiura, T., Itani, S., and Tanaka, T. (2015). “Strength improvement in injection-molded jute-fiber-reinforced polylactide green-composites.” *Compos. Part B Eng.*, 68, 200–206.

Arbelaiz, A., Fernandez, B., Ramos, J. A., Retegi, A., Llano-Ponte, R., and Mondragon, I. (2005). “Mechanical properties of short flax fibre bundle / polypropylene composites : Influence of matrix / fibre modification , fibre content , water uptake and recycling.” *Compos. Sci. Technol.*, 65(10), 1582–1592.

Aruchamy, K., Subramani, S. P., Palaniappan, S. K., Sethuraman, B., and Kaliyannan, G. V. (2019). “Study on mechanical characteristics of woven cotton/bamboo hybrid reinforced composite.” *J. Mater. Res. Technol.*, 9(1), 718–726.

Asaithambi, B., Ganesan, G., and Kumar, S. A. (2014). “Bio-composites : Development and Mechanical Characterization of Banana/Sisal Fibre Reinforced Poly Lactic Acid (PLA) Hybrid Composites.” *Fibers Polym.*, 15(4), 847–854.

Ashori, A., and Nourbakhsh, A. (2009). “Characteristics of wood – fiber plastic composites made of recycled materials.” *Waste Manag.*, 29(4), 1291–1295.

Awal, A., Rana, M., and Sain, M. (2015). “Thermorheological and mechanical properties of cellulose reinforced PLA bio-composites.” *Mech. Mater.*, 80, 87–95.

Aznar, M., Ubeda, S., Dreolin, N., and Nerin, C. (2019). “Determination of non-volatile components of a biodegradable food packaging material based on polyester and polylactic acid (PLA) and its migration to food simulants.” *J. Chromatogr. A*, 1583, 1–8.

Bairstow. (2018). “Ropeand Fiber Comparison Guides.” *Bairstow Lift. Prod. Co.* (April 22, 2021).

Bajpai, P. K., Singh, I., and Madaan, J. (2012). “Frictional and adhesive wear performance of natural fibre reinforced polypropylene composites.” *J. Eng. Tribol.*, 227(4), 385–392.

Bajpai, P. K., Singh, I., and Madaan, J. (2013). “Tribological behavior of natural fiber reinforced PLA composites.” *Wear*, 297(1–2), 829–840.

Baran, I. J., Nowak, M. B., Chłopek, J. P., and Konsztowicz, K. J. (2018). “Acoustic Emission from Microcrack Initiation in Polymer Matrix Composites in Short Beam Shear Test.” *J. Nondestruct. Eval.*, 37(1), 1–10.

Bax, B., and Müssig, J. (2008). “Impact and tensile properties of PLA/Cordenka and PLA/flax composites.” *Compos. Sci. Technol.*, 68(7–8), 1601–1607.

- Bayerl, T., Geith, M., Somashekar, A. A., and Bhattacharyya, D. (2014). "Influence of fibre architecture on the biodegradability of FLAX/PLA composites." *Int. Biodeterior. Biodegradation*, 96, 18–25.
- Behera, A. K., Avancha, S., Basak, R. K., Sen, R., and Adhikari, B. (2012). "Fabrication and characterizations of biodegradable jute reinforced soy based green composites." *Carbohydr. Polym.*, 88(1), 329–335.
- Ben, G., Kihara, Y., Nakamori, K., and Aoki, Y. (2012). "Examination of heat resistant tensile properties and molding conditions of green composites composed of kenaf fibers and PLA resin." *Adv. Compos. Mater.*, 16(4), 361–376.
- Bhagat, V., George, N., Jeyaraj, P., and Murigendrappa, S. M. (2018). "Buckling and Free Vibration Behavior of Cylindrical Panel Under Thermal Load: Influence of Graphene Grading." *AIP Conf. Proc.*, 1943(1), 020012.
- Bhagat, V., and Jeyaraj, P. (2018). "Experimental investigation on buckling strength of cylindrical panel: Effect of non-uniform temperature field." *Int. J. Non. Linear. Mech.*, 99, 247–257.
- Bijwe, J. Ā., Rattan, R., and Fahim, M. (2007). "Abrasive wear performance of carbon fabric reinforced polyetherimide composites: Influence of content and orientation of fabric." *Tribol. Int.*, 40(5), 844–854.
- Bledzki, A. K., Jaszkiwicz, A., and Scherzer, D. (2009). "Mechanical properties of PLA composites with man-made cellulose and abaca fibres." *Compos. Part A Appl. Sci. Manuf.*, 40(4), 404–412.
- Bodros, E., Pillin, I., Montrelay, N., and Baley, C. (2007). "Could biopolymers reinforced by randomly scattered flax fibre be used in structural applications?" *Compos. Sci. Technol.*, 67(3–4), 462–470.
- Bogoeva-Gaceva, M., Avella, M., Malinconico, M., Buzarovska, A., Grozdanov, A., Gentile, G., and Errico, M. E. (2007). "Natural Fiber Eco-Composites." *Polym. Compos.*, 28(1), 98–107.
- Bouazza, M., Benseddiq, N., and Zenkour, A. M. (2019). "Thermal buckling analysis of laminated composite beams using hyperbolic refined shear deformation theory." *J. Therm. Stress.*, 42(3), 332–340.
- Bouazza, M., Zenkour, A. M., and Benseddiq, N. (2018). "Closed-form solutions for thermal buckling analyses of advanced nanoplates according to a hyperbolic four-variable refined theory with small-scale effects." *Acta Mech.*, 229(5), 2251–2265.
- Bourmaud, A., Shah, D. U., Beaugrand, J., and Dhakal, H. N. (2020). "Property changes in plant fibres during the processing of bio-based composites." *Ind. Crop. Prod.*, 154, 112705.
- Bozkurt, Ö. Y., Bulut, M., Erkliğ, A., and Faydh, W. A. (2019). "Axial and lateral buckling analysis of fiber reinforced S-glass/epoxy composites containing nano-clay particles." *Compos. Part B*, 158(August 2018), 82–91.

- Byun, J. H., and Chou, T. W. (1989). "Modelling and characterization of textile structural composites: A review." *J. Strain Anal. Eng. Des.*, 24(4), 253–262.
- Cantero, G., Arbelaiz, A., Llano-ponte, R., and Mondragon, I. (2003). "Effects of fibre treatment on wettability and mechanical behaviour of flax/polypropylene composites." *Compos. Sci. Technol.*, 63(9), 1247–1254.
- Cao, X., Mohamed, A., Gordon, S. H., Willett, J. L., and Sessa, D. J. (2003). "DSC study of biodegradable poly (lactic acid) and poly (hydroxy ester ether) blends." *Thermochimica acta*, 406(1–2), 115–127.
- Chabba, S., and Netravali, A. N. (2005). "'Green' composites Part 1: Characterization of flax fabric and glutaraldehyde modified soy protein concentrate composites." *J. Mater. Sci.*, 40(23), 6263–6273.
- Chaitanya, S., and Singh, I. (2017). "Processing of PLA/sisal fiber biocomposites using direct- and extrusion-injection molding." *Mater. Manuf. Process.*, 32(5), 468–474.
- Chalid, M., and Prabowo, I. (2015). "The Effects of Alkalization to the Mechanical Properties of the Ijuk Fiber Reinforced PLA Biocomposites." *Int. J. Chem. Mol. Nucl. Mater. Metall. Eng.*, 9(2), 342–346.
- Chan, C. M., Vandi, L., Pratt, S., Halley, P., Richardson, D., Werker, A., and Laycock, B. (2018). "Composites of Wood and Biodegradable Thermoplastics: A Review." *Polym. Rev.*, 58(3), 444–494.
- Chapple, S. C., and Nandjiwala, R. A. (2010). "Flammability of Natural Fiber-reinforced Composites and Strategies for Fire Retardancy: A Review." *J. Thermoplast. Compos. Mater.*, 23(6), 871–893.
- Cheng, S., Lau, K., Liu, T., Zhao, Y., Lam, P., and Yin, Y. (2009). "Mechanical and thermal properties of chicken feather fiber/PLA green composites." *Compos. Part B*, 40(7), 650–654.
- Crawford, B., Pakpour, S., Kazemian, N., Klironomos, J., Stoeffle, K., Rho, D., Denault, J., and Milani, A. S. (2017). "Effect of Fungal Deterioration on Physical and Mechanical Properties of Hemp and Flax Natural Fiber Composites." *Materials (Basel)*, 10(11), p.1252.
- Cruz Demosthenes, C. L. da, Nascimento, L. F. C., Monteiro, S. N., Costa, U. O., Filho, F. da C. G., Luz, F. S. da, Oliviera, M. S., James, F., Ramos, F. J. H. V., Periera, A. C., and Braga, F. O. (2019). "Thermal and structural characterization of buriti fibers and their relevance in fabric reinforced composites." *J. Mater. Res. Technol.*, Nov-13, 1–9.
- Deo, C., and Acharya, S. K. (2009). "Effects of load and sliding velocity on abrasive wear of Lantana camara fibre-reinforced." *J. Eng. Tribol.*, 224(5), 491–496.
- Devallencourt, C., and Capitaine, D. (1996). "Characterization of recycled celluloses: thermogravimetry/Fourier transform infra-red coupling and

thermogravimetry investigations.” *Polym. Degrad. Stab.*, 52(3), 327–334.

Dhakal, H. N., Zhang, Z. Y., and Richardson, M. O. W. (2007). “Effect of water absorption on the mechanical properties of hemp fibre reinforced unsaturated polyester composites.” *Compos. Sci. Technol.*, 67(7–8), 1674–1683.

Dhal, J. P., and Mishra, S. C. (2013). “Processing and Properties of Natural Fiber-Reinforced Polymer Composite.” *J. Mater.*, 1–6.

Diamant, Y., Marom, G., and Broutman, L. J. (1981). “The Effect of Network Structure on Moisture Absorption of Epoxy Resins.” *J. Appl. Polym. Sci.*, 26(9), 3015–3025.

Dittenber, D. B., and Gangarao, H. V. S. (2012). “Critical review of recent publications on use of natural composites in infrastructure.” *Compos. Part A*, 43(8), 1419–1429.

Dobircan, L., Sreekumar, P. A., Saiah, R., Leblanc, N., Terrié, C., Gattin, R., and Saiter, J. M. (2009). “Wheat flour thermoplastic matrix reinforced by waste cotton fibre: Agro-green-composites.” *Compos. Part A*, 40(4), 329–334.

Du, Y., Wu, T., Yan, N., Kortschot, M. T., and Farnood, R. (2014). “Fabrication and characterization of fully biodegradable natural fiber-reinforced poly (lactic acid) composites.” *Compos. Part B*, 56, 717–723.

Duigou, A. Le, Barbé, A., Guillou, E., and Castro, M. (2019). “3D printing of continuous flax fibre reinforced biocomposites for structural applications.” *Mater. Des.*, 180, 4–11.

Duigou, A. Le, Bourmaud, A., and Baley, C. (2015). “In-situ evaluation of flax fibre degradation during water ageing.” *Ind. Crop. Prod.*, 70, 204–210.

Duigou, A. Le, Davies, P., and Baley, C. (2009). “Seawater ageing of flax/poly (lactic acid) biocomposites.” *Polym. Degrad. Stab.*, 94(7), 1151–1162.

El-Sayed, A. A., El-Sherbiny, M. G., Abo-E-Ezz, A. S., and Aggag, G. A. (1995). “Friction and wear properties of polymeric composite materials for bearing applications.” *Wear*, 184(1), 45–53.

El-Tayeb, N. S. M. (2008). “A study on the potential of sugarcane fibers/polyester composite for tribological applications.” *Wear*, 265(1–2), 223–235.

El-Tayeb, N. S. M., Yousif, B. F., and Yap, T. C. (2006). “Tribological studies of polyester reinforced with CSM 450-R-glass fiber sliding against smooth stainless steel counterface.” *Wear*, 261(3–4), 443–452.

Eselini, N., Tirkes, S., Akar, A. O., and Tayfun, U. (2019). “Production and characterization of poly (lactic acid)-based biocomposites filled with basalt fiber and flax fiber hybrid.” *J. Elastomers Plast.*, 52(8), 701–716.

Espert, A., Vilaplana, F., and Karlsson, S. (2004). “Comparison of water absorption in

natural cellulosic fibres from wood and one-year crops in polypropylene composites and its influence on their mechanical properties.” *Compos. Part A Appl. Sci. Manuf.*, 35, 1267–1276.

Faruk, O., Bledzki, A. K., Fink, H., and Sain, M. (2012). “Biocomposites reinforced with natural fibers: 2000 – 2010.” *Prog. Polym. Sci.*, 37(11), 1552–1596.

Fazita, N., Rawi, M., Jayaraman, K., and Bhattacharyya, D. (2014). “Bamboo Fabric Reinforced Polypropylene and Poly (lactic acid) for Packaging Applications : Impact , Thermal , and Physical Properties.” *Polym. Compos.*, 35(10), 1888–1899.

Fleck, N. A., and Sridhar, I. (2002). “End compression of sandwich columns.” *Compos. Part A*, 33(3), 353–359.

Foruzanmehr, M., Vuillaume, P. Y., Elkoun, S., and Robert, M. (2016). “Physical and mechanical properties of PLA composites reinforced by TiO₂ grafted flax fibers.” *Mater. Des.*, 106, 295–304.

George, N., Jeyaraj, P., and Murigendrappa, S. M. (2016). “Buckling of non-uniformly heated isotropic beam : Experimental and theoretical investigations.” *Thin-Walled Struct.*, 108, 245–255.

George, N., Jeyaraj, P., and Murigendrappa, S. M. (2017). “Buckling and Free Vibration of Nonuniformly Heated Functionally Graded Carbon Nanotube Reinforced Polymer Composite Plate.” *Int. J. Struct. Stab. Dyn.*, 17(6), 1750064.

Georgiopoulos, P., Kontou, E., and Georgousis, G. (2018). “Effect of silane treatment loading on the flexural properties of PLA/flax unidirectional composites.” *Compos. Commun.*, 10, 6–10.

Gill, N. S., and Yousif, B. F. (2008). “Wear and frictional performance of betelnut fibre-reinforced polyester composite.” *J. Eng. Tribol.*, 223(2), 183–194.

Gilorkar, A., Murugan, R., and Pitchaimani, J. (2020). “Thermal buckling of sisal and glass hybrid woven composites : Experimental investigation.” *Compos. Part C Open Access*, 2, 100012.

Goriparthi, B. K., Suman, K. N. S., and Mohan Rao, N. (2012). “Effect of fiber surface treatments on mechanical and abrasive wear performance of polylactide/jute composites.” *Compos. Part A Appl. Sci. Manuf.*, 43(10), 1800–1808.

Goutianos, S., Peijs, T., Nystrom, B., and Skrifvars, M. (2006). “Development of Flax Fibre based Textile Reinforcements for Composite Applications.” *Appl. Compos. Mater.*, 13(4), 199–215.

Graupner, N., Herrmann, A. S., and Müssig, J. (2009). “Natural and man-made cellulose fibre-reinforced poly (lactic acid) (PLA) composites : An overview about mechanical characteristics and application areas.” *Compos. Part A Appl. Sci. Manuf.*, 40(6–7), 810–821.

Gunning, M. A., Geever, L. M., Killion, J. A., Lyons, J. G., and Higginbotham, C. L.

- (2013). “Mechanical and biodegradation performance of short natural fibre polyhydroxybutyrate composites.” *Polym. Test.*, 32(8), 1603–1611.
- Gunti, R., Prasad, A. V. R., and Gupta, A. V. S. S. K. S. (2016). “Preparation and Properties of Successive Alkali Treated Completely Biodegradable Short Jute Fiber-Reinforced PLA Composites.” *Polym. Compos.*, 37(7), 2160–2170.
- Guo, F., Zhang, Z., Zhang, H., Wang, K., and Jiang, W. (2010). “Tribological behavior of spun Kevlar fabric composites filled with fluorinated compounds.” *Tribology Int.*, 43(8), 1466–1471.
- Hamdan, S., Talib, Z. A., Rahman, M. R., Ahmed, A. S., and Islam, M. S. (2010). “Dynamic young’s modulus measurement of treated and post-treated tropical wood polymer composites (wpc).” *BioResources*, 5, 324–342.
- Harnnecker, F., Rosa, S., and Lenz, D. M. (2012). “Biodegradable Polyester-Based Blend Reinforced with Curaua Fiber: Thermal, Mechanical and Biodegradation Behaviour.” *J. Polym. Environ.*, 20(1), 237–244.
- Holbery, J., and Houston, D. (2006). “Natural-Fiber-Reinforced Polymer Composites in Automotive Applications.” *JOM*, 58(11), 80–86.
- Hong, G., Meng, Y., Yang, Z., Cheng, H., Zhang, S., and Song, W. (2017). “Mussel-Inspired Polydopamine Modification of Bamboo Fiber and Its Effect on the Properties of Bamboo Fiber/Polybutylene Succinate Composites.” *BioResources*, 12(4), 8419–8442.
- Hu, R., and Lim, J.-K. (2007). “Fabrication and mechanical properties of completely biodegradable hemp fiber reinforced polylactic acid composites.” *J. Compos. Mater.*, 41(13), 1655–1669.
- Huang, X., and Netravali, A. (2007). “Characterization of flax fiber reinforced soy protein resin based green composites modified with nano-clay particles.” *Compos. Sci. Technol.*, 67(10), 2005–2014.
- Huang, Z. ming. (2000). “The mechanical properties of composites reinforced with woven and braided fabrics.” *Compos. Sci. Technol.*, 60(4), 479–498.
- Huang, Z., Qian, L., Yin, Q., Yu, N., Liu, T., and Tian, D. (2018). “Biodegradability studies of poly (butylene succinate) composites filled with sugarcane rind fiber.” *Polym. Test.*, 66(February), 319–326.
- Huda, M. S., Drzal, L. T., Mohanty, A. K., and Misra, M. (2006). “Chopped glass and recycled newspaper as reinforcement fibers in injection molded poly (lactic acid) (PLA) composites : A comparative study.” *Compos. Sci. Technol.*, 66(11–12), 1813–1824.
- Huerta-cardoso, O., Durazo-cardenas, I., Longhurst, P., Simms, N. J., and Encinas-oropesa, A. (2020). “Fabrication of agave tequilana bagasse/PLA composite and preliminary mechanical properties assessment.” *Ind. Crop. Prod.*, 152, 112523.

Islam, M. S., Pickering, K. L., and Foreman, N. J. (2010a). "Influence of accelerated ageing on the physico-mechanical properties of alkali-treated industrial hemp fibre reinforced poly (lactic acid) (PLA) composites." *Polym. Degrad. Stab.*, 95(1), 59–65.

Islam, M. S., Pickering, K. L., and Foreman, N. J. (2010b). "Influence of Hygrothermal Ageing on the Physico-Mechanical Properties of Alkali Treated Industrial Hemp Fibre Reinforced Polylactic Acid Composites." *J. Polym. Environ.*, 18(4), 696–704.

Islam, M. S., Pickering, K. L., and Foreman, N. J. (2010c). "Influence of alkali treatment on the interfacial and physico-mechanical properties of industrial hemp fibre reinforced polylactic acid composites." *Compos. Part A Appl. Sci. Manuf.*, 41(5), 596–603.

Jang, Y. J., Jeong, K. T., Oh, J. H., Youn, R. J., and Song, Y. S. (2012). "Thermal stability and flammability of coconut fiber reinforced poly (lactic acid) composites." *Compos. Part B Eng.*, 43(5), 2434–2438.

Jawaid, M., Khalil, H. P. S. A., Bakar, A. A., and Khanam, P. N. (2011). "Chemical resistance , void content and tensile properties of oil palm/jute fibre reinforced polymer hybrid composites." *Mater. Des.*, 32(2), 1014–1019.

Jiang, N., Yu, T., Li, Y., Pirzada, T. J., and James, T. (2019). "Hygrothermal aging and structural damage of a jute/poly (lactic acid) (PLA) composite observed by X-ray tomography." *Compos. Sci. Technol.*, 173, 15–23.

Jin, X., Wang, W., Xiao, C., Lin, T., Bian, L., and Hauser, P. (2016). "Improvement of coating durability, interfacial adhesion and compressive strength of UHMWPE fiber/epoxy composites through plasma pre-treatment and polypyrrole coating." *Compos. Sci. Technol.*, 128, 169–175.

Jirawattanasomkul, T., Ueda, T., Likitlersuang, S., Zhang, D., Hanwiboonwat, N., Wuttiwannasak, N., and Horsangchai, K. (2019). "Effect of natural fibre reinforced polymers on confined compressive strength of concrete." *Constr. Build. Mater.*, 223, 156–164.

John, M. J., and Thomas, S. (2008). "Biofibres and biocomposites." *Carbohydr. Polym.*, 71(3), 343–364.

Kandola, B. K., Mistik, S. I., Pornwannachai, W., and Anand, S. C. (2018). "Natural fibre-reinforced thermoplastic composites from woven-nonwoven textile preforms : Mechanical and fire performance study." *Compos. Part B*, 153, 456–464.

Kannan, T. G., Wu, C. M., and Cheng, K. B. (2012). "Effect of different knitted structure on the mechanical properties and damage behavior of Flax/PLA (Poly Lactic acid) double covered uncommingled yarn composites." *Compos. Part B Eng.*, 43(7), 2836–2842.

Katherine. (2012). "Growing Fibers." <http://oneinchworld.com/blog/index.php/2012/05/growing-fibers/> (April 22, 2021).

- Khan, G. M. A., Terano, M., Gafur, M. A., and Alam, M. S. (2016). "Studies on the mechanical properties of woven jute fabric reinforced poly(L-lactic acid) composites." *J. King Saud Univ. - Eng. Sci.*, 28(1), 69–74.
- Khondker, O. A., Ishiaku, U. S., Nakai, A., and Hamada, H. (2006). "A novel processing technique for thermoplastic manufacturing of unidirectional composites reinforced with jute yarns." *Compos. Part A Appl. Sci. Manuf.*, 37(12), 2274–2284.
- Khuntia, T., and Biswas, S. (2020). "An investigation on the flammability and dynamic mechanical behavior of coir fibers reinforced polymer composites." *J. Ind. Text.*, 1528083720905031.
- Kim, H. S., Kim, H. J., Lee, J. W., and Choi, I. G. (2006). "Biodegradability of bio-flour filled biodegradable poly (butylene succinate) bio-composites in natural and compost soil." *Polym. Degrad. Stab.*, 91(5), 1117–1127.
- Koronis, G., Silva, A., and Furtado, S. (2016). "Applications of Green Composite Materials." *Biodegrad. Green Compos.*, 312.
- Kowalczyk, M., Piorkowska, E., Kulpinski, P., and Pracella, M. (2011). "Mechanical and thermal properties of PLA composites with cellulose nanofibers and standard size fibers." *Compos. Part A*, 42(10), 1509–1514.
- Kozłowski, R., and Władyka-Przybylak, M. (2008). "Flammability and fire resistance of composites reinforced by natural fiber." *Polym. Adv. Technol.*, 19(6), 446–453.
- Krishnasamy, S., Thiagamani, K. S. M., Kumar, C. M., Nagarajan, R., Shahroze, R. M., Siengchin, S., Ismail, S. O., and M.P, I. D. (2019). "Recent advances in thermal properties of hybrid cellulosic fiber reinforced polymer composites." *Int. J. Biol. Macromol.*, 141, 1–13.
- Kumar, P., Singh, I., and Madaan, J. (2013). "Tribological behavior of natural fiber reinforced PLA composites." *Wear*, 297(1–2), 829–840.
- Kumar, R., Irfan, M., Haq, U., Raina, A., Anand, A., and Raina, A. (2018). "Industrial applications of natural fibre- reinforced polymer composites – challenges and opportunities." *Int. J. Sustain. Eng.*, 12(3), 212–220.
- Kumar, R., Kumar, K., Bhowmik, S., and Sarkhel, G. (2019). "Tailoring the performance of bamboo filler reinforced epoxy composite : insights into fracture properties and fracture mechanism." *J. Polym. Res.*, 26(2), 54.
- Kumar, R., Yakabu, M. K., and Anandjiwala, R. D. (2010). "Effect of montmorillonite clay on flax fabric reinforced poly lactic acid composites with amphiphilic additives." *Compos. Part A Appl. Sci. Manuf.*, 41(11), 1620–1627.
- Kumar, R., and Yakubu, M. K. (2010). "Biodegradation of flax fiber reinforced poly lactic acid." *EXPRESS Polym. Lett.*, 4(7), 423–430.
- Kymäläinen, H., and Sjöberg, A. (2008). "Flax and hemp fibres as raw materials for thermal insulations." *Build. Environ.*, 43(7), 1261–1269.

- Kyosev, Y. (2015). "Introduction: the main types of braided structure using maypole braiding technology." *Braid. Technol. Text. Princ. Des. Process.*, 1–25.
- Lee, S., and Wang, S. (2006). "Biodegradable polymers/bamboo fiber biocomposite with bio-based coupling agent." *Compos. Part A Appl. Sci. Manuf.*, 37, 80–91.
- Li, Z., and Qiao, P. (2015). "Buckling and postbuckling behavior of shear deformable anisotropic laminated beams with initial geometric imperfections subjected to axial compression." *Eng. Struct.*, 85, 277–292.
- Linganiso, L. Z., Bezerra, R., Bhat, S., John, M., Braeuning, R., and Anandjiwala, R. D. (2014). "Pultrusion of flax/poly (lactic acid) commingled yarns and nonwoven fabrics." *J. Thermoplast. Compos. Mater.*, 27(11), 1553–1572.
- Liu, W., Drzal, L. T., Mohanty, A. K., and Misra, M. (2007). "Influence of processing methods and fiber length on physical properties of kenaf fiber reinforced soy based biocomposites." *Compos. Part B*, 38(3), 352–359.
- Liu, W., Misra, M., Askeland, P., Drzal, L. T., and Mohanty, A. K. (2005). "Green composites from soy based plastic and pineapple leaf fiber : fabrication and properties evaluation." *Polymer (Guildf)*, 46(8), 2710–2721.
- Luckachan, G. E., and Pillai, C. K. S. (2011). "Biodegradable Polymers- A Review on Recent Trends and Emerging Perspectives." *J. Polym. Environ.*, 19(3), 637–676.
- Lv, S., Zhang, Y., Gu, J., and Tan, H. (2017). "Biodegradation behavior and modelling of soil burial effect on degradation rate of PLA blended with starch and wood flour." *Colloids Surfaces B Biointerfaces*, 159, 800–808.
- Macedo, J. N. De, and Rosa, D. dos S. (2016). "Effect of fiber and starch incorporation in biodegradation of PLA-TPS- Cotton composites." *Key Eng. Mater.*, 668, 54–62.
- Mamun, A. A., Heim, H., Hossen, D., Kim, T. S., and Ahmad, S. H. (2013). "PLA and PP composites with enzyme modified oil palm fibre : A comparative study." *Compos. Part A*, 53, 160–167.
- Masirek, R., Kulinski, Z., Chionna, D., Piorkowska, E., and Pracella, M. (2006). "Composites of Poly (L -lactide) with Hemp Fibers : Morphology and Thermal and Mechanical Properties." *J. Appl. Polym. Sci.*, 105(1), 255–268.
- Matsunaga, H. (1996). "Free Vibration and Stability of Thin Elastic Beams Subjected to Axial Forces." *J. Sound Vib.*, 191(5), 917–933.
- Mirzabeigy, A., and Madoliat, R. (2016). "Large amplitude free vibration of axially loaded beams resting on variable elastic foundation." *Alexandria Eng. J.*, 55(2), 1107–1114.
- Morales, A. P., Güemes, A., Fernandez-lopez, A., Valero, V. C., La, S. De, and Llano, R. (2017). "Bamboo – Polylactic Acid (PLA) Composite Material for Structural Applications." *Materials (Basel)*, 10(11), 1286.

- Muñoz, E., and García-Manrique, J. A. (2015). “Water Absorption Behaviour and Its Effect on the Mechanical Properties of Flax Fibre Reinforced Bioepoxy Composites.” *Int. J. Polym. Sci.*, 2015, 16–18.
- Mustapha, K., Annan, E., Azeko, S. T., Kana, M. G. Z., and Soboyejo, W. O. (2015). “Strength and fracture toughness of earth- based natural fiber-reinforced composites.” *J. Compos. Mater.*, 0(0), 1–16.
- Nagarajan, V., Mohanty, A. K., and Misra, M. (2016). “Perspective on Polylactic Acid (PLA) based Sustainable Materials for Durable Applications: Focus on Toughness and Heat Resistance.” *ACS Sustain. Chem. Eng.*, 4(6), 2899–2916.
- Naik, R. A. (1995). “Failure analysis of woven and braided fabric reinforced composites.” *J. Compos. Mater.*, 29(17), 2334–2363.
- Naik, R. A., Ifju, P. G., and Masters, J. E. (1994). “Effect of Fiber Architecture Parameters on Deformation Fields and Elastic Moduli of 2-D Braided Composites.” *J. Compos. Mater.*, 28(7), 656–681.
- Nam, T. H., Ogihara, S., and Kobayashi, S. (2012). “Interfacial , Mechanical and Thermal Properties of Coir Fiber-Reinforced Poly (Lactic Acid) Biodegradable Composites.” *Adv. Compos. Mater.*, 21(1), 103–122.
- Nam, T. H., Ogihara, S., Tung, N. H., and Kobayashi, S. (2011). “Effect of alkali treatment on interfacial and mechanical properties of coir fiber reinforced poly (butylene succinate) biodegradable composites.” *Compos. Part B*, 42(6), 1648–1656.
- Narish, S., Yousif, B. F., and Rilling, D. (2010). “Adhesive wear of thermoplastic composite based on kenaf fibres.” *J. Eng. Tribol.*, 225(2), 101–109.
- Nassiopoulos, E., and Njuguna, J. (2015). “Thermo-mechanical performance of poly (lactic acid)/flax fibre-reinforced biocomposites.” *Mater. Des.*, 66, 473–485.
- Netravali, A. N., and Chabba, S. (2003). “Composites get greener.” *Mater. Today*, 4(6), 22–29.
- Ngaowthong, C., Boruvka, M., Behálek, L., Lenfeld, P., Švec, M., Dangtugee, R., Siegchin, S., and Rangappa, Sanjay Mavinkere Parameswaranpillai, J. (2019). “Recycling of sisal fiber reinforced polypropylene and polylactic acid composites: Thermo-mechanical properties, morphology, and water absorption behavior.” *Waste Manag.*, 97, 71–81.
- Nosbi, N., Akil, H., Ishak, Z. A. M., and Bakar, A. A. (2010). “Degradation of compressive properties of pultruded kenaf fiber reinforced composites after immersion in various solutions.” *Mater. Des.*, 31(10), 4960–4964.
- Ochi, S. (2008). “Mechanical properties of kenaf fibers and kenaf/PLA composites.” *Mech. Mater.*, 40, 446–452.
- Ohkita, T., and Lee, S. (2005). “Thermal Degradation and Biodegradability of Poly (lactic acid)/Corn Starch Biocomposites.” *J. Appl. Polym. Sci.*, 100(4), 3009–3017.

Oksman, K., Skrifvars, M., and Selin, J. F. (2003). "Natural fibres as reinforcement in polylactic acid (PLA) composites." *Compos. Sci. Technol.*, 63(9), 1317–1324.

Omrani, E., Menezes, P. L., and Rohtagi, P. K. (2016). "State of the art on tribological behavior of polymer matrix composites reinforced with natural fibers in the green materials world." *Eng. Sci. Technol. an Int. Journal*, 19(2), 717–736.

Orue, A., Eceiza, A., and Arbelaiz, A. (2018a). "Preparation and characterization of poly (lactic acid) plasticized with vegetable oils and reinforced with sisal fibers." *Ind. Crop. Prod.*, 112, 170–180.

Orue, A., Eceiza, A., and Arbelaiz, A. (2018b). "The effect of sisal fiber surface treatments, plasticizer addition and annealing process on the crystallization and the thermo-mechanical properties of poly (lactic acid) composites." *Ind. Crop. Prod.*, 118, 321–333.

Özbek, Ö. (2021). "Axial and lateral buckling analysis of kevlar/poxy fiber-reinforced composite laminates incorporating silica nanoparticles." *Polym. Compos.*, 42(November 2020), 1109–1122.

Pappu, A., Pickering, K. L., and Kumar, V. (2019). "Manufacturing and characterization of sustainable hybrid composites using sisal and hemp fibres as reinforcement of poly (lactic acid) via injection moulding." *Ind. Crop. Prod.*, 137, 260–269.

Pei, X., Shang, B., Chen, L., Li, J., and Tang, Y. (2016). "Compression properties of multilayer-connected biaxial weft knitted carbon fiber fabric reinforced composites." *Compos. Part B*, 91, 296–305.

Pickering, K. L., and Efendy, M. G. A. (2016). "Preparation and mechanical properties of novel bio-composite made of dynamically sheet formed discontinuous harakeke and hemp fibre mat reinforced PLA composites for structural applications." *Ind. Crop. Prod. jo*, 84, 139–150.

Pickering, K. L., Efendy, M. G. A., and Le, T. M. (2016). "A review of recent developments in natural fibre composites and their mechanical performance." *Compos. Part A Appl. Sci. Manuf.*, 83, 98–112.

Pickering, K. L., Sawpan, M. A., Jayaraman, J., and Fernyhough, A. (2011). "Influence of loading rate, alkali fibre treatment and crystallinity on fracture toughness of random short hemp fibre reinforced polylactide bio-composites." *Compos. Part A*, 42(9), 1148–1156.

Pietrak, K., and Wi, T. S. (2015). "A review of models for effective thermal conductivity of composite materials." *J. Power Technol.*, 95(1), 14–24.

Pilla, S., Gong, S., Neill, E. O., Yang, L., and Rowell, R. M. (2008). "Polylactide-Recycled Wood Fiber Composites." *J. Appl. Polym. Sci.*, 111(1), 37–47.

Pilla, S., Kramschuster, A., Lee, J., Auer, G. K., Gong, S., and Turng, L. (2012). "Microcellular and Solid Polylactide – Flax Fiber Composites." *Compos. Interfaces*,

16(7–9), 869–890.

Plackett, D., Andersen, T. L., Pedersen, W. B., and Nielsen, L. (2003). “Biodegradable composites based on L-poly lactide and jute fibres.” *Compos. Sci. Technol.*, 63(9), 1287–1296.

Poole, C. (2020). “Unique Ropecraft: How to Tie the Diamond Braid Stitch.” <http://uniqeropecraft.blogspot.com/2012/01/how-to-tie-diamond-braid-stitch.html> (Dec. 14, 2020).

Porras, A., and Maranon, A. (2012). “Development and characterization of a laminate composite material from polylactic acid (PLA) and woven bamboo fabric.” *Compos. Part B Eng.*, 43(7), 2782–2788.

Porras, A., Maranon, A., and Ashcroft, I. A. (2016). “Thermo-mechanical characterization of Manicaria Saccifera natural fabric reinforced poly-lactic acid composite lamina.” *Compos. Part A Appl. Sci. Manuf.*, 81, 105–110.

Rajesh, G., Prasad, A. V. R., and Gupta, A. V. S. S. K. S. (2019). “Soil Degradation Characteristics of Short Sisal / PLA Composites.” *Mater. Today Proc.*, 18, 1–7.

Rajesh, M., and Pitchaimani, J. (2016). “Dynamic Mechanical and Free Vibration Behavior of Natural Fiber Braided Fabric Composite: Comparison with Conventional and Knitted Fabric Composites.” *Polym. Compos.*, 39(7), 2479–2489.

Rajesh, M., and Pitchaimani, J. (2017a). “Mechanical characterization of natural fiber intra-ply fabric polymer composites: Influence of chemical modifications.” *J. Reinf. Plast. Compos.*, 0(0), 1–14.

Rajesh, M., and Pitchaimani, J. (2017b). “Mechanical Properties of Natural Fiber Braided Yarn Woven Composite: Comparison with Conventional Yarn Woven Composite.” *J. Bionic Eng.*, 14(1), 141–150.

Rajesh, M., and Pitchaimani, J. (2017c). “Experimental investigation on buckling and free vibration behavior of woven natural fiber fabric composite under axial compression.” *Compos. Struct.*, 163, 302–311.

Rajesh, M., Singh, S. P., and Pitchaimani, J. (2018a). “Mechanical behavior of woven natural fiber fabric composites: Effect of weaving architecture, intra-ply hybridization and stacking sequence of fabrics.” *J. Ind. Text.*, 47(5), 938–959.

Rajesh, M., Sultan, H. M. T., Uthayakumar, M., Jayakrishna, K., and Shah, A. U. M. (2018b). “Dynamic Behaviour of Woven Bio Fiber Composite.” *BioResources*, 13(1), 1951–1960.

Rashid, B., Leman, Z., Jawaid, M., Ghazali, M. J., Ishak, M. R., and Abdelgnei, M. A. (2017). “Dry sliding wear behavior of untreated and treated sugar palm fiber filled phenolic composites using factorial technique.” *Wear*, 381, 26–35.

Rawal, A., Saraswat, H., and Sibal, A. (2015). “Tensile response of braided structures: A review.” *Text. Res. J.*, 85(19), 2083–2096.

- Rawi, N. F. M., Jayaraman, K., and Bhattacharyya, D. (2013). "A performance study on composites made from bamboo fabric and poly (lactic acid)." *J. Reinf. Plast. Compos.*, 32(20), 1513–1525.
- Razak, I. N. A., Ibrahim, N. A., Zainuddin, N., Rayung, M., and Saad, W. Z. (2014). "The Influence of Chemical Surface Modification of Kenaf Fiber using Hydrogen Peroxide on the Mechanical Properties of Biodegradable Kenaf Fiber/Poly(Lactic Acid) Composites." *molecules*, 19(3), 2957–2968.
- Ren, J., Kim, Y. K., and Rice, J. (2010). "Comparing the fracture toughness of 3-D braided preform composites with z- fiber-reinforced laminar composites." *Text. Res. J.*, 81(4), 335–343.
- Rezaiee-Pajand, M., Mokhtari, M., and Hozhabrossadati, S. M. (2019). "Application of Hencky bar-chain model to buckling analysis of elastically restrained Timoshenko axially functionally graded carbon nanotube reinforced composite beams." *Mech. Based Des. Struct. Mach.*, 47(5), 599–620.
- Rosa, I. M. De, Iannoni, A., Kenny, J. M., Puglia, D., Santulli, C., Sarasini, F., Terenzi, A., and Eudossiana, V. (2011). "Poly (lactic acid)/Phormium tenax Composites: Morphology and Thermo-Mechanical Behavior." *Polym. Compos.*, 32(9), 1362–1368.
- Sadasivuni, K. K., Saha, P., Adhikari, J., Deshmukh, K., Ahamed, M. B., and Cabibihan, J.-J. (2019). "Recent advances in mechanical properties of biopolymer composites: a review." *Polym. Compos.*, 41(1), 32–59.
- Saeed, U., Nawaz, M. A., and Al-turaif, H. A. (2018). "Wood flour reinforced biodegradable PBS/PLA composites." *J. Compos. Mater.*, 52(19), 2641–2650.
- Sair, S., Mandili, B., Taqi, M., and Bouari, A. El. (2019). "Development of a new eco-friendly composite material based on gypsum reinforced with a mixture of cork fibre and cardboard waste for building thermal insulation." *Compos. Commun.*, 16(August), 20–24.
- Sakaguchi, M., Nakai, A., Hamada, H., and Takeda, N. (2000). "The mechanical properties of unidirectional thermoplastic composites manufactured by a micro-braiding technique." *Compos. Sci. Technol.*, 60(5), 717–722.
- Samantrai, S. P., Raghavendra, G., and Acharya, S. K. (2014). "Effect of carbonization temperature and fibre content on the abrasive wear of rice husk char reinforced epoxy composite." *J. Eng. Tribol.*, 228(4), 463–469.
- Sanjay, M. R., Arpitha, G. R., Naik, L. L., Gopalakrishna, K., and Yogesha, B. (2016). "Applications of Natural Fibers and Its Composites: An Overview." *Nat. Resour.*, 7(3), 108–114.
- Sawpan, M. A., Pickering, K. L., and Fernyhough, A. (2011). "Improvement of mechanical performance of industrial hemp fibre reinforced polylactide biocomposites." *Compos. Part A*, 42(3), 310–319.

Sgriccia, N., Hawley, M. C., and Misra, M. (2008). "Characterization of natural fiber surfaces and natural fiber composites." *Compos. Part A Appl. Sci. Manuf.*, 39(10), 1632–1637.

Shanks, R. A., Hodzic, A., and Ridderhof, D. (2005). "Composites of Poly (lactic acid) with Flax Fibers Modified by Interstitial Polymerization." *J. Appl. Polym. Sci.*, 99(5), 2305–2313.

Shen, X., Jia, J., and Chen, C. (2014). "Enhancement of mechanical properties of natural fiber composites via carbon nanotube addition." *J. Mater. Sci.*, 49(8), 3225–3233.

Shibata, M., Ozawa, K., Teramoto, N., Yosomiya, R., and Takeishi, H. (2003). "Biocomposites Made from Short Abaca Fiber and Biodegradable Polyesters." *Macromol. Mater. Eng.*, 288(1), 35–43.

Shonaike, G. O., Hamada, H., Maekawa, Z., Matsuda, M., Yuba, T., and Matsuo, T. (1996). "The influence of cooling conditions on the mechanical properties of commingled yarn composites." *J. Thermoplast. Compos. Mater.*, 9(1), 76–89.

Shrivastava, A. (2018). "Introduction to Plastics Engineering." *Introd. to Plast. Eng.*, 1–16.

Siengchin, S. (2014). "Reinforced Flax mat/modified Polylactide (PLA) Composites: Impact, Thermal, and Mechanical Properties." *Mech. Compos. Mater.*, 50(2), 257–266.

Siengchin, S., Pohl, T., Medina, L., and Mitschang, P. (2013). "Structure and properties of flax/ polylactide/alumina nanocomposites." *J. Reinf. Plast. Compos.*, 32(1), 23–33.

Singh, S., Mohanty, A. K., Sugie, T., Takai, Y., and Hamada, H. (2008). "Renewable resource based biocomposites from natural fiber and polyhydroxybutyrate-co-valerate (PHBV) bioplastic." *Compos. Part A Appl. Sci. Manuf.*, 39(5), 875–886.

Sombatsompop, N., and Chaochanchaikul, K. (2004). "Effect of moisture content on mechanical properties , thermal and structural stability and extrudate texture of poly (vinyl chloride)/ wood." *Polym. Int.*, 1218(9), 1210–1218.

Song, Y. S., Lee, J. T., Ji, D. S., Kim, M. W., Lee, S. H., and Youn, J. R. (2012). "Viscoelastic and thermal behavior of woven hemp fiber reinforced poly (lactic acid) composites." *Compos. Part B*, 43(3), 856–860.

Song, Y., Wang, D., Wang, X., Lin, L., and Wang, Y. (2011). "A method for simultaneously improving the flame retardancy and toughness of PLA." *Polym. Adv. Technol.*, 22(12), 2295–2301.

"Standard Test Methods for Plane-Strain Fracture Toughness and Strain Energy Release Rate of Plastic Materials 1." (n.d.). *ASTM D5045-99*.

Sujaritjun, W., Uawongsuwan, P., Pivsa-art, W., and Hamada, H. (2013).

“Mechanical property of surface modified natural fiber reinforced PLA biocomposites.” *Energy Procedia*, 34, 664–672.

Sun, H., and Qiao, X. (1997). “Prediction of the Mechanical Properties of Three-dimensionally Braided Composites.” *Compos. Sci. Technol.*, 57(6), 623–629.

Taib, R. M., Hassan, H. M., and Ishak, Z. A. M. (2014). “Mechanical and Morphological Properties of Polylactic Acid/Kenaf Bast Fiber Composites Toughened with an Impact Modifier.” *Polym. Plast. Technol. Eng.*, 53(2), 199–206.

Tan, P., Tong, L., and Steven, G. P. (1997). “Modelling for predicting the mechanical properties of textile composites -A review.” *Compos. Part A Appl. Sci. Manuf.*, 28(11), 903–922.

Tao, Y. U., Yan, L. I., and Jie, R. E. N. (2009). “Preparation and properties of short natural fiber reinforced poly (lactic acid) composites.” *Trans. Nonferrous Met. Soc. China*, 19, s651–s655.

Tate, J. S., Kelkar, A. D., and Whitcomb, J. D. (2006). “Effect of braid angle on fatigue performance of biaxial braided composites.” *Int. J. Fatigue*, 28(10 SPEC. ISS.), 1239–1247.

Thiagamani, S. M. K., Krishnasamy, S., Muthukumar, C., Tengsuthiwat, J., Nagarajan, R., Siengchin, S., and Ismail, S. O. (2019). “Investigation into mechanical, absorption and swelling behaviour of hemp/sisal fibre reinforced bioepoxy hybrid composites: Effects of stacking sequences.” *Int. J. Biol. Macromol.*, 140, 637–646.

Triki, A., Guicha, M., Hassen, M. Ben, and Arous, M. (2013). “Comparative Study of the Dielectric Properties of Natural-Fiber – Matrix Composites and E-Glass – Matrix Composites.” *J. Appl. Polym. Sci.*, 129(1), 487–498.

Tuttle, M., Singhatanadgid, P., and Hinds, G. (1999). “Buckling of Composite Panels Subjected to Biaxial Loading.” *Exp. Mech.*, 39(3), 191–201.

Waddar, S., Pitchaimani, J., and Doddamani, M. (2018). “Snap-through buckling of fly ash cenosphere/epoxy syntactic foams under thermal environment.” *Thin-Walled Struct.*, 131(March), 417–427.

Waddar, S., Pitchaimani, J., and Doddamani, M. (2020). “Effect of thermal loading on syntactic foam sandwich composite.” *Polym. Compos.*, [https://doi, 1–11](https://doi.org/10.1002/polb.25000).

Waddar, S., Pitchaimani, J., Doddamani, M., and Barbero, E. (2019). “Buckling and vibration behaviour of syntactic foam core sandwich beam with natural fiber composite facings under axial compressive loads.” *Compos. Part B*, 175(July), 1–11.

Wambua, P. M., and Anandjiwala, R. (2011). “A Review of Preforms for the Composites Industry.” *Compos. Part A Appl. Sci. Manuf.*, 40(4), 310–333.

Wang, B., Panigrahi, S., Tabil, L., and Crerar, W. (2007). “Pre-treatment of Flax Fibers for use in Rotationally Molded Biocomposites.” *J. Reinf. Plast. Compos.*, 26(5), 447–463.

- Wang, G., Zhang, D., Li, B., Wan, G., Zhao, G., and Zhang, A. (2019). “Strong and thermal-resistance glass fiber-reinforced polylactic acid (PLA) composites enabled by heat treatment.” *Int. J. Biol. Macromol.*, 129, 448–459.
- Weidong, Y., and Yan, L. I. (2012). “Sound absorption performance of natural fibers and their.” *Sci. China Technol. Sci.*, 55(8), 2278–2283.
- Wu, H., Kitipornchai, S., and Yang, J. (2015). “Free Vibration and Buckling Analysis of Sandwich Beams with Functionally Graded Carbon Nanotube-Reinforced.” *Int. J. Struct. Stab. Dyn.*, 15(7), 1–17.
- Xie, D., Salvi, A. G., Sun, C., and Waas, A. M. (2006). “Discrete Cohesive Zone Model to Simulate Static Fracture in 2D Triaxially Braided Carbon Fiber Composites.” *J. Compos. Mater.*, 40(22), 2025–2046.
- Yan, L., and Chouw, N. (2015). “Behavior and analytical modeling of natural flax fibre-reinforced polymer tube confined plain concrete and coir fibre-reinforced concrete.” *J. Compos. Mater.*, 47(17), 2133–2148.
- Yan, L., Chouw, N., and Jayaraman, K. (2014). “Flax fibre and its composites – A review.” *Compos. Part B*, 56, 296–317.
- Yang, W., Fortunati, E., Dominici, F., Giovanale, G., Mazzaglia, A., Balestra, G. M., Kenny, J. M., and Puglia, D. (2016). “Synergic effect of cellulose and lignin nanostructures in PLA based systems for food antibacterial packaging.” *Eur. Polym. J.*, 79, 1–12.
- Yatigala, N. S., Bajwa, D. S., and Bajwa, S. G. (2018). “Compatibilization improves physico-mechanical properties of biodegradable biobased polymer composites.” *Compos. Part A*, 107(August 2017), 315–325.
- Yew, G. H., Yusof, A. M. M., Ishak, Z. A. M., and Ishiaku, U. S. (2005). “Water absorption and enzymatic degradation of poly (lactic acid)/ rice starch composites.” *Polym. Degrad. Stab.*, 90(3), 488–500.
- Yousif, B. F. (2008). “Frictional and wear performance of polyester composites based on coir fibres.” *J. Eng. Tribol.*, 223(1), 51–59.
- Yousif, B. F., and El-tayeb, N. S. M. (2008). “Adhesive Wear Performance of T-OPRP and UT-OPRP Composites.” *Tribol. Lett.*, 32(3), 199–208.
- Yousif, B. F., and El-Tayeb, N. S. M. (2015). “High-stress three-body abrasive wear of treated and untreated oil palm fibre-reinforced.” *J. Eng. Tribol.*, 222(5), 637–646.
- Yousif, B. F., and EL-Tayeb, N. S. M. (2007). “The effect of oil palm fibers as reinforcement on tribological performance of polyester composite.” *Surf. Rev. Lett.*, 14(6), 1095–1102.
- Yousif, B. F., Lau, S. T. W., and Mcwilliam, S. (2010). “Polyester composite based on betelnut fibre for tribological applications.” *Tribology Int.*, 43(1–2), 503–511.

Yu, T., Jiang, N., and Li, Y. (2014). "Study on short ramie fiber/poly (lactic acid) composites compatibilized by maleic anhydride." *Compos. Part A Appl. Sci. Manuf. Part A*, 64, 139–146.

Yussuf, A. A., Massoumi, I., and Hassan, A. (2010). "Comparison of Polylactic Acid/Kenaf and Polylactic Acid/Rise Husk Composites: The Influence of the Natural Fibers on the Mechanical , Thermal and Biodegradability Properties." *J. Polym. Environ.*, 18(3), 422–429.

Zhang, Y., Li, Y., Ma, H., and Yu, T. (2013). "Tensile and interfacial properties of unidirectional flax/glass fiber reinforced hybrid composites." *Compos. Sci. Technol.*, 88, 172–177.

Zhong, Y., Godwin, P., Jin, Y., and Xiao, H. (2020). "Biodegradable polymers and green-based antimicrobial packaging materials: A mini-review." *Adv. Ind. Eng. Polym. Res.*, 3(1), 27–35.

Zhou, Y., Fan, M., and Chen, L. (2016). "Interface and bonding mechanisms of plant fibre composites: An overview." *Compos. Part B Eng.*, 101, 31–45.

Zsidai, L., Baets, P. De, Samyn, P., Kalacska, G., Peteghem, A. P. Van, and Parys, F. Van. (2002). "The tribological behaviour of engineering plastics during sliding friction investigated with small-scale specimens." *Wear*, 253(5–6), 673–688.

LIST OF PUBLICATIONS

INTERNATIONAL JOURNALS

1. Sateeshkumar Kanakannavar, Jeyaraj Pitchaimani and M.R. Ramesh, (2020). “Tribological behaviour of natural fibre 3D braided woven fabric reinforced PLA composites”. *Proceedings of the Institution of Mechanical Engineers, Part J: Journal of Engineering Tribology*, 235, 1-12. (SAGE, SCIE, IF=1.674).
2. Sateeshkumar Kanakannavar and Jeyaraj Pitchaimani, (2020). “Thermal buckling of braided flax woven polylactic acid composites”. *Journal of Reinforced Plastics and Composites*, 40 (7-8), 261-272. (SAGE, SCIE, IF: 3.710).
3. Sateeshkumar Kanakannavar and Jeyaraj Pitchaimani, 2021. “Fracture Toughness of Flax Braided Yarn Woven PLA Composites”. *International Journal of Polymer Analysis and Characterization*, 26 (4), 364-379. (Taylor & Francis, SCIE, IF: 2.583).
4. Sateeshkumar Kanakannavar and Jeyaraj Pitchaimani, 2021. “Fabrication and mechanical properties of braided flax fabric polylactic acid bio-composites”. *The Journal of The Textile Institute*, 112, 1-13. (Taylor & Francis, SCIE, IF: 1.880).
5. Sateeshkumar Kanakannavar, Jeyaraj Pitchaimani, Arunkumar Thalla and M. Rajesh, 2021. “Biodegradation properties and thermogravimetric analysis of 3D braided flax PLA textile composites”. *Journal of Industrial Textiles*, 51 (2), 1-26. (SAGE, SCIE, IF=3.721).
6. Sateeshkumar Kanakannavar and Jeyaraj Pitchaimani, (2021). “Free vibration of flax braided fabric PLA beam under edge compression”. *Journal of Natural Fibers*, 1-14. (Taylor & Francis, SCIE, IF-5.323).

INTERNATIONAL CONFERENCES

1. Sateeshkumar Kanakannavar and Jeyaraj Pitchaimani (2019).
“Comparative study of natural fibre 3D braided yarn woven fabric and simply twisted yarn woven fabric reinforced epoxy composites”. ICDEM, Second International conference on Design, Materials and Manufacture, December 6th to 8th 2019, National Institute of Technology Karnataka, Surathkal, India.
2. Sateeshkumar Kanakannavar and Jeyaraj Pitchaimani, (2020).
“Compressive properties of 3D braided flax fiber textile fabric reinforced PLA composites”. ICFEST, 1st International Conference on Frontiers in Engineering Science and Technology, Decemember 18th to 19th 2020, Yenepoya Institute of Technology, Moodbidri, Mangalore, India.

BIO-DATA

1. Name : Sateeshkumar Kanakannavar
2. Father's Name : Ashok Kanakannavar
3. Date of Birth : 20th July 1988
4. Nationality : Indian
5. Marital Status : Single
6. Address : Department of Mechanical Engineering,
National Institute of technology Karnataka,
Surathkal, P.O. Srinivasnagar – 575 025
Karnataka, India.
7. Mobile Number : +91 9538519935
8. E-mail id. : *skanakannavar@gmail.com*
9. Educational Qualification :

Qualification	University/Board	Year of Passing
Ph.D. (Mechanical engineering)	National Institute of Technology Karnataka, Surathkal, Mangalore	Pursuing
M. Tech (Engineering Analysis and Design)	Visvesvaraya Technological University, Belgaum	2017
B.E. (Mechanical Engineering)	Visvesvaraya Technological University, Belgaum	2012